

REPORT TO THE WATER RESEARCH COMMISSION

**THE ENGINEERING CHARACTERISTICS OF IMPORTANT
SOUTHERN AFRICAN ROCK TYPES WITH EMPHASIS ON
SHEAR STRENGTH OF CONCRETE DAM FOUNDATIONS.**

by

A J GEERTSEMA

DEPARTMENT OF CIVIL ENGINEERING
TECHNIKON PRETORIA

DECEMBER 2000

WRC REPORT NO: 433/1/00

ISBN: 1 86845 602 1

ACKNOWLEDGEMENTS

This report is the result of a research project on the engineering characteristics of important southern African rocks with the emphasis on the shear strength of concrete dam foundations. The study was made possible by the financial support of the Water Research Commission (WRC) over a period of seven years. This support is acknowledged with thanks to the WRC, in particular the late Mr. A G Reynders (Research Manager on the project) as well as Mr. D S van der Merwe as subsequent Research Manager.

The steering committee responsible for the project consisted of the following members:

Mr. AG Reynders*(deceased)	Water Research Commission (first Chairman)
Mr. DS van der Merwe	Water Research Commission (later Chairman)
Mr. FHWM Druyts	Department of Water Affairs and Forestry
Dr JM Jordaan	University of Pretoria
Dr HAD Kirsten	Steffen Robertson & Kirsten
Dr C Oosthuizen	Department of Water Affairs and Forestry
Prof. A Rooseboom	University of Stellenbosch
Dr A Schall *	Council for Geoscience
Mr. AT van Coller	National Department of Agriculture
Mr. CL van den Berg	Department of Water Affairs and Forestry
Mr. MA van der Walt *	Department of Water Affairs and Forestry
Prof. A van Schalkwyk *	University of Pretoria
Mr. UW Vogler *	CSIR and later consultant

The contribution of each of these members of the steering committee is acknowledged with thanks.

Members marked with an * were the members of the subcommittee for the project. The subcommittee met approximately every three months to discuss progress and results of the project. These members are thanked for their time and input into the project.

A special word of thanks to Mr. UW Vogler for the valuable contribution he made on the evaluation of the shear results on large-scale rock specimens as well as for editing of the report.

Thanks are also due to Mr. MA van der Walt, Head of the Materials Laboratory of the Department of Water Affairs and Forestry and a member of the Technical Sub Committee who made the large shearbox available for testing purposes and who's comments on testing procedures and evaluation of results were invaluable.

Mr. C Millman, Technician (1992 - 1994) and Mr. GF Filmalter, Technician (1995 - 2000) both of the Department of Civil Engineering, Technikon Pretoria, who conducted most of the testing on rock specimens. Without their co-operation this project would not have been possible.

The following contributors who conducted specialized tests are acknowledged with thanks:

Mr. C Schutte and Ms E Texiera of the Directorate of Surveying of the Department of Water Affairs and Forestry who annualized the results of the scanning device and printed the contours of shear surfaces.

Mrs. S Verryn of the Department of Geology, University of Pretoria who conducted the petrographic descriptions of rock material specimens.

Mr. UW Vogler, then of EMATEK, CSIR who conducted the tests on the swelling properties of rock material specimens. Mr. Vogler was appointed as consultant at the latter stage of the project to assist with the interpretation of the results.

Mr. GF Filmalter, then of the Council for Geoscience who conducted porosity and slake durability tests on rock material specimens.

Mr. MA van der Walt, Head of the Materials Laboratory of the Department of Water Affairs and Forestry who conducted abrasiveness testing on rock material specimens.

Prof. GGS Pegram of the University of Natal who helped to design and supervised the building of the laser scanning device.

To the Technikon Pretoria in the person of Prof. K Vorster, Dean of Engineering, who supported the project and who made time available to the researcher, a word of thanks.

EXECUTIVE SUMMARY

Introduction

The stability along joint planes is one of the most important characteristics of a rock mass forming the foundation of a concrete dam. The shear strength of discontinuities within the foundation rock is probably the most important characteristic.

Objectives and Purpose of the study

The objectives of this research project were:

- (a) to determine and to analyse the shear strength of joints in a number of rock types, sampled at different locations, and to link these strengths to the condition of the foundations and, in particular, the condition of the surfaces of the rock joints. The information so obtained can then serve as a databank for the design of new dams and for the evaluation of the safety of existing dams, and
- (b) to determine the characteristics of a number of southern African rock types to serve as preliminary design parameters to allow safer and more economical designs for the foundations of concrete dam walls.

Stages of investigation

The study was carried out in four identifiable phases. The first phase that took place during 1992 and 1993 was to do a literature study in order to determine the engineering characteristics of different rock types world-wide and in southern Africa. During this stage a visit was undertaken to the UK, Norway and the USA to study shear apparatus and the rock testing methods in these countries. The second phase was to determine the general characteristics of important southern African rock types. During the period 1993 to 1995 the shear apparatus and surface-scanning device to be used in the third stage were designed and constructed. The third phase (1994 to 1999) comprised of shear tests on NX-size borehole core samples (base shear and direct shear) and the testing and characterisation of large shear surfaces. The last phase (1999 to 2000) was used to compile the report.

Several delays were encountered mainly due to the following reasons: (a) the late delivery of the large shearbox and subsequent problems with the computer controlling the shearbox, (b)

resignation of the technician working full-time on the project and (c) illness of the researcher during 1996.

Format of the report

The text of the report start by stating the problems to be investigated followed in Chapter two by the findings of a literature study. Chapter three describes the determination of the engineering characteristics: methods and equipment, and Chapter four the presentation and discussion of results. This is followed in Chapter five by a description of the estimation of shear strength using a geotechnical characterization of the joint surface followed in Chapters six, seven and eight by conclusions, recommendations and references.

The Compact Disc (CD) contains the appendixes in electronic form as reports, graphs and photo's.

Results

A comprehensive literature study on test methods and engineering characteristics of different rock types was conducted. It was found that although engineering characteristics of rock material have been investigated on a regular basis for civil and other engineering applications, this information is not readily available to the engineering community at large. It is often regarded as confidential information by clients and filed for possible use in claims situations. This document is probably the most comprehensive source of engineering characteristics of southern African rock types available today.

This report describes the strength, deformation and general characteristics of quartzite, shale, sandstone, dolerite, mudstone, granite, rhyolite and tillite. Chapter 4 describes each of these rock types in detail. The results are too comprehensive to describe here. These rock types were selected because they cover a very large portion of the surface area of southern Africa, and as such many dams and other civil engineering structures have been built on them.

Emphasis was placed on the shear strength parameters of joints, especially the angle of friction. Two types of joints are recognised in nature: (a) joints with no or little fill material where the shear strength is determined by the characteristics of the rock material and (b) joints with fill material where the shear strength is determined by the characteristics of the fill material. The major part of this research concentrated on (a) joints with no or little fill material.

The three major characteristics determining the shear strength parameters of this type of joint are (i) the base shear strength of the rock material, (ii) the roughness profile along the joint surface and (iii) the hardness of the material on the joint surface.

The base shear strength parameters of the different rock materials were determined as part of the determination of rock material characteristics. The angle of friction obtained for the different materials corresponds very well to those published in the literature. The values for cohesion obtained through testing is zero to very small.

As part of this research project a laser-scanning device was developed and built in association with the Department of Civil Engineering of the University of Natal. This device measure x, y and z co-ordinates on a rock joint surface on a grid pattern. This information can be analyzed with software on a computer to produce a contour diagram of the joint surface area. From this contour diagram, joint roughness profiles were obtained. These, as well as profiles obtained with a carpenter's comb, were compared with typical roughness profiles as published by Barton.

Because of the importance of joint roughness in connection with the shear strength of joints, a further attempt was made to obtain a method of quantifying this phenomenon. The volume of material (asperities) above the lowest point on a joint surface was determined for each specimen tested with the large shear apparatus. The volume was then divided by the surface area of the specimen to obtain a value called the volume-area ratio. This was then correlated to the shear strength (in particular to the angle of friction) of a joint plane. Although no good correlation could be found, it is believed that this ratio could be a method of expressing joint roughness. Further investigation will be needed to verify this.

Conclusions

This study provides a useful guide to engineering parameters of several important rock types in southern Africa for planning and preliminary design purposes. It is probably the most comprehensive document describing the rock material, the testing procedure, and the engineering characteristics of so many rock types in southern Africa.

This research project was the first attempt to determine the shear strength characteristics of joints in southern African rock types with a large shear apparatus.

This study also contributes to the knowledge on shear strength of southern African rocks, in particular on (i) the sampling and preparation of specimens for testing in the large shear apparatus, (ii) the measurement of the roughness of the joint surfaces and (iii) the testing procedure. The shear strength characteristics of the rock joints of southern African rocks are described and an attempt was made to classify joints using a geotechnical description of the joint surface. Geotechnical parameters include rock type, roughness, hardness, and description of fill joint material. The joint fill material could be a clay or secondary mineral like smectite, it could be staining or it could be clean. This classification is a first attempt and further work still needs to be done in this regard.

Recommendations

It is recommended that a project be initiated to investigate the shear strength of southern African rock types in further detail in a systematic manner. Such an investigation can build on the knowledge obtained in this investigation. It is important to keep the variables such as rock type, weathering, and hardness be kept a minimum to investigate influence of joint roughness. An appropriate rock type to start with could be mudstone from the Qeduzisi Dam area near Ladysmith. This is a relative soft rock with smooth joints that gave low shear strength results during testing. These results should be confirmed. This could then be extended to other rock types once the influence of roughness has been established.

Acknowledgement

The author wishes to express his gratitude to the Water Research Commission for funding this project and hope that the report will contribute to dams and other civil engineering structures be built more cost effectively and safely.

It could be noted that this project was the first project at a Technikon to be funded by the Water Research Commission. As such it contributed to the building of capacity at the Department of Civil Engineering at Technikon Pretoria: Two technicians had the opportunity to gain experience in testing rock specimen on the newly built shear apparatus belonging to the Department of Water Affairs and Forestry: Staff of the above-mentioned department were trained on the use and procedures of the machine. The researcher had the opportunity to gain experience and knowledge on many aspects of rock mechanics with the emphases on shear strength. This abundant source of information established during the project will lead to publication in of articles in scientific and engineering journals.

LIST OF CONTENTS.

	page
Acknowledgements	ii
Executive Summary	iv
List of Contents	viii
List of Tables	xiii
List of Figures	xviii
List of Symbols/Acronyms	xxi
Definition of terms	xxii
List of Appendices	xxiv
 1. Introduction	
1.1 Motivation and objectives.	1.1
1.2 Engineering characteristics investigated during this study.	1.2
1.2.1 Engineering characteristics of rock materials.	1.2
1.2.2 Shear properties of joints in rock.	1.3
1.3 The history of the study conducted.	1.3
1.4 Outline of the report.	1.5
 2. Review of the related literature	
2.1 Introduction	2.1
2.2 Literature study on testing procedures for engineering characteristics of rock material.	2.1
2.3 Shear strength of discontinuities in rock.	2.2
2.3.1 Types of discontinuities in rock.	2.2
2.3.2 Factors influencing the shear strength of rock joints	2.5
2.4 Review of equipment for direct shear testing of large specimens (testing machines).	2.9
2.4.1 Norwegian Geotechnical Institute's apparatus.	2.9
2.4.2 US Bureau of Reclamation's apparatus.	2.9
2.4.3 US Army Corps of Engineer's apparatus.	2.10

2.4.4	Imperial College's apparatus.	2.10
2.5	Review of shear strength assessment method by Barton and others	2.11
2.5.1	Introduction	2.11
2.5.2	Measurement of the hardness of joint surfaces.	2.13
2.5.3	Review of measurement of the roughness of joint surfaces.	2.16
	(a) Joint Roughness Coefficient (JRC).	2.16
	(b) Physical roughness measurement by Pegram and Pennington.	2.19
2.5.4	Scale effects	2.19
2.5.5	The empirical equation of shear strength	2.20
2.6	Literature study on the engineering characteristics of southern African rocks	
2.6.1	Strength properties of rock material	2.22
	(a) Uniaxial compressive strength (UCS)	
	(i) Uniaxial compressive strength	2.22
	(ii) Point load strength index (PLSI)	2.23
	(b) Triaxial compressive strength	2.23
	(c) Tensile strength	2.24
	(i) Direct tensile strength	2.24
	(ii) Indirect tensile strength (Brazilian method)	2.24
	(d) Shear strength.	2.25
	(i) Base shear strength	2.25
	(ii) Shear strength of joints (Peak and Residual)	2.25
	(iii) Punch shear strength (Intact shear strength)	2.26
2.6.2	Deformation properties of rock material	
	(a) E-modulus (Young's modulus)	2.26
	(b) Poisson's ratio	2.27
2.6.3	Other general rock properties	2.28
	(a) Hardness (Schmidt hammer)	2.28
	(b) Abrasiveness	2.28
	(c) Seismic wave velocity	2.29

4.3.7 Sandstone of the Ventersdorp Supergroup	4.20
4.3.8 Granite of the Basement Complex	4.22
4.3.9 Sandstone of the Karoo Supergroup	4.26
4.3.10 Siltstone of the Karoo Supergroup	4.28
4.3.11 Rhyolite of the Karoo Supergroup	4.30
4.3.12 Tillite of the Karoo Supergroup	4.31
4.4 Correlation of some rock properties	4.32
4.4.1 The relation of uniaxial compressive strength and point load strength	4.32
4.4.2 The relation between Schmidt hammer hardness and uniaxial compressive strength	4.33
4.4.3 The relation between punch shear strength and uniaxial compressive strength	4.34
4.4.4 The relation between modulus of elasticity and uniaxial compressive strength	4.35
4.4.5 The relation between punch shear strength and Brazilian tensile strength.	4.35
4.4.6 The relation between density and seismic wave velocity	4.36
4.4.7 The relation between punch shear strength and cohesion of triaxial testing	4.37
4.4.8 Conclusion	4.37
4.5 Results of shear testing on large shear apparatus	4.38
4.5.1 Phases of testing and testing procedure	4.38
4.5.2 Data analysis	4.39
4.5.3 Rock types tested	4.40
4.5.2.1 Basalt	4.41
4.5.2.2 Dolerite	4.43
4.5.2.3 Granite	4.45
4.5.2.4 Sandstone	4.51
4.5.2.5 Mudstone	4.53

4.7	Determination of hardness and roughness of joint surfaces tested in the large shear apparatus	4.55
4.7.1	Hardness of joint surfaces	4.55
4.7.2	Determination of roughness of joint surfaces	4.56
4.7.3	Correlation of joint roughness, hardness and shear strength	4.59
4.8	Discussion of testing and results of Phase 2	4.61
4.9	Discussion of testing and results of Phase 3	4.65
5.	Estimation of shear strength using a geotechnical characterisation of the joint surface	
5.1	Introduction	5.1
5.2	Joint surface parameters	5.1
5.3	The theory of shear strength of joints in rock.	5.2
5.4	Classification of joint surfaces for the determination of shear strength	5.3
5.4.1	Joint surfaces in hard rock.	5.3
5.4.2	Joints with staining on hard and rough joints.	5.4
5.4.3	Joints in rock with fill material present	5.5
5.5	Application of shear strength in the design of concrete dam foundations	5.6
5.6	Guidelines for the use of information contained in this report	5.6
6.	Conclusions	6.1
7.	Recommendations	7.1
8.	References	8.1
9.	Appendixes	see: Compact Disc

LIST OF TABLES

Table 2.1 Parameters controlling the shear strength of infilled discontinuities (After De Toledo et al, 1993)

Table 2.2 Basic friction angles of various unweathered rocks. (After Barton and Choubey, 1977)

Table 2.3. Descriptive classification of Rock Joints (After Barton and Choubey, 1977)

Table 2.4 Roughness descriptors by Pegram and Pennington (1996)

Table 2.5 Rock types described in the literature.

Table 2.6 Uniaxial compressive strengths of selected southern African rock types.

Table 2.7 Point load strength index of selected southern African rock types.

Table 2.8 Triaxial compressive strengths of selected southern African rock types.

Table 2.9 Direct tensile strength of selected southern African rock types.

Table 2.10 Indirect tensile strength of selected southern African rock types.

Table 2.11 Basic shear strength of selected southern African rock types.

Table 2.12 Punch shear strength of selected southern African rock types.

Table 2.13 E-moduli of selected southern African rock types.

Table 2.14 Poisson's ratios of selected southern African rock types.

Table 2.15 Schmidt hammer hardnesses of selected southern African rocks.

Table 2.16 Abrasiveness of selected southern African rocks.

Table 2.17 Seismic wave velocities of selected southern African rocks.

Table 2.18 Water absorption capacities of selected southern African rocks.

Table 2.19 Porosity of selected southern African rocks.

Table 2.20 Densities of selected southern African rocks.

Table 2.21 Swelling properties of selected southern African rocks.

Table 2.22 Slake durability properties of selected southern African rocks.

Table 4.1 Selected southern African rock types tested for engineering characteristics.

Table 4.2 Selected rock types (large block samples) tested with the large shear box.

Table 4.3 Characteristics of selected specimens of Quartzite (1A) of the Cape Supergroup.

Table 4.4 Characteristics of selected specimens of Quartzite (1B) of the Cape Supergroup.

Table 4.5 Characteristics of selected specimens of Quartzite (8A) of the Cape Supergroup.

Table 4.6 Characteristics of selected specimens of Quartzite (8B) of the Cape Supergroup.

Table 4.7 Characteristics of selected specimens of Shale (2A) of the Cape Supergroup.

Table 4.8 Characteristics of selected specimens of Sandstone (2B) of the Cape Supergroup.

Table 4.9 Characteristics of selected specimens of fine grained Dolerite (3A)

Table 4.10 Characteristics of selected specimens of coarse grained Dolerite (3B)

Table 4.11 Characteristics of selected specimens of coarse grained Dolerite (5D)

Table 4.12 Friction angle of selected specimen of post Karoo Dolerite (similar to Dolerite 3A).

Table 4.13 Characteristics of selected specimen of Mudstone (3C) of the Cape Supergroup.

Table 4.14 Friction angle of selected test specimens of Mudstone of the Karoo Supergroup (similar to Mudstone 3C).

Table 4.15 Characteristics of selected specimen of Shale (4A) of the Ventersdorp Supergroup

Table 4.16 Characteristics of selected specimen of Sandstone (4B) of the Ventersdorp Supergroup.

Table 4.17 Characteristics of selected specimen of Granite (5A) of the Basement Complex.

Table 4.18 Friction angles of selected specimens of Granite of the Basement Complex (similar to Granite 5A).

Table 4.19 Characteristics of selected specimen of Sandstone (5B) of the Karoo Supergroup.

Table 4.20 Characteristics of selected specimen of Siltstone (5C) of the Karoo Supergroup.

Table 4.21 Characteristics of selected specimen of Rhyolite (6A) of the Karoo Supergroup.

Table 4.22 Characteristics of selected specimen of Tillite (7A) of the Karoo Supergroup.

Table 4.23 Specimens tested during the first and second phases of testing.

Table 4.24 Granite specimens tested during the third phase of the investigation.

Table 4.25 Shear strength parameters of basalt as determined during test Phases 2A and 2B.

Table 4.26 Friction angles and apparent cohesion for Dolerite as determined by this study.

Table 4.27 Shear strength parameters of Granite as determined during phases 2A and 2B.

Table 4.28 Results of shear testing on Granite 1C.

Table 4.29 Results of shear testing on Granite 2C.

Table 4.30 Results of shear testing on Granite 3C.

Table 4.31 Shear strength parameters of Sandstone as determined by this study.

Table 4.32 Shear strength parameters of Mudstone as determined by this study.

Table 4.33 Hardness of joint surfaces determined by Schmidt hammer and expresses in terms of uniaxial compressive strength.

Table 4.34 Measured joint roughness coefficient (JRC) for large samples tested.

Table 4.35 Calculated roughness index for large samples tested during Phase 2.

Table 4.36 Shear strength parameters for samples tested in the large shear apparatus during Phases 2.

Table 4.37 Friction angle for rock types as calculated with the Barton and Choubey (1977) empirical equation for shear strength at normal stress equal to 1000kPa.

Table 4.38 Difference between the calculated and tested residual friction angles for rock types tested during Phase 2.

Table 4.39 Difference between dry and saturated friction angles.

Table 4.40 Friction angles for granite as calculated with the Barton and Choubey (1977) empirical equation for shear strength at normal stress equal to 1000kPa.

Table 4.41 Difference between the calculated and tested residual friction angles for rock types tested during Phase 3.

Table 4.42 Difference between dry and saturated friction angles of granite specimens tested.

Table 5.1 Friction angle characteristics of Granite 1C.

Table 5.2 Friction angle characteristics of Granite 2C.

Table 5.3 Comparison of basic, calculated peak, measured maximum residual and measured saturated maximum friction angles of some rock types tested.

LIST OF FIGURES

Figure 2.1 Shear stress vs. normal stress illustrating peak and residual shear strength.

Figure 2.2 Shear stress vs. normal stress illustrating friction angle and apparent cohesion.

Figure 2.3 The relationship between Schmidt hardness and the uniaxial compressive strength of rock. (After Miller 1965 as reported by Barton and Choubey, 1977)

Figure 2.4 Typical roughness profiles (After Barton and Choubey, 1977)

Figure 3.1 Farnell test press used for testing of rock specimens.

Figure 3.2 Point load test apparatus.

Figure 3.3 The triaxial cell or Hoek cell used to determine the triaxial strength of intact rock specimens.

Figure 3.4 Brazilian tensile test apparatus.

Figure 3.5 The modified soil shearbox for shear testing of NX-size rock core samples.

Figure 3.6 The large shear testing machine.

Figure 3.7 Schematic sketch of large shear testing machine (side view).

Figure 3.8 Schematic sketch of large shear box (front view).

Figure 3.9 Bottom half of shearbox assembly with test specimen.

Figure 3.10 Rock sample with associated joint surface tied up with wire ready to be cast.

Figure 3.11 The laser scanning device.

Figure 3.12 Carpenters comb on rough joint surface.

Figure 3.13 Punch shear apparatus.

Figure 3.14 The Schmidt hammer.

Figure 4.1 Location where samples of rock material were taken.

Figure 4.2 Correlation of point load strength vs uniaxial compressive strength.

Figure 4.3 Correlation of Schmidt rebound number vs uniaxial compressive strength.

Figure 4.4 Correlation of punch shear strength vs uniaxial compressive strength.

Figure 4.5 Correlation of tangent modules vs uniaxial compressive strength.

Figure 4.6 Correlation of punch shear strength vs tensile strength.

Figure 4.7 Correlation of density vs seismic wave velocity.

Figure 4.8 Correlation of punch shear strength vs triaxial cohesion.

Figure 4.9 Shear stress vs normal stress of Basalt - Phases 2A and 2B of shearing of Basalt 1, 2 & 3.

Figure 4.10 Shear stress vs normal stress of Dolerite - Phases 2A and 2B of shearing of Dolerite 1 & 3.

Figure 4.11 Shear stress vs normal stress of Granite – Phases 2A and 2B of shearing (dry and submerged).

Figure 4.12 Shear stress vs normal stress observations for Granite 1C.

Figure 4.13 Shear stress vs. normal stress observations for Granite 2C.

Figure 4.14 Shear stress vs. normal stress observations for Granite 3C.

Figure 4.15 Shear stress vs. normal stress observations for Sandstone - Phases 2A and 2B of shearing (dry and saturated).

Figure 4.16 Shear stress vs. normal stress of Mudstone - Phases 2A and 2B of shearing (dry and saturated).

Figure 4.17 A comparison between profiles along the centreline of specimen determined by (a) the laser apparatus vs. (b) the carpenters comb and (c) roughness profile by Barton and Choubey.

Figure 4.18 Correlation of friction angle to effective roughness.

LIST OF SYMBOLS AND ACRONYMS

A	= cross-sectional area (m^2)
c	= cohesion (kPa, MPa)
d	= diameter (m)
E_t	= Tangent modulus (GPa)
E_{av}	= Average modulus (GPa)
E_{sec}	= Secant Modulus (GPa)
g	= acceleration due to gravity ($9,81 \text{ ms}^{-2}$)
l	= length (m)
m	= meter (m)
N	= Newton
ν	= Poisson's ratio
ρ	= density (kg/m^3)
γ	= unit weight (kN/m^3)
σ	= normal stress (MPa)
τ	= shear stress (MPa)
ϕ	= friction angle (degrees)
ϕ_b	= base friction angle (degrees)
ϕ_r	= residual friction angle (degrees)

ISRM	= International Society for Rock Mechanics
JCS	= Joint wall compressive strength (MPa)
JRC	= Joint roughness coefficient
PLSI	= Point load strength index
SHI	= Shear strength index
UCS	= Uniaxial compressive strength (MPa)
XRD	= X-ray diffraction

DEFINITION OF TERMS

Average modulus (E_{av}) = The average modulus is the Young's modulus measured at the linear portion of the axial stress-strain curve.

Base friction angle (ϕ_b) = The base friction angle is the friction angle of rock material measured on a artificial saw cut joint in a rock specimen.

Density (ρ) = Density is defined as the mass of a specimen divided by its volume and is usually expressed in g/cm^3 (ml) or kg/m^3 .

Effective normal stress (σ_n) = Effective normal stress is the total stress level acting on a joint surface in the field minus the hydrostatic pressure.

Friction angle (ϕ) = Friction angle is the angle in degrees at which an object on an inclined surface is just stable.

Joint wall compressive strength (JCS) = Joint wall compressive strength is the strength of rock material at the surface of a joint plane, in terms of uniaxial compressive strength in MPa.

Joint roughness coefficient (JRC) = Joint roughness coefficient is a number developed by Barton and Choubey (1977) describing the roughness of a joint surface.

Normal stress (σ) = Normal stress is defined by a force acting on a determined surface area.

Peak shear strength (ϕ_p) = Peak shear strength represent the maximum shear resistance.

Poisson's ratio (ν) = Poisson's ratio is the ratio of the slope of the axial stress-strain curve to the slope of the diametric stress-strain curve.

Punch shear strength = Punch shear strength is the shear resistance to punch.

Residual friction angle (ϕ_r) = The residual friction angle is the friction angle parameter at the residual shear strength after substantial movement along the joint plane has taken place.

Secant Modulus (E_{sec}) = Secant Young's modulus (E_{sec}), is usually measured from zero stress to some fixed percentage of the ultimate strength, generally 50%.

Shear strength (τ) = Shear stress is a combination of the angle of friction and the cohesion, given by the Mohr Coulomb expression $\tau = c + \sigma \tan \phi$.

Tangent modulus (E_t) = Tangent Young's modulus (E_t), is measured at a stress level which is usually some fixed percentage of the ultimate strength.

Uniaxial compressive strength (UCS) = The uniaxial compressive strength is the strength of a rock specimen two and a half to three times the diameter in length broken in compression, expressed in MPa.

LIST OF APPENDICES

Appendix A & B – Basic shear strength: Test results (Software: Corel Quattro Pro 8)

Appendix C & D – Shear strength on small specimens: Test results (Software: Corel Quattro Pro 8).

Appendix E - Shear strength on large specimens: Test results of Phase 1 Graphs of shear load vs. shear displacement (Software: MS Word 97).

Appendix F - Shear strength on large specimens: Test results of Phase 1 Graphs of normal stress vs. shear stress. (Software: Corel Quattro Pro 8).

Appendix G - Shear strength on large specimens: Test results of Phase 2A and 2B. Graphs of shear load vs. shear displacement (Software: MS Word 97).

Appendix H - Shear strength on large specimens: Test results of Phase 2A and 2B. Graphs of normal stress vs. shear stress. (Software: Corel Quattro Pro 8).

Appendix I - Shear strength on large specimens: Test results of Phase 2A and 2B. Tables and graphs of normal stress vs. shear stress. (Software: MS Excell 97).

Appendix J - Shear strength on large specimens: Test results of Phase 3A and 3B. Graphs of shear load vs. shear displacement (Software: MS Word 97).

Appendix K - Shear strength on large specimens: Test results of Phase 3A and 3B. Tables and graphs of normal stress vs. shear stress. (Software: MS Excell 97).

Appendix L - Shear strength on large specimens: Plates of shear surfaces. (Software: MS Word 97).

Appendix M - Shear strength on large specimens: Topography of shear surfaces of Phases 2A, 2B, 3A and 3B. (Software: Microstation).

Appendix N - Shear strength on large specimens: Roughness profiles of shear surfaces of Phases 2A, 2B, 3A and 3B. (Software: Microstation).

Appendix O – Principal stress diagrams for the determination of triaxial compressive strength of some southern African rock types. (Software: Corel Quattro Pro 8).

Appendix P – Stress strain diagrams for the determination of youngs modulus and poissons ration of some southern African rock types. (Software: Corel Quattro Pro 8).

Appendix Q – Test report on microscopic identification of rock samples. Department of Geology, University of Pretoria. January 1994. (Software: MS Word 97).

Appendix R – Test report on porosity and slake durability of rock samples. Geological Survey. Pretoria, December 1993. (Software: MS Word 97).

Appendix S – Test report on free swell strain tests. EMATEC, CSIR Report. November, 1993.
(Software: MS Word 97).

Appendix T – Test report on Los Angeles abrasion testing on coarse aggregate, SABS Report.
May 1996. (Software: MS Word 97).

CHAPTER ONE

INTRODUCTION

1.1 Motivation and objectives.

The engineering characteristics of rocks and particularly, the shear strength of discontinuities in rock masses play a key role in civil engineering and specifically in geotechnical engineering. Civil engineers are confronted with the problem of shear strength when designing excavations in rock masses for structures such as dam foundations, rock slopes, tunnels etc.

A large proportion of South Africa's economically most active population lives in the Gauteng province, which is situated on a watershed. Furthermore, South Africa is a relatively dry country, which necessitates that water storage dams have to be built in suitable riverbeds from where the water has to be transferred to the end users by means of pump stations, pipelines, tunnels and canals. A number of major water schemes have been constructed, e.g. the Drakensberg Pumped Storage Scheme, the Orange-Fish River Scheme and the Lesotho Highlands Water Project, phase 1B of the latter currently under construction. Increasing the capacity of existing schemes will become necessary and further, similar schemes will have to be constructed in the future to satisfy the ever-increasing demand for water in the RSA. A number of dams in our country have reached ages of 40 years and more with the result that their safety and stability will have to be re-evaluated.

The stability of a dam depends on its design, on the materials and methods used during its construction and on the stability of the foundations on which it is built. The characteristics (properties) of the rocks and particularly the shear resistance of the joints in the rocks are very important design parameters. The latter parameter has generally not received the necessary attention, mainly because it can not be determined quickly and cheaply. An additional explanation is that obtaining representative rock samples is very difficult and often only the more competent materials survive the sampling processes.

The original objectives of this research project were thus:

(a) to determine and to analyse the shear strength of joints in a number of rock types, sampled at different locations and to link these strengths to the conditions of the foundations and in particular the condition of the surfaces of the rock joints. The information so obtained can then serve as a data bank for the design of new dams and for the evaluation of the safety of existing dams, and

(b) To determine the engineering and geological characteristics of a number of southern African rock types to serve as preliminary design parameters to allow safer and more economical designs for the foundations of concrete dam walls.

The shear strength of joints in rock is also of importance for the design of slopes in rock for roads and for mining excavations as well as for the design of tunnels for civil and mining engineering applications. The information presented in this report will therefore also be of use to engineers designing such structures.

1.2 The engineering characteristics investigated during this study.

For the purpose of this investigation the engineering characteristics have been subdivided into two groups:

- (a) The **GENERAL** engineering characteristics that include: strength-, deformability- and other characteristics and
- (b) The **SHEAR STRENGTH** characteristics of joints.

1.2.1 The engineering characteristics of rock materials

The **strength characteristics** of rock materials can be subdivided into compressive, tension and shear, depending on the mode of application of stresses. The compressive strength must be split further into uniaxial and triaxial. The **deformation behaviour** is characterised by Young's Modulus and Poisson's ratio. **Other engineering properties** include hardness, abrasive resistance, seismic wave velocities, water absorption, porosity, and density, swelling characteristics and slake durability. An attempt was made to determine the characteristics of

the most important southern African rock types. The types of rocks tested include: Quartzite, shale and sandstone of the Cape Supergroup; post-Karoo dolerite; siltstone, mudstone, sandstone, tillite and rhyolite of the Karoo Supergroup; shale and sandstone of the Ventersdorp Supergroup and granite of the Basement Complex.

1.2.2 Shear properties of joints in rock

To evaluate the stability of a dam foundation, the shear strength of those joints with the most unfavourable orientations relative to the applied loads is required. Determination of the orientation of joints in a foundation by means of a joint survey is relatively easy. From this the most unfavourably oriented joints can be selected. The design parameters for shear strength of these joints are usually not available during the early stages of the design and it is thus necessary to estimate these. It is therefore the aim of this investigation to provide a guideline for the estimation of these shear strength characteristics as accurately as possible.

1.3 The history of the study conducted.

It should be noted that this was the first project proposed by a Technikon to be financed by the Water Research Commission.

The study has been executed in five distinct phases. The first phase, taking place between 1992 and 1993 consisted of a literature survey with the aim of collecting and studying data on the engineering properties of different types of rock from southern Africa and elsewhere, as well as of world wide origin. During this phase the United Kingdom, Norway and the United States were visited to study inter alia their methods of determination of the engineering characteristics of rocks and particularly also their equipment for shear testing. During the same period, the Department of Water Affairs and Forestry (DWAF) designed a large shear box. This shear box was later used in the research project.

During the second phase a sampling programme was undertaken and the general engineering properties of the sampled southern African types of rocks were determined. During this phase, which lasted from 1993 to 1995, the DWAF's large shear box was manufactured. Also during 1995 a scanning apparatus was developed and built in co-operation with the University of Natal. This apparatus scans the surface of a rock specimen and can produce a

contour map of the scanned surface, which can be used to describe quantitatively the surface topography and thus the roughness of the rock joints to be tested.

The third phase, from 1994 to 1999, consisted of an intensive testing programme during which NX-size cores were used to determine the shear strength (basic and residual) of the selected rock materials. In addition, the large specimens collected for testing in the large shear box at the DWAF were characterised and a number of these were tested.

During the fourth and last phase a number of shear tests on large specimens were conducted at the DWAF – both ‘wet’ and ‘dry’ - and the report was written.

The last phase conducted between 1999 and 2000 included a sampling and testing programme of three specimens of granite. The purpose of this phase was to apply the knowledge and experience gained during the previous part of the project, to calibrate the results obtained previously.

The investigation experienced a number of serious delays for which the main reasons were: (a) The large shear box developed by the DWAF was delivered late and in addition, problems were experienced with its computerised control system. (b) The resignation of the technician who had been appointed in a full-time capacity to work on the project and (c) the serious illness of the researcher during 1996.

Deviations from the first objective occurred as a result of the test machine being new and that a learning curve had to be followed by the investigators to familiarise themselves with the equipment. The taking of large rock samples was also more complicated than originally anticipated. Just as these problems were solved the researcher fell ill while the technician continued with the testing programme. The result of this sequence of events led to a situation where data could only be analysed after the testing programme was almost completed. A second attempt was made after consultation with a consultant to put the available already tested samples through a further set of tests. It should be emphasised that a specific sample could only be tested once to determine the peak shear strength. All these factors contributed to a rather small number of rock samples being tested.

1.4 Outline of the report.

In this report a description of the problem is presented, followed by the literature survey. The following three chapters deal with the determination of the engineering properties, the interpretation and discussion of the results and the estimation of the shear strength by making use of the geotechnical description of the joint surfaces. The next chapters present conclusions and recommendations. The report closes with a list of literature references. Appendixes are available in electronic form on compact disc.

CHAPTER TWO

REVIEW OF THE RELATED LITERATURE

2.1 Introduction.

Rock mechanics for civil engineering applications world-wide is a relatively young subject in comparison with related engineering sciences such as soil mechanics. This is especially true in southern Africa as far as civil engineering applications are concerned. Rock mechanics in mining applications has been studied for many years. The International Society for Rock Mechanics (ISRM) has since 1966 played a major part in communication between workers in the field of rock mechanics.

One of the ISRM's indispensable contributions is the standardisation of test methods. Representative sampling and determination of the engineering characteristics (rock material properties) of rock specimens can be carried out using ISRM standardised methods. This does however not represent the engineering characteristics of the rock mass, as often the best materials (unweathered and without discontinuities) are tested, because the weaker rock materials get damaged or lost during the sampling process.

The literature study on southern African rock types was mainly confined to information contained in the books (four volumes) by Brink (1979-1983), and publications by Ward et al (1985), Maschek (1989) and van Rooy (1991). With the exception of Pegram and Pennington (1995) literature referred to dates earlier than 1993. The reason for this is that information on engineering characteristics is mainly found in contract reports on site investigations conducted by consultants for clients. Consultants regard this information as confidential.

2.2 Literature study on test procedures for the determination of engineering characteristics of rock materials.

Engineering characteristics of rock materials are usually tested in a laboratory using ISRM test methods, Brown (1981). The most common rock material properties include: (i) Strength parameters such as uniaxial compressive strength (UCS), point load strength testing is used as an indicator test for the UCS, triaxial strength, tensile strength and shear strength (direct and

punch shear). (ii) Deformation testing such as E-modulus (Young's modulus) and Poisson's ratio and (iii) Other rock material properties including hardness, abrasiveness, seismic wave velocity, water absorption, porosity, density, swelling and slake durability. A petrographic description of the rock is usually also carried out.

2.3 Shear strength of discontinuities in rock.

Hoek and Bray (1977) define discontinuities or weakness planes as those structural features, which separate intact rock blocks within a rock mass. Many engineers describe these features collectively as joints but this is perhaps an over-simplification since the mechanical properties of these features will vary according to the process of their formation. Faults, bedding planes, cleavage, tension joints and shear joints all will exhibit distinct characteristics and will respond in different ways to applied loads.

2.3.1 Types of discontinuities in rock.

Gabrielsen (1990), discussing the characteristics of joints and faults from a geological perspective, concludes that even a single fracture may have a long and complex history of changing stress, temperature, strain rate, mineralisation and recrystallisation. Because of this complexity, geologists have adopted a range of terms to describe discontinuities and also to indicate their dominant mode of formation and geological history as determined by observational studies. The following sections summarize the most widely accepted terms:

(a) Faults

Price (1966) defines a fault as a plane of shear failure that exhibits obvious signs of differential movement of the rock mass on either side of the plane. It is assumed that a fault is induced when changing tectonic stresses produce a shear stress that exceeds the shear strength on a particular plane in the rock mass. Evidence of shear displacement includes the offset of identifiable features such as bedding planes or veins, or the creation of slickensides and fault gouge by the scraping and grinding action associated with slip. Although shear displacements can range from just a few millimeters to several hundred meters, the term 'fault' is usually reserved for the more extensive features on which significant displacement has taken place.

Faults that have experienced very large shear displacements often accumulate a significant thickness of powdered rock, called fault gouge, or generate a zone of broken rock, called fault breccia. Fault breccia can extend up to several meters on each side of the shear plane.

During formation of faults shear displacements of a few millimeters can, in theory, be accommodated as elastic displacements of the surrounding rock. Larger displacements have to be accommodated by subsidiary structures such as folds, hinge lines or secondary faults at each end of the primary fault.

(b) Joints

Price(1966) defines joints as *cracks and fractures in rock along which there has been extremely little or no movement*. Joints are found in rock masses within 1000 m or more of the earth's surface, at all orientations and at extents ranging from a few millimeters to several hundred meters. Joints occur many thousand times more frequently than faults; indeed it is rare to find a cubic meter of rock that does not contain any joints. Many geologists believe that studying joints and their origins can provide valuable clues to the history of tectonic processes in near-surface rocks. It is, however, worth considering the following factors when debating the mechanisms that may have created joints:

- (i) Joints can form in materials ranging from relatively fresh, partly-consolidated sediments to rocks that have lain intact for thousands of millions of years.
- (ii) Mechanisms such as thermal metamorphism and pressure solution, which can lead to the healing or removal of joints, are rare in near-surface rocks encountered in rock engineering.
- (iii) The formation of a joint will lead to a complex redistribution of the local stress field in a rock mass.

The origins of certain types of joints are clearly related to relatively simple mechanisms such as the columnar jointing formed by stresses induced during the cooling of basalts and the slabbing joints caused by diurnal temperature changes on exposed rock faces. The ubiquitous nature of other joints suggests that their formation is related to some other, more complex, geological process.

(c) Bedding planes

A bedding plane is a surface created by a change in such factors as layering due to sedimentation, grain size, grain orientation, mineralogy or chemistry during the deposition of a sedimentary rock. Bedding does not always create discontinuities; in many cases it forms only a slight change in colour or texture in an otherwise intact rock material. In sedimentary rocks, some of the bedding planes find expression as discontinuities. In fine grained sedimentary rocks such as shales, bedding planes can form discontinuities that are only a few millimetres apart, dominating the discontinuous structure of the mass.

(d) Cleavage

Some minerals break in a characteristic way. Where the break forms flat surfaces which are parallel to defined crystal directions it is known as cleavage. Spencer (1969) and Whitten and Brooks (1972) identify two broad types of rock cleavage: viz fracture cleavage and flow cleavage. *Fracture cleavage* (also known as false cleavage and strain slip cleavage) is a term describing incipient, cemented or welded parallel discontinuities that are independent of any parallel alignment of minerals. Spencer (1969) lists six possible mechanisms for the formation of fracture cleavage. In each mechanism, lithology and stress conditions are assumed to have produced shearing, extension or compression, giving rise to numerous closely-spaced discontinuities separated by thin slivers of intact rock. Fracture cleavage is generally associated with other structural features such as faults, folds and kink bands. *Flow cleavage*, which can occur as slaty cleavage or schistosity, is dependent upon the recrystallisation and parallel alignment of platy minerals such as mica, producing an interleaving or *foliation* structure. It is generally accepted that flow cleavage is produced by the high temperatures and/or pressures associated with metamorphism in fine grained rocks. Spencer (1969) suggests that mechanisms such as the rotation and flattening of existing minerals, and the recrystallisation and growth of new minerals, produce the parallel alignment of crystals and the associated cleavage observed in rocks such as slates, phyllites and schists.

(e) Fractures, fissures and other features

Bridges (1975) defines a *fracture* as a discrete break in a rock which is not parallel with a visible fabric. In coining this term he presumably excludes discontinuities that have been produced by the exfoliation of cleavage, and, in so doing, concurs with one of the definitions given by Whitten and Brooks (1972). Bridges specifically avoids the term 'joint' to prevent

confusion arising from the range of different definitions. The terms 'fracture' and 'crack' have been adopted, but not explicitly defined, by most of the authors cited in this section for describing joints and other discontinuities that have arisen from brittle fracture mechanisms. Rock mechanics engineers also use these terms to describe the cracks generated during rock material testing, blasting and brittle rock failure. It must also be recognised that these terms are widely used in general speech so it is inappropriate and unwise to claim specific meanings for them.

Fookes and Denness (1969) define the term 'fissure' as follows: discontinuity dividing an otherwise continuous material without separation of units. According to Fourmaintraux (1975), fissures are planar discontinuities that are extensive in two directions but restricted in the third, which corresponds to the thickness or aperture of the discontinuity. Unfortunately the term 'fissure' also has a range of other, less formally defined meanings. Goodman (1976) distinguishes fissures as the small fractures that can be found in specimens of rock material. Price (1966) refers to 'gashes' or 'fissures' as fractures that *are open or, more usually, filled with quartz or some carbonate material*. In concurring with this general definition Whitten and Brooks (1972) point out that fissures and other discontinuities that have become filled with extraneous material are also referred to as 'veins', 'lodes', 'dykes' and 'sills' depending on their geometry, composition and mode of formation. In the author's opinion, the term 'fissure' is somewhat ambiguous and should not be used to describe any specific types of discontinuities unless the meaning has been defined locally.

Although discontinuities in rock masses could be described as any one of the above-mentioned terms by structural geologists, terminology usually used by civil engineers and also in this report is limited to joint and joint plane to describe any discontinuity in a rock mass.

2.3.2 Factors influencing the shear strength of rock joints

(a) Introduction

According to De Toledo et al (1993) the shear strength characteristics of rock discontinuities have been studied for a long time but a complete understanding of the mechanisms and of the parameters controlling the process has never been reached. Infilled joints are likely to be the weakest elements of any rock mass in which they occur and exert a dominant influence on its behaviour. The behaviour of infilled rock joints in shear has been investigated for decades. The results of field and laboratory tests started to be published frequently in the 1960's and

were reviewed by Barton (1974). From then on, investigations became more systematic and concentrated mainly on laboratory testing.

Different materials and test procedures were employed in an attempt to study primarily the influence of filler thickness on peak shear strength. However, other physical properties were less frequently studied, mainly because of experimental difficulties. Previously published test results lead to contradictory conclusions so far as the influence of filler thickness is concerned.

Rocks of medium strength (e.g. sandstone) have been widely used by researchers in this field, although harder materials such as basalt and granite have also been used.

Systematic research on this subject has mainly been done on laboratory made joints. Three types of surfaces have been used:

- (i) flat surfaces produced by saw cutting
- (ii) rough surfaces generated by tensile fracture
- (iii) regularly profiled surfaces produced by cutting instruments.

A laboratory investigation always has to choose between testing real joints and artificially created ones. Natural joints, either filled or unfilled, are virtually impossible to use in systematic research, but the benefits of adopting either a copy of a natural joint or a regularly profiled one are clear. It is a matter of choice between the study of the behaviour of the interaction of infill with a real joint shape as opposed to the study of infill within a boundary whose geometry is well constrained but made from real rock material. Idealized profiles allow a better understanding of specific joint properties, yet both methods of testing laboratory-prepared joints may face serious shortcomings, such as inappropriate representation of an infilled joint in the field. In most cases, laboratory shear box tests have been adopted for this work with sample sizes of 50 -250 mm and normal stresses of 20-1500 kPa, producing results relevant to conditions of zero normal stiffness, i.e. constant normal stress. Peak shear strength was always investigated and in some cases residual strength was also studied. However, the ability of equipment to study the residual strength of joints infilled with soil is limited by maximum displacements which may lead to significant errors. Kutter (1974), using a simplified rotary machine, showed the need to use large displacements in order to define properly the residual strength of an unfilled and rough rock joint. In fact, displacements of up to 100 mm are usually required to achieve the residual strength in soils (Lupini, Skinner & Vaughan, 1981) and as much as 200 mm have been observed for some

rough unfilled rock joints. It is doubtful whether a shear box apparatus or the ring shear apparatus is capable of producing a correct measure of the residual shear strength characteristics of natural infilled joints.

When comparing published results in the literature, it is important to remember that there are eight basic parameters to be considered in the study of the shear strength of infilled joints; some relate to the material properties, some to the joint itself and to the geological formation to which the joint belongs, and others to the equipment and the particular problem under consideration. Table 2.1 summarizes the parameters involved in both drained and undrained shear strengths, which should be borne in mind in the testing of infilled joints.

Some of these parameters will be discussed in the following paragraphs.

a. <u>Material parameters</u>	Infilling properties Infilling thickness Joint stress history Rock properties Joint wall roughness Orthogonal joints
b. <u>Equipment parameters</u>	Rate of shear Stiffness of the shearing equipment

Table 2.1 Parameters controlling the shear strength of infilled discontinuities (After De Toledo et al, 1993)

(b) Effect of the rock boundaries

In practice, the assumption that the minimum shear strength of an infilled rock joint is the shear strength of the filler itself is frequently made.

De Toledo et al (1993) tested flat saw-cut and polished surfaces of limestone and basalt in shear boxes using different soils as the infilling material. The results of the ratio of the shear strength of the infilled joint to that of the soil alone are between 0,61 and 0,95, which means that an infilled joint is normally weaker than the soil that constitutes its filler. The magnitude

of the strength reduction seems to be a function of the surface roughness and of the clay minerals present in the soil. Boundary effects have also been found by other authors.

Sun et al. (1981) performed shear box tests on joints in concrete blocks filled with clayey sand and sandy clay with variable normal stresses and filler thicknesses. The failure surfaces occurred either at the top or at the bottom concrete contact or as a combination of both surfaces. Pereira (1990), using mainly sand filling between two flat granite blocks, also reported failure along the solid boundaries due to the rolling of sand grains. Solid boundaries affect the strength of a joint in two ways: In clay fillers, sliding occurs along the contact due to the particle alignment, whereas in sands the rolling of grains seems to be the major factor responsible for the greater weakness of a joint as compared with its filler. The magnitude of the influence of surface roughness depends on the particle size of the soil. In a simple form, when sand as infilling material is considered, the influence of the rock boundary may begin to be felt when its surface is smoother than the roughness of the sand surface defined by its particle size distribution. This is because dilation is reduced.

(c) The influence of filler thickness

Research tests are generally not conducted on natural joints, only on model infill joint material. The influence of filler thickness has been studied by several authors, whose results can be divided into two categories. The first category includes the matching toothed joints that have a ratio filler thickness to asperity height t/a of less than three. The second category comprises planar joints using either saw-cut, sandblasted or polished surfaces, where t/a is usually much greater than three.

Ladanyi & Archambault (1977) performed direct shear tests using kaolin clay between two series of juxtaposed concrete blocks. Different asperity heights and different normal stresses were used. The results obtained seem to confirm the results obtained by Goodman (1970).

(d) Conclusions

The analysis of the results of recent tests on infilled joints by De Toledo et al (1993) has shown that when studying the results in the literature it is important to appreciate not only the mechanical properties of the materials involved (filler or rock) but also the mechanisms involved in the shearing process. The careful consideration of soil mechanics principles, in particular the filler molding conditions, the draining capacity of the boundaries and the shear velocity, are vital to the acquisition of consistent test results. To allow full understanding of the test results, research reports should include a detailed description of the experimental

procedures followed as well as of the filler material. Further, the adequacy of the equipment used is of paramount importance.

The research has also shown that the stress-displacement curve for an infilled joint presents, in principle, two peaks. The first peak is a function of the filler material; the second (usually the higher) is controlled by the rock.

The literature study was conducted before 1993 and information contained in this report is based on publications up to 1993. The only exception is information on the hydraulic roughness by Pegram and Pennington (1996).

2.4 Review of equipment for direct shear testing of large specimens (testing machines).

2.4.1 Norwegian Geotechnical Institute's apparatus.

Barton and Choubey (1977) developed a simple shear apparatus based on tilting a sample together with a joint until the top half slides due to gravity to measure the shear strength parameters of discontinuities. The residual tilt test allows a rock containing a joint surface to tilt until sliding of the upper half relative to the lower half just occurs. The residual tilt test is essentially a shear test under very low normal stress.

2.4.2 US Bureau of Reclamation's (USBR) apparatus.

The equipment developed by the USBR incorporates a controlled strain rate system that permits selection of shear displacement rates. The shear load is generated by two screw jacks developing a total of 60 tons force and having a maximum stroke of 250-mm (10 inches). Speeds from 0,025 mm (0,001 inch) to 6,25 mm (0,25 inch) per minute can be obtained at the full rated load. The shear test equipment provides for a constant initial normal load using a dead-weight system that permits the specimen to dilate or consolidate with little change in the initial normal load. A 350-mm (14-inch) diameter flat jack placed between the shear specimen and the top platen of the reaction frame provides the normal load. Hydraulic oil is supplied to the flat jack by the dead-weight pressure system. Limit switches allow for repositioning of the piston and dead-weight pressure system to accommodate compression or dilation of the specimen maintaining a constant pressure to the flat jack system. The shear box is rigidly constructed of 150 mm (6 inch) by 50 mm (2 inch) steel channels and 6,25 mm (¼ inch) steel plate and has inside dimensions of 600 mm (2 feet) x 600 mm (2 feet) x 300 mm (12 inches). A 12,5 mm (½ inch) gap is left between the top and bottom halves of the

shear box. Since it is often desirable to inundate the shear zone, a water tank is constructed in which the test specimen can be completely submerged.

2.4.3 US Army Corps of Engineers apparatus.

Nicholsen (1983) describes a shear device designed by the US Army Corps of Engineers (USACE) for laboratory testing of rock core specimen from 75 mm (3 inches) to 150 mm (6 inches) in diameter. The shear box is made of two square boxes 75 mm (3 inches) deep and tapered from 212,5 mm (8 ½ inches) at their widest point to 187,5 mm (7 ½ inches) at their base. The tapered housing permits easy extrusion of the specimen after testing. Each box is equipped with reinforced angle iron bars. Shear and reaction loads are transmitted to the shear box by pinned swivel eyebolts. The centre line of the pinholes passes through a plane flush with each shear box. The normal load system consists of a single 60 ton jack driven by a 69 MPa (10000 psi) maximum capacity, manually operated hydraulic pump equipped with a bleed-off valve. A constant normal load is maintained by carefully monitoring the required load and either applying or relieving the hydraulic pressure as needed throughout the test. The shear load system consists of a loading frame, screw jack and a pair of roller bearing platens. The load frame is constructed of 200 mm x 60mm (8 by 2 ¼ inch) steel channels. The inside dimensions of the frame are 300 mm x 600 mm (1-x 2 feet). The frame provides reaction for both shear and normal loads. The shear loads are generated by a screw jack powered by variable speed transmission coupled to a constant velocity electric motor.

2.4.4 Imperial College's apparatus.

Work conducted at the Imperial College, London, led to the development of a simple portable shear box device for laboratory and field use. The device is unique in that the shear box, normal load component and the shear load component were constructed as one unit. The shear box was designed to accept rock specimens of up to 125-mm (5-inch) cube and rock core specimens of up to 100 mm (4 inch) in diameter. Normal and shear loads are applied by 5-ton hydraulic rams. An additional ram could be fitted to the shear box to facilitate the reversal of shear direction for conducting the residual shear test if required. Hydraulic pressures are monitored by Bourdon type pressure gauges, alternatively the shear load could be monitored by a 69 MPa (10 000 psi) pressure transducer and a strain indicator. Both rams are driven independently by hand-operated hydraulic pumps. An adjustable pressure maintainer, incorporated into the normal loading system, allows a constant normal load to be

achieved throughout the duration of the test. A dial gauge is used to monitor the shear displacement.

2.5 Review of shear strength assessment methods.

2.5.1 Introduction.

Barton and Choubey (1977) describe the term rock joints as the mechanical discontinuities of geological origin, that intersect almost all near-surface rock masses. The most important external factor affecting shear strength is the magnitude of the effective normal stress (σ_n) acting across the joint. In many rock engineering problems the maximum effective normal stress will lie in the range 0.1 to 2.0 MPa for those joints considered critical for stability. This is about three orders of magnitude lower than that used by tectonophysicists, when studying the shear strength of laboratory induced faults, under stress levels of for example 100 to 2000 MPa. In consequence, the literature contains shear strength data for rock joints spanning a stress range of at least four orders of magnitude. It is partly for this reason that opinions concerning shear strength vary so widely. It has been customary to fit Coulomb's linear relation

$$\tau = c + \sigma_n \tan \phi$$

to the results of shear strength investigations on rock joints. (τ = shear strength, c = cohesion intercept, ϕ = internal friction angle). If this equation is applied to the results of shear tests on rough joints, under both high normal stress and low normal stress, one finds the tectonophysicist's recording a cohesion intercept of tens of MPa and a friction angle of perhaps only 20°, while the rock slope engineer finds that he has a friction angle of perhaps 70° and zero cohesion. Figure 2.1 is a graph of shear stress vs. normal stress that illustrates peak and residual shear strength. The peak shear strength envelopes for non-planar rock joints are in fact strongly curved. This curved envelope also has the effect that it seems as if there is some cohesion present. This is called the apparent cohesion. (see figure 2.2 where cohesion is indicated with c) This fact has been known for many years, however many engineers still describe shear strength in terms of Coulomb's constants c and ϕ . Both are in fact stress dependent variables. They are also scale dependent.

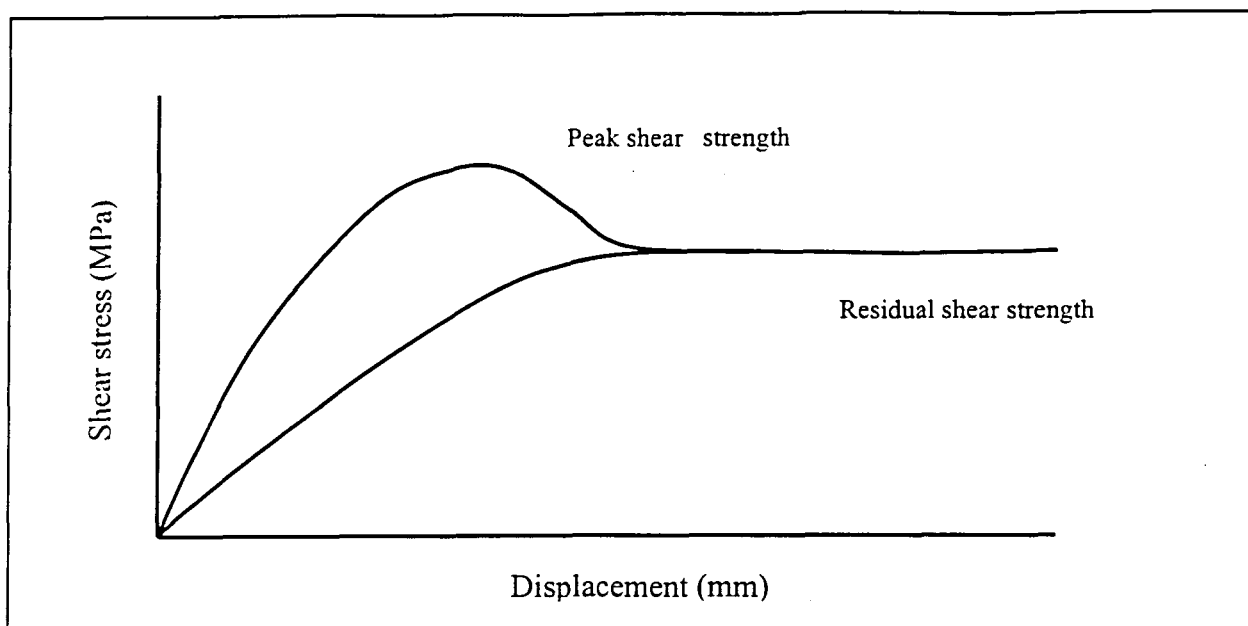


Figure 2.1 Shear stress vs. normal stress illustrating peak and residual shear strength.

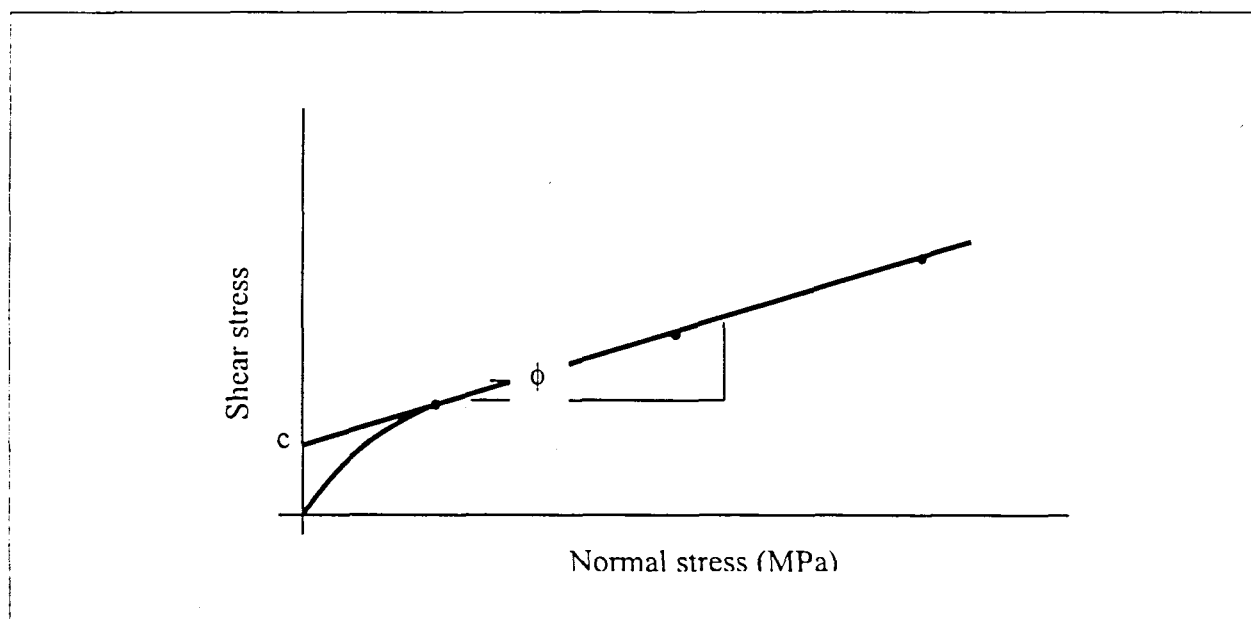


Figure 2.2 Graph of shear stress vs. normal stress.

2.5.2 Measurement of hardness of joint surfaces.

(a) Joint Wall Compressive Strength (JCS)

Barton and Choubey (1977) studied this characteristic and stated that the measurement of this parameter is of fundamental importance in rock engineering since it is largely the wall characteristics that control the strength and deformation properties of the rock joints. Naturally the importance of the parameter is accentuated if the joint walls are weathered, since then the *JCS* value may be only a small fraction of the uniaxial compressive strength of the rock material associated with the majority of the rock mass, as typically sampled by borehole core.

The depth of penetration of weathering into joint walls depends on the rock type, in particular on its permeability. A permeable rock will tend to be weakened throughout, while impermeable rocks will just develop weakened joint walls, leaving relatively unweathered rock in the interior of each block. Barton and Choubey (1977) propose that the weathering process of a rock mass can be summarized in the following simplified stages:

- (i) Formation of joint in intact unweathered rock; *JCS* value same as the uniaxial compressive strength, σ_c
- (ii) Slow reduction of joint wall strength if joints are water-conducting; *JCS* becomes less than σ_c
- (iii) Common intermediate stage; weathered, water conducting joints, impermeable rock blocks between; *JCS* some fraction of σ_c .
- (iv) Penetration of joint weathering effect into rock blocks; progressive reduction of σ_c from the walls of the blocks inwards, *JCS* continues to reduce slowly.
- (v) Advanced stage of weathering; more uniformly reduced σ_c drops to same level as *JCS*; rock mass permeable throughout.

The *JCS* values corresponding to stages (i) and (v) can be obtained by conventional unconfined compression tests on intact cylinders or from point load tests on rock core or irregular lumps, though there might be sampling problems in the case of stage (v). Point load testing has been described in detail by Broch and Franklin (1972). In view of the fact that point load tests can be performed on core discs down to a few centimeters in thickness, it might also be possible to use this test for stage (iv) on the core pieces on each side of deeply weathered joints. However, the *JCS* values relevant to stages (ii) and (iii) cannot be evaluated by these standard rock mechanics tests. The thickness of material controlling shear strength may be as little as a fraction of a millimeter (for planar joints) up to perhaps a few millimeters

(for rough, weathered joints) with the limits depending on the ratio JCS / σ_c which basically controls the amount of asperity damage for a given joint roughness.

(b) Schmidt Hammer Index Test

Barton and Choubey (1977) state that the Schmidt hammer provides the ideal solution to determine JCS. The Schmidt hammer is a simple device for recording the rebound of a spring loaded plunger after its impact with a surface. The L-hammer used here (L for light, impact energy = 0.075 mkg) is described by the manufacturers as being “suitable for testing small and impact-sensitive parts of concrete or artificial stone”. It is suitable for measuring JCS values down to about 20 MPa and up to at least 300 MPa. A wide ranging assessment of the suitability of the Schmidt hammer for use in rock mechanics was done by Miller (1965) as reported by Barton and Choubey (1977). He found a reasonable correlation between the rebound number (range 10 to 60) and the unconfined compressive strength (σ_c) of the rock. However, a better correlation was obtained when he multiplied the rebound number by the dry density of the rock.

$$\text{Log}_{10} (\sigma_c) = 0.00088 \phi R + 1.01$$

where (σ_c) = unconfined compressive strength of surface material (MPa)
 ϕ = dry unit weight of rock (kN/m³), and
 R = rebound number

Example:

$$\begin{aligned}\text{Log}_{10} (\sigma_c) &= 0.00088 \phi R + 1.01 \\ \text{Log}_{10} (\sigma_c) &= 0.00088 * 27 * 48 + 1.01 \\ \sigma_c &= 141 \text{ MPa}\end{aligned}$$

Deere and Miller (1966) investigated the relationship between Schmidt hardness and the uniaxial compressive strength of rock. This relationship is presented by Figure 2.3. Suppose that a vertical downwards held type L-hammer gave a reading of 48 on a rock with a unit weight of 27 kN/m³, the uniaxial compressive strength σ_c is given by the graph as 140 ± 50 MPa. Note that the hammer should always be perpendicular to the rock surface.

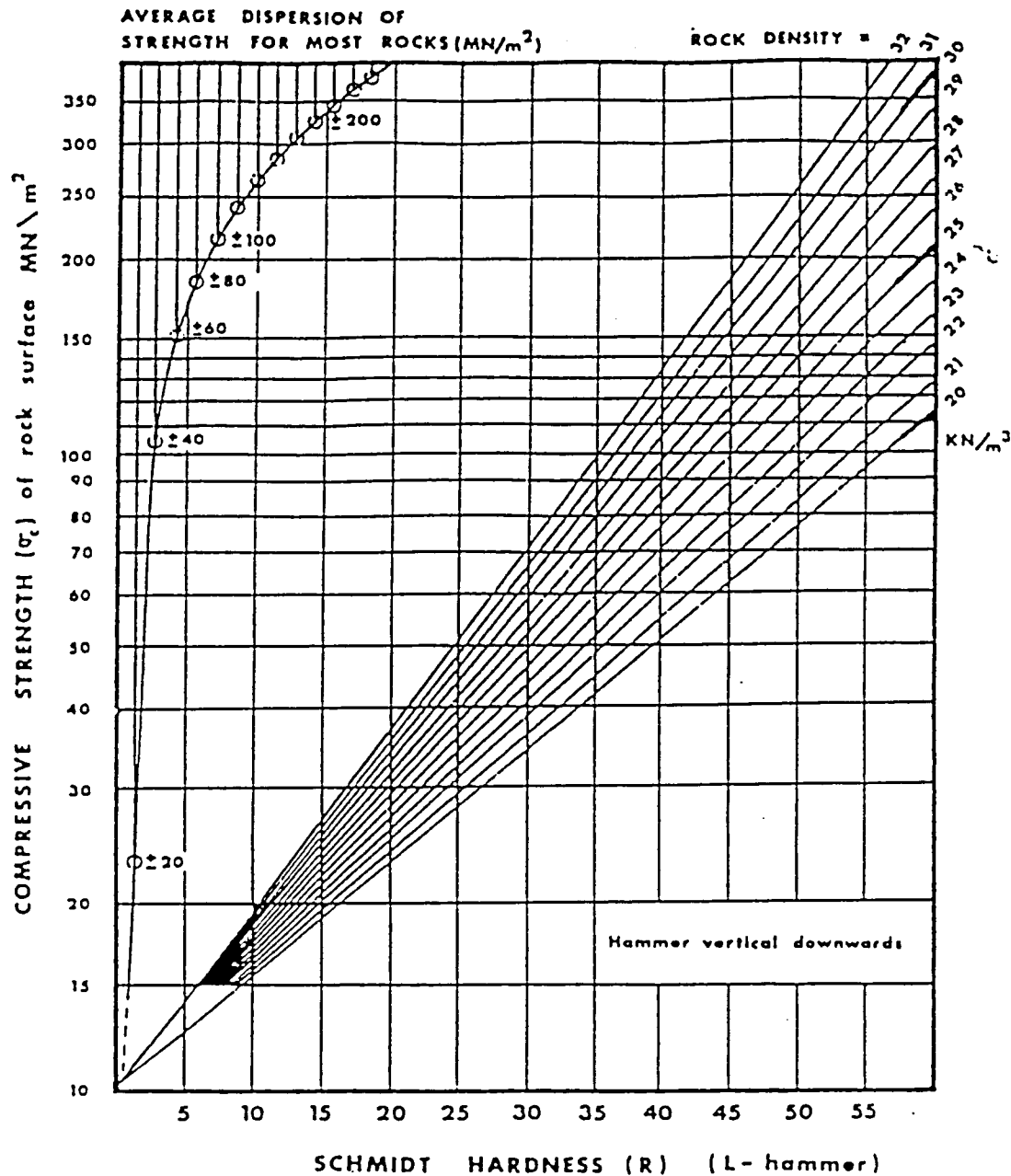


Figure 2.3 The relationship between Schmidt hardness and the uniaxial compressive strength of rock. (After Deere and Miller 1966 as reported by Barton and Choubey, 1977)

(c) Basic Friction Angle (ϕ_b)

A useful list of basic friction angle (ϕ_b) values in Table 2.2 are for the most part based on the basic strength exhibited by flat unweathered rock surfaces, which were most frequently prepared by diamond saw. In some cases these surfaces were sandblasted between tests.

ROCK TYPE	BASIC FRICTION ANGLE(ϕ_b) (Degrees)	REFERENCE
A. Sedimentary Rocks		
Sandstone	26 - 35	Patton, 1966
Sandstone	31 - 33	Krsmanovic, 1967
Sandstone	31 - 34	Coulson, 1972
Siltstone	31 - 33	Coulson, 1972
B. Igneous Rocks		
Basalt	35 - 38	Coulson, 1972
Granite (Fine)	31 - 35	Coulson, 1972
Granite (Coarse)	31 - 35	Coulson, 1972
Porphyry	31	Barton, 1971
Dolerite	36	Richards, 1975
C. Metamorphic Rocks		
Gneiss	26 - 29	Coulson, 1972
Slate	25 - 30	Barton, 1971

Table 2.2 Basic friction angles of various unweathered rocks. (After Barton and Choubey, 1977)

The friction angles obtained are applicable to unweathered joint surfaces, and will not be applicable to weathered rock joints unless the level of effective normal stress applied is high enough for the thin layers of weathered rock to be worn away, thereby allowing contact between the fresher underlying rock (Richards, 1975). Under low levels of effective normal stress the thin layers of weathered material, perhaps less than 1 mm in thickness, may continue to control the shear strength past peak strength and even for displacements up to residual strength. Barton and Choubey (1977) also describe the tilt test as a means to determine the base shear strength of joints. The residual tilt test is basically a shear test under very low normal stress. Most specimens slide at a joint surface tilt angle of about 30° that correspond to a normal stress of approximately of 1 to 5 kPa.

2.5.3 Review of measurement of roughness of joint surfaces.

(a) Joint Roughness Coefficient (JRC)

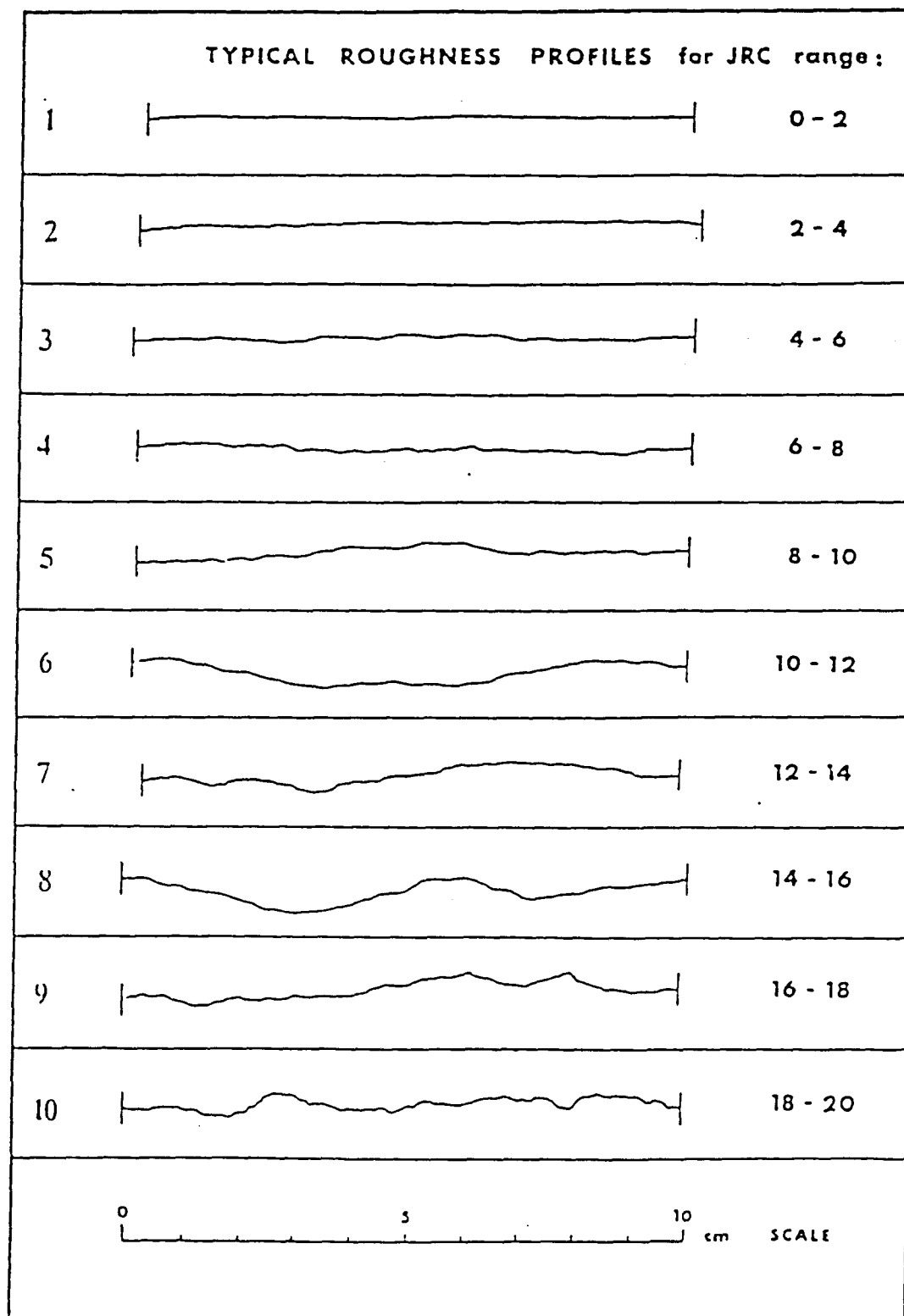
During the preliminary stages of a rock engineering project, it might be possible to establish whether the shear strength of the joints is required for design purposes. If so, closer

investigation is required. A method was developed for estimating the JRC by measuring the roughness. Figure 2.2 and Table 2.3 gives a description of the 10 surfaces. (Barton and Choubey, 1977). The verbal description of roughness, i.e. “undulating” and “planar” refers to small scale and intermediate scale features, in that order.

Sample	Rock type	Description of joint	JRC
1	Slate	smooth, planar: cleavage joints, iron stained	0.4
2	Aplite	smooth, planar: tectonic joints, unweathered	2.8
3	Gneiss (muscovite)	undulating, planar: foliation joints unweathered	5.8
4	Granite rough,	planar: tectonic joints, slightly weathered	6.7
5	Granite rough,	planar: tectonic joints, slightly weathered	9.5
6	Hornfels (nodular)	rough, undulating: bedding joints, calcite coatings	10.8
7	Aplite	rough, undulating: tectonic joints, slightly weathered	12.8
8	Aplite	rough, undulating: relief joints, partly oxidized	14.5
9	Hornfels (nodular)	rough, irregular: bedding joints, calcite coatings	16.7
10	Soapstone	rough, irregular: artificial tension fractures, fresh surfaces	18.7

Table 2.3. Descriptive classification of Rock Joints (After Barton and Choubey, 1977)

The crude estimates of JRC (5, 10 and 20) given by Barton (1971) were proposed as a preliminary guide for those unable to investigate the parameter JRC more closely. In most cases, three profiles were measured on each specimen. The JRC values back calculated from each shear box test were grouped in the following ranges 0-2, 2-4 etc. up to 18-20. An attempt was then made to select the most typical profiles of each group. It should be noted that in all cases where the mean joint plane was not within $\pm 1^\circ$ of horizontal when placed in the shear box, the shear strengths and corresponding JRC values were corrected to the horizontal plane.



(vertical scale = horizontal scale)

Figure 2.4 Typical roughness profiles (After Barton and Choubey, 1977)

(b) Physical roughness measurement by Pegram and Pennington (1996)

Pegram and Pennington (1996) studied the roughness created by a tunnel boring machine (TBM) on a rock surface. The roughness pattern produced is comprised of features on both micro and macro scales. An apparatus was developed that uses a laser distance measuring device to read the physical roughness and store it in digital form. A printout of the roughness can then be made. A set of roughness descriptors was developed from the data obtained. These descriptors are tabulated in table 2.4.

Descriptor	Definition
Wavy	Obvious repetitive grooved pattern with “wavelength” typically 5 - 50 mm
Stippled	Very rough surface with no directional trends in roughness character (unlike wavy)
Rutted	Ruts or grooves typically 3 - 10 mm deep over surface in one or more directions
Uneven	Term to describe non-uniform shotcrete layer thickness, causing slight radius changes
Irregular	Surface has at least one outstanding feature not described by other descriptors
Stepped	Steps in wall profile due to steering adjustment made during TBM operation
Coarse	Surface has coarse grain texture with minimum bump dimension greater than 3 mm
Fine	Converse of coarse. Maximum bump dimension 3mm or less
Chipped	Non-directional, angular surface without sharp crests

Table 2.4 Roughness descriptors by Pegram and Pennington (1996)

2.5.4 Scale effects.

Scale effects are particularly well documented for joint behaviour in shear. Fundamental geometrical scale effects are evident when sampling (i) angles at different scale. These are

evident in the JRC scale effect. Since asperities may fail in shear, the size of asperity that is under stress, may cause an additional compression or tensile scale effect.

Barton (1991) states that discontinuities in rock can exhibit both higher and lower shear strength when size is increased. Large scale undulations may become relevant in slope design which could not be sampled in samples for laboratory testing or in-situ tests. Small steps on a joint surface caused by cross jointing would tend to be avoided in any sampling programme, likewise would intact portions between joints (intact bridges). These phenomena complicate testing and interpretation but are components in shear strength that may not be ignored.

2.5.5 The empirical equation of shear strength.

Barton and Choubey's (1977) empirical relationship on shear strength parameters is unusual in that it can be used both to fit to or to extrapolate experimental data and even to predict it. The three constants involved can be determined so accurately from simple index tests that it has been possible to predict the mean peak shear strength angle $(\arctan \sigma / \sigma_n)^\circ$ for over 100 joint specimens to within $1/2^\circ$. The derivation of the empirical relationship was described by Barton (1977). It is written as follows:

$$\tau = \sigma_n \tan [JRC \log_{10} (JCS/\sigma_n) + \phi_b]$$

where τ = peak shear strength

σ_n = effective normal stress

JRC = joint roughness coefficient

JCS = joint wall compressive strength

ϕ_b = basic friction angle (obtained from residual shear tests on flat unweathered rock surfaces)

2.6 Literature study on the engineering characteristics of southern African rock types.

In South Africa the Department of Water Affairs and Forestry, CSIR, Council for Geoscience, Department of Transport and various geotechnical consultants and researchers have investigated the behaviour of southern African rock materials. Various materials have been tested. Tests are usually conducted using the ISRM suggested methods (Brown, 1981). Results discussed in this chapter were taken from the available literature (mainly Brink,

1983). In many cases the test methods were not stated. The material type, geological setting and reference are set out in table 2.5 Results of this search are also presented below. "Material type" describes the rock type described in the literature, "geological setting" describes the geological formation or site, and the "reference" the author. The following tables contain the engineering characteristics of a number of different rock types. Some of these values are suspicious and should be used with caution in the design of any engineering structure. It must be stressed that the test procedure and the degree of weathering are not always given in the literature.

MATERIAL TYPE	GEOLOGICAL SETTING	REFERENCE
Dolerite ¹	Gariep (Hendrik Verwoerd) Dam	Brink (1983)
Dolerite ²	Pietermaritzburg (Quarry)	Brink (1983)
Sandstone ³	Clarence Formation (Warmbaths)	Brink (1983)
Mudrock ⁴	Beaufort Group	Brink (1983)
Mudrock ⁵	Beaufort Group (Orange-Fish tunnel)	Brink (1983)
Sandstone ⁶	Ecca Group (Ellisras)	Brink (1983)
Sandstone ⁷	Vryheid Formation (Coal fields) - hard	Brink (1983)
Sandstone ⁸	Vryheid Formation (Coal fields) - medium	Brink (1983)
Sandstone ⁹	Vryheid Formation (Coal fields) - soft	Brink (1983)
Siltstone ¹⁰	Vryheid Formation (Facies A)	Ward et al (1985)
Silt/sandstone ¹¹	Vryheid Formation (Facies C)	Ward et al (1985)
Sandstone ¹²	Vryheid Formation (Facies E)	Ward et al (1985)
Sandstone ¹³	Vryheid Formation (Facies G)	Ward et al (1985)
Sandstone ¹⁴	Vryheid Formation (Facies F)	Ward et al (1985)
Sandstone ¹⁵	Estcourt Formation	Brink (1983)
Sandstone ¹⁶	Vryheid Formation	Brink (1883)
Tillite ¹⁷	Dwyka Formation (Goedertrouw Dam)	Brink (1983)
Tillite ¹⁸	Dwyka Formation (Ulundi - tunnel)	Brink (1983)
Tillite ¹⁹	Dwyka Formation - Natal (Webb)	Brink (1983)
Sandstone ²⁰	Natal Group - Mvumase dam site	Geertsema (1986)
Shale ²¹	Natal Group - Mvumase dam site	Geertsema (1986)
Dolomite ²²	Transvaal Supergroup - Mafikeng	Brink (1983)
Quartzite ²³	Turffontein Subgroup - Witwatersrand	Brink (1983)
Quartzite ²⁴	Johannesburg Subgroup - Witwatersrand	Brink (1983)
Granite ²⁵	Archaean granite (Eastern Tvl - Sabie River)	Maschek (1989)
Basalt I ²⁶	Karoo volcanics - Lesotho Highland Scheme	Van Rooy (1991)
Basalt II ²⁷	Karoo volcanics - Lesotho Highland Scheme	Van Rooy (1991)
Basalt III ²⁸	Karoo volcanics - Lesotho Highland Scheme	Van Rooy (1991)
Basalt IV ²⁹	Karoo volcanics - Lesotho Highland Scheme	Van Rooy (1991)
Basalt V ³⁰	Karoo volcanics - Lesotho Highland Scheme	Van Rooy (1991)

Table 2.5 Rock types described in the literature. (The use of superscript ^{1, 2 and 3} in the left-hand column refers to the number of a specific sample)

2.6.1 Strength properties of rock material.

The uniaxial compressive strength of rock materials can be determined directly by means of the direct compressive strength test or indirectly by means of the point load strength index test. (a) Uniaxial compressive strength (UCS)

Rock specimens are prepared and tested in accordance with ISRM (Brown, 1981). The UCS is calculated by dividing the load (N) by the area (m²) and expressed in Pa or multiples.

(i) Uniaxial compressive strength

The uniaxial compressive strength of different rock materials is listed in table 2.6

Rock Type	Degree of weathering	UCS (MPa)			
		Min	Max	Mean	Number
A Sedimentary rock					
Mudrock ⁴	unweathered	33	169	-	-
Mudrock ⁵	unweathered	40	168	-	-
Sandstone ⁶	unweathered	46,6	83,2	69,1	19
Siltstone ¹⁰	unweathered	57	65	61	-
Sandstone ¹²	unweathered	74	108	86	-
Sandstone ¹³	unweathered	68	114	92	-
Sandstone ¹⁴	unweathered	59	110	90	-
Sandstone ¹⁵	unweathered	57	271	116	20
Sandstone ¹⁶	unweathered	8,6	44,7	27	17
Tillite ¹⁷	unweathered	122	298	225	-
Tillite ¹⁸	unweathered	142	194	180	4
Tillite ¹⁹	moderately	22	62	47	4
Sandstone ²⁰	unweathered	144	323	212	51
Shale ²¹	unweathered	76	83	79	4
Dolomite ²²	unweathered	51	256	181	6
B Igneous rock					
Dolerite ¹	unweathered	133	551	388	82
Dolerite ²	unweathered	269	368	336	9
Granite ²⁵	unweathered	44	200	137	30
Basalt I ²⁶	unweathered			180	31
Basalt II ²⁷	unweathered			162	831
Basalt III ²⁸	unweathered			157	408
Basalt IV ²⁹	unweathered			166	375
Basalt V ³⁰	unweathered			146	343
C Metamorphic rock					
Quartzite ²³	unweathered	-	-	284	12
Quartzite ²⁴	unweathered	-	-	237	10

Table 2.6 Uniaxial compressive strength of selected southern African rock types. (The use of superscript ^{1, 2 and 3} in the left-hand column refers to the number of a specific sample)

(ii) Point load strength index

The point load strength index can be determined by testing a rock specimen with a portable point load testing apparatus as described by Broch and Franklin (1972). The PLSI (I_s) is calculated by dividing the load (kN.) by the diameter (m) square and corrected to $I_{s(50)}$. This $I_{s(50)}$ value can be converted to UCS (Broch and Franklin, 1972). The point load strengths of rock materials are listed in table 2.7. Note that the orientation of fabric is not given. This has an influence on the strength.

Rock Type	Degree of weathering	PLSI			
		Min	Max	Mean	n
A Sedimentary rock					
Sandstone ⁶	unweathered	0,1	7,2	2,9	20
Sandstone ¹²	unweathered	1,4	2,3	2,0	
Sandstone ¹³	unweathered	1,6	2,4	2,1	
Sandstone ¹⁴	unweathered	1,6	2,5	2,2	
Tillite ¹⁸	unweathered	0,5	9,8	5,5	25
Tillite ¹⁸	moderately	0,5	3,1	1,1	32
Sandstone ²⁰	unweathered	0,8	19,3	7,75	638
Shale ²¹	unweathered	0,56	2,45	1,45	5
B Igneous rock					
Basalt I ²⁶	unweathered			7,81	41
Basalt I ²⁷	unweathered			6,92	813
Basalt III ²⁸	unweathered			7,02	394
Basalt IV ²⁹	unweathered			7,12	384
Basalt V ³⁰	unweathered			6,25	341

Table 2.7 Point load strengths of selected southern African rock types. (The use of superscript ¹, ² and ³ in the left-hand column refers to the number of a specific sample)

(b) Triaxial compressive strength

The triaxial compressive strength of rock material is usually determined on NX-size core in a triaxial (Hoek) cell in accordance with the ISRM suggested test method (Brown, 1981). The cohesion (c, MPa) and the internal angle of friction (ϕ) are graphically determined with Mohr circles. The triaxial compressive strengths of rock materials are listed in table 2.8

Rock Type	Degree of weathering	Triaxial strength parameters			
			Min	Max	Mean n
Sandstone ²⁰	unweathered	(ϕ)	20	55	45 20
		(c,MPa)	13	75	42 20
Shale ²¹	unweathered	(ϕ)	45,6	47,6	46,6 5
		(c,MPa)	9,7	16,9	13,3 5

Table 2.8 Triaxial compressive strengths of selected southern African rock types.

(c) Tensile strength

(i) Direct tensile strength

Direct tensile strength tests are performed on core specimens of less than NX-size. Metal caps are cemented to the specimen and a tensile load is applied (Brown, 1981). The tensile strength is calculated by dividing the maximum load by the original cross-sectional area and expressed in MPa. The direct tensile strengths of rock materials are listed in table 2.9

Rock Type	Degree of weathering	Direct tensile strength (MPa)			
		Min	Max	Mean	n
A Sedimentary rock					
Sandstone ¹⁰	unweathered	0,66	0,80	0,73	-
Sandstone ¹²	unweathered	0,91	1,31	1,10	-
Sandstone ¹³	unweathered	3,42	3,89	3,69	-
Sandstone ¹⁴	unweathered	2,46	3,42	3,10	-
B Igneous rock					
Basalt I ²⁶	unweathered			12	5
Basalt II ²⁷	unweathered			9,91	25
Basalt III ²⁸	unweathered			12,07	12
Basalt IV ²⁹	unweathered			13,89	15
Basalt V ³⁰	unweathered			11,71	17

Table 2.9 Direct tensile strengths of selected southern African rock types.

(ii) Indirect tensile strength (Brazilian method)

This test is intended to measure the uniaxial tensile strength of rock material. The principle of the test is based on the experimental fact that most rocks in uniaxial stress fields fail in tension (Brown, 1981). A Brazilian test apparatus is required to conduct the test. A cylindrical specimen is loaded in a diametrical direction until it fails. The indirect tensile strengths of rock materials are listed in table 2.10

Rock Type	Degree of weathering	Indirect tensile strength (MPa)			
		Min	Max	Mean	n
B Igneous rock					
Dolerite ¹	unweathered	9,5	46,3	30,5	81
Dolerite ²	unweathered	34,9	38,5	37,6	6

Table 2.10 Indirect tensile strengths of selected southern African rock types.

(d) Shear strength

The shear strength of rock material can be determined in a number of ways all based on the Suggested Methods for Determining Shear Strength of the ISRM (1974). All these tests are designed for laboratory application.

(i) Basic shear strength

This test measures the basic shear strength as a function of stress normal to the shear plane. The shear plane coincides with a plane created in the rock, in this case a saw cut plane. Determination of the shear strength comprises of three (or more) specimens of the same geological horizon with each specimen tested at a different but constant normal stress. The test apparatus and procedure is suggested by ISRM (1974). Normal stress, ϕ_n is plotted against shear stress, σ . The shear strength parameters ϕ (angle of friction) and c (cohesion) can be read off the graph. The base shear strengths of rock materials are listed in table 2.11. Note that cohesion is high - for base shear strength it should be zero.

Rock Type	Degree of weathering	Direct shear strength (basic)				
		Min	Max	Mean	n	
A Sedimentary rock Sandstone ²⁰	unweathered	(ϕ)	25,6	45,9	35,8	20
		(c,kPa)	80	150	119	20
Shale ²¹	unweathered	(ϕ)	35,0	41,2	36,6	5
		(c,kPa)	30	215	142	5
Tillite ¹⁹	unweathered	(ϕ)	-	-	53	1
		(c,kPa)	-	-	30	1
Tillite ¹⁹	moderately	(ϕ)	-	-	51	1
		(c,kPa)	-	-	8	1

Table 2.11 Basic shear strengths of selected southern African rock types. (The use of superscript ^{1, 2 and 3} in the left-hand column refers to the numbers of specific samples)

(ii) Direct shear strength of joints

The direct shear strength of joints is determined as in (i) but the shear plane is an open joint. Peak and residual shear strength can be determined in this manner (Brown, 1981).

No results of direct shear strength of rock joints could be found.

(iii) Punch shear strength

The punch shear strength of intact rock material is determined with the punch shear apparatus. The punch shear strength (SHI) in MPa can be calculated with the formula:

$$SHI = F / \pi a t$$

Where F = load at failure (N), t = average thickness of specimen (mm), and a = diameter of punch (mm). This applies to the round punch. The punch shear strength of sandstone is given in table 2.12

Rock Type	Degree of weathering	Punch shear (MPa)			
		Min	Max	Mean	n
A Sedimentary rock Sandstone ²⁰	unweathered	29,1	43,4	34,8	36

Table 2.12 Punch shear strength of a southern African sandstone. (The use of superscript ^{1, 2 and 3} in the left-hand column refers to the numbers of specific samples)

2.6.2 Deformation properties of rock material.

(a) E-modulus (Young's modulus)

This test is intended to determine stress-strain curves, Young's moduli and Poisson's ratio in uniaxial compression of a rock specimen of regular geometry. Electrical resistance strain gauges are used to measure both axial and circumferential deformation. Axial strain ϵ^a is plotted against axial stress σ and the different E-moduli determined from the slope of the graph. $E = d\sigma/d\epsilon^a$. The E-modulus can be determined at different points on the axial stress (σ) vs axial strain (ϵ^a) curve. The following methods of E-modulus determination have been described by Brown (1981):

(i) Tangent Young's modulus (E_t), is measured at a stress level which is usually some fixed percentage of the ultimate strength.

(ii) Average Young's modulus (E_{av}), is determined from the more or less straight line portion of the axial stress-axial strain curve.

(iii) Secant Young's modulus (E_{sc}), is usually measured from zero stress to some fixed percentage of the ultimate strength, generally 50%.

The E-moduli of rock materials are listed in table 2.13

Rock Type	Degree of weathering	E-modulus (GPa)			
		Min	Max	Mean	n
A Sedimentary rock					
Sandstone ⁶	unweathered	E _{sec} 19,6	49,7	36,1	19
Sandstone ¹⁵	unweathered	E ₅₀ 5,9	13,4	9,9	9
Sandstone ¹⁶	unweathered	E _t 0,6	11,3	2,4	17
Tillite ¹⁸	unweathered	E _t 39	70,0	54,0	4
Tillite ¹⁸	moderately	E _t 13,5	15,4	14,8	4
Sandstone ²⁰	unweathered	E ₅₀ 46,4	70,4	61,8	20
Shale ²¹	unweathered	E ₅₀ 3,7	7,5	5,4	4
B Igneous rock					
Basalt I ²⁶	unweathered			46,9	8
Basalt II ²⁷	unweathered			38,2	20
Basalt III ²⁸	unweathered			32,3	16
Basalt IV ²⁹	unweathered			47,2	8
Basalt V ³⁰	unweathered			49,5	16

Table 2.13 E-moduli of selected southern African rock types. (The use of superscript ^{1, 2 and 3} in the left-hand column refers to the numbers of specific samples)

(b) Poisson's ratio

Poisson's ratio, ν , may be calculated from the equation: ν = slope of axial stress-strain curve/slope of diametric stress-strain curve. The Poisson's ratios of rock materials are listed in table 2.14. Note that the value of the sandstone is on the low side.

Rock Type	Degree of weathering	Poisson's ratio			
		Min	Max	Mean	n
A Sedimentary rock					
Sandstone ⁶	unweathered	0,11	0,21	0,16	19
Sandstone ¹⁵	unweathered	0,06	0,28	0,14	9
Tillite ¹⁸	unweathered	0,22	0,33	0,27	4
Tillite ¹⁸	moderately	0,29	0,31	0,30	4
Sandstone ²⁰	unweathered	0,171	0,238	0,212	20
Shale ²¹	unweathered	0,246	0,371	0,298	4
B Igneous rock					
Basalt I ²⁶	unweathered			0,25	2
Basalt II ²⁷	unweathered			0,23	11
Basalt III ²⁸	unweathered			0,28	10
Basalt IV ²⁹	unweathered			0,23	7
Basalt V ³⁰	unweathered			0,23	16

Table 2.14 Poisson's ratios of selected southern African rock types. (The use of superscript ^{1, 2 and 3} in the left-hand column refers to the numbers of a specific sample)

2.6.3 Other engineering rock properties.

(a) Hardness (Schmidt hammer)

The ISRM suggested method (Brown, 1981) for determination of the Schmidt rebound hardness is used. The Schmidt hammer hardness of rock materials is listed in table 2.15.

Rock Type	Degree of weathering	Schmidt hammer hardness	
		Mean	n
B Igneous rock			
Basalt I ²⁶	unweathered	44,48	3
Basalt II ²⁷	unweathered	39,17	5
Basalt III ²⁸	unweathered	36,26	4
Basalt IV ²⁹	unweathered	41,46	13
Basalt V ³⁰	unweathered	37,55	5

Table 2.15 Schmidt hammer hardness of selected southern African rocks. (The use of superscript ^{1, 2 and 3} in the left-hand column refers to the numbers of specific samples)

(b) Abrasiveness

The method for determination of the resistance to abrasion of aggregate by use of the Los Angeles machine (ISRM, (c) 1977) is used. The abrasiveness of rock materials is listed in table 2.16.

Rock Type	Degree of weathering	Abrasiveness (% , Los Angeles)			
		Min	Max	Mean	n
A Sedimentary rock Sandstone ²⁰	unweathered	18,3	32,9	23,1	22
B Igneous rock Dolerite ¹	unweathered	-	-	0	1

Table 2.16 Abrasiveness of selected southern African rocks. (The use of superscript ^{1, 2 and 3} in the left-hand column refers to the numbers of specific samples)

(c) Seismic wave velocity

The suggested method for determination of the Sound Velocity (Brown, 1981) is used. The seismic wave velocities of rock materials are listed in table 2.17.

Rock Type	Degree of weathering	Seismic wave velocity (m/s)			
		Min	Max	Mean	n
A Sedimentary rock					
Tillite ¹⁷	unweathered	4960	5512	-	-
Tillite ¹⁷	slightly	3858	4960	-	-
Tillite ¹⁷	moderately	1654	3858	-	-
Tillite ¹⁷	highly	551	1654	-	-
Sandstone ²⁰	unweathered	3745	4837	4360	12

Table 2.17 Seismic wave velocities of selected southern African rocks. (The use of superscript ^{1, 2 and 3} in the left-hand column refers to the numbers of specific samples)

(d) Water absorption

The suggested method for determination of the water absorption of a rock sample (ASTM C64) is used. The water absorption indices of rock materials are listed in table 2.18.

Rock Type	Degree of weathering	Water absorption by weight (%)			
		Min	Max	Mean	n
A Sedimentary rock					
Sandstone ²⁰	unweathered	0,55	1,35	0,92	40
B Igneous rock					
Basalt I ²⁶	unweathered	0,09	1,49	0,91	14
Basalt II ²⁷	unweathered	0,66	4,41	3,08	16
Basalt III ²⁸	unweathered	1,35	6,50	2,93	8
Basalt IV ²⁹	unweathered	1,39	8,06	3,79	35
Basalt V ³⁰	unweathered	2,99	7,29	4,53	11

Table 2.18 Water absorption indices of selected southern African rocks. (The use of superscript ^{1, 2 and 3} in the left-hand column refers to the numbers of specific samples)

(e) Porosity

The suggested method for porosity/density determination (Brown, 1981) is used. The porosities of rock materials are listed in table 2.19.

Rock Type	Degree of weathering	Porosity (%)			
		Min	Max	Mean	n
A Sedimentary rock					
Sandstone ³	unweathered	0,77	4,68	1,99	12
Tillite ¹⁹	unweathered	0,21	0,76	0,42	3
Sandstone ²⁰	unweathered	0,92	2,85	2,62	12
Shale ²¹	unweathered	0,07	2,94	1,42	3

Table 2.19 Porosity of selected southern African rocks. (The use of superscript ^{1, 2 and 3} in the left-hand column refers to the numbers of specific samples)

(f) Density

The suggested method for porosity/density determination (Brown, 1981) is used. The densities of rock materials are listed in table 2.20.

Rock Type	Degree of weathering	Density (kg/m ³)			
		Min	Max	Mean	n
A Sedimentary rock					
Sandstone ³	unweathered	1910	2120	-	-
Sandstone ⁶	unweathered	2332	2452	2394	19
Sandstone ⁷	unweathered	1990	2340	2190	25
Sandstone ⁸	unweathered	1910	2340	2150	21
Sandstone ⁹	unweathered	1850	2250	2100	14
Sandstone ¹⁵	unweathered	2350	2660	2473	3
Sandstone ¹⁶	unweathered	2356	2493	2421	17
Tillite ¹⁷	unweathered	2560	2650	2610	40
Tillite ¹⁹	unweathered	2508	2690	2647	-
Sandstone ²⁰	unweathered	2508	2690	2647	-
Shale ²¹	unweathered	2550	2750	2659	10
Dolomite ²²	unweathered	2710	2880	2820	38
C Metamorphic rock					
Quartzite ²³	unweathered	-	-	2650	-
Quartzite ²⁴	unweathered	-	-	2710	-

Table 2.20 Densities of selected southern African rocks. (The use of superscript ^{1, 2 and 3} in the left-hand column refers to the numbers of specific samples)

(g) Swelling (Free swell)

The suggested method for determination of the swelling strain developed in an unconfined rock specimen (Brown, 1981) is used. The free swelling properties of rock materials are listed in table 2.21

Rock Type	Degree of weathering	Swelling properties (%)			
		Min	Max	Mean	n
A Sedimentary rock Tillite ¹⁷	unweathered	0,003	2,39	0,85	-

Table 2.21 Free swelling properties of selected southern African rocks. (The use of superscript ^{1, 2 and 3} in the left-hand column refers to the numbers of specific samples)

(h) Slake durability

The suggested method for determination of the slake-durability index (ISRM, 1977) is used. The slake durability of rock materials are listed in table 2.22.

Rock Type	Degree of weathering	Slake durability (%) (7cycles)			
		Min	Max	Mean	n
A Sedimentary rock Tillite ¹⁷	unweathered	-	-	99,54	-
Tillite ¹⁷	slightly	-	-	99,02	-
Tillite ¹⁷	moderately	-	-	95,24	-
Tillite ¹⁷	highly	-	-	57,5	-
Sandstone ²⁰	unweathered	-	-	99,3	-

Table 2.22 Slake durability of selected southern African rocks. (The use of superscript ^{1, 2 and 3} in the left-hand column refers to the numbers of specific samples)

2.6.4 Petrographic description of rocks.

The suggested (ISRM) method for petrographic description of rocks (ISRM, 1977) is used. No results of petrographic descriptions relevant to the materials investigated were found in the available literature.

CHAPTER THREE

DETERMINATION OF ENGINEERING CHARACTERISTICS DURING THIS STUDY: METHODS AND EQUIPMENT

3.1 Introduction.

This chapter describes the methods and equipment used to determine the engineering characteristics of selected southern African rock types. Special emphasis is placed on the shear strength of joints of small NX-size core samples as well as large block samples. A laser apparatus for the determination of the joint surface roughness of the large specimens is also described.

3.2 Strength properties of rock material.

3.2.1 Uniaxial compressive strength (UCS).

Uniaxial compressive strength testing was carried out on a number of rock specimens taken from NX-size (54,5 mm diameter) borehole cores. The specimens were prepared and tested in accordance with the ISRM suggested methods (Brown, 1981). Testing was done in the rock mechanics laboratory of the Technikon Pretoria.

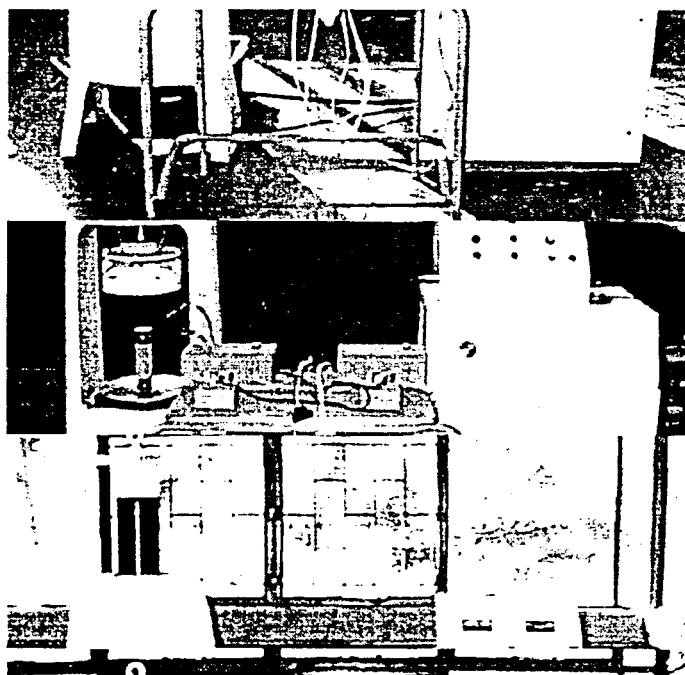


Figure 3.1 Farnell test press used for testing of rock specimens.

The apparatus used was a Farnell concrete cube press, illustrated in Figure 3.1, capable of producing a force of 2000 kN.

A more convenient field test that is normally used on site to determine rock strength is the point load test. The point load test apparatus is a portable hydraulic press illustrated in Figure 3.2 that can test a NX-size (or any other size) specimen in point load compression.

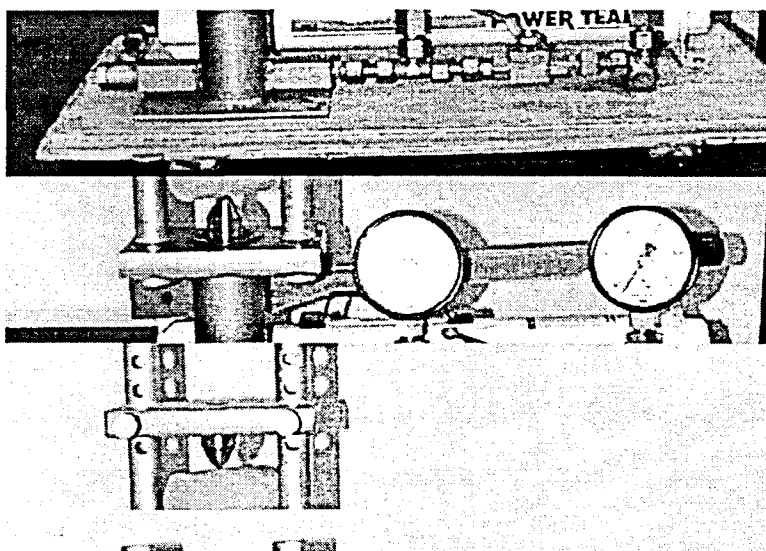


Figure 3.2 Point load test apparatus

The specimens were prepared and tested in accordance with the relevant ISRM suggested methods (Brown, 1981). Testing was done in the Rock mechanics laboratory of the Technikon Pretoria.

3.2.2 Triaxial compressive strength.

Triaxial compressive strength testing was carried out on a number of rock specimens taken from NX-size (54,5 mm diameter) borehole cores. The specimens were prepared and 5 specimens tested in-groups of three in accordance with the relevant ISRM suggested methods (Brown, 1981) in a triaxial (Hoek) cell illustrated in Figure 3.3. The same test press was used as for UCS testing. Testing was done in the rock mechanics laboratory of the Technikon Pretoria.

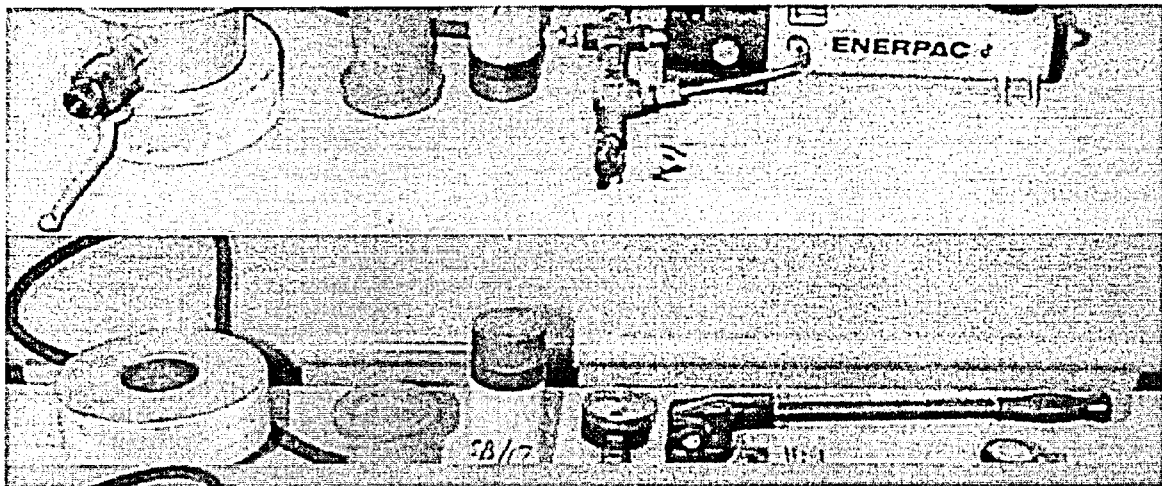


Figure 3.3 The triaxial cell or Hoek cell used to determine the triaxial strength of intact rock specimens.

3.2.3 Tensile strength (Indirect tensile strength - Brazilian method)

Tensile strength testing was carried out on a number of rock specimens taken from NX-size (54,5 mm diameter) borehole cores. The specimens were prepared and tested in accordance with the relevant ISRM suggested methods (Brown, 1981) in the Brazilian apparatus illustrated in Figure 3.4. Testing was done in the rock mechanics laboratory of the Technikon Pretoria.

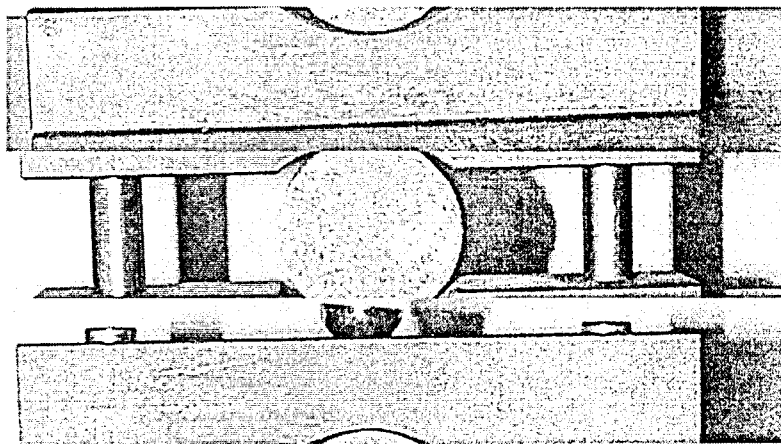


Figure 3.4 Brazilian tensile test apparatus

3.2.4 Shear strength.

Two types of shear tests were conducted. These were on samples with (i) saw cut surfaces and (ii) natural joint surfaces.

3.2.4.1 The small shearbox.

Base shear strength and shear strength of joints (Peak and Residual)

A Soiltech soil shearbox was modified for this purpose. The original sample box was removed and replaced by a clamp mechanism to accommodate the NX size rock core samples. The bottom sample holder is vertically fixed to the frame of the apparatus while the upper sample holder can move along the line of shear. The normal load is applied through a yoke and hanger system where the normal load is increased by adding additional weights. The shear load is applied by a motorized worm drive acting on a load cell transferring the load to the upper sample holder assembly. Vertical dilation and horizontal movement are measured by means of linear variable displacement transducers (LVDT's). The shear process is computer controlled and data retrieval is done through a data acquisition unit connected to the PC. See figure 3.5 for the laboratory setup.

Three loading cycles were carried out on each sample. Normal stresses of 55 kPa, 105 kPa and 1,55 MPa were applied and the corresponding shear loads were measured.

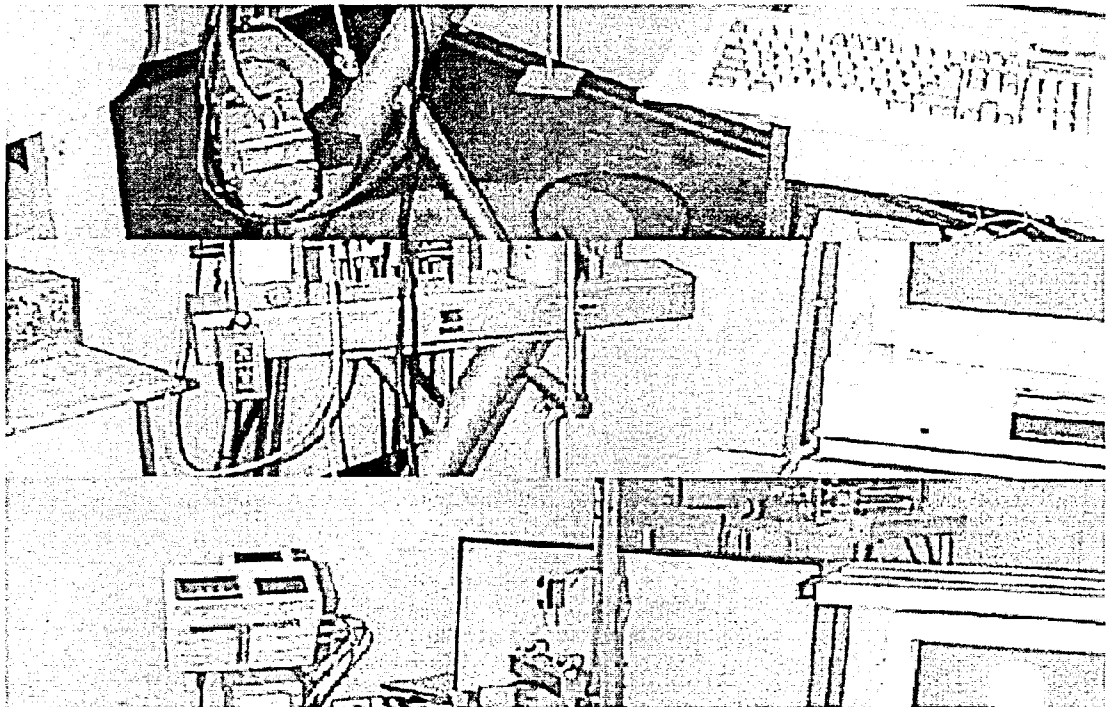


Figure 3.5 The modified soil shearbox for shear testing of NX-size rock core samples.

The maximum travel was 10 mm. After each cycle the upper sample holder containing the sample was returned to its original position before applying the next higher load. The measurements are illustrated in graphic form as shear load vs shear displacement and shear stress vs normal stress.

3.2.4.2 Large shear box of the Department of Water Affairs and Forestry

(a) The apparatus

The machine was designed and built in such a way, that specimens of rock or soil of a maximum size of 350 x 350 mm can be tested under normal loads of up to 200 kN and shear loads of up to 500 kN - illustrated in Figure 3.6

The machine consists essentially of an arrangement to accommodate the specimen to be tested, a mechanism to apply different constant vertical loads on the specimen and a mechanism to apply shear loads, in a direction perpendicular to the normal load.

A line drawing of the machine is presented in Figure 3.7 (side view) and Figure 3.8 (front view).

Suitable instrumentation to measure and record forces and displacements is also provided.

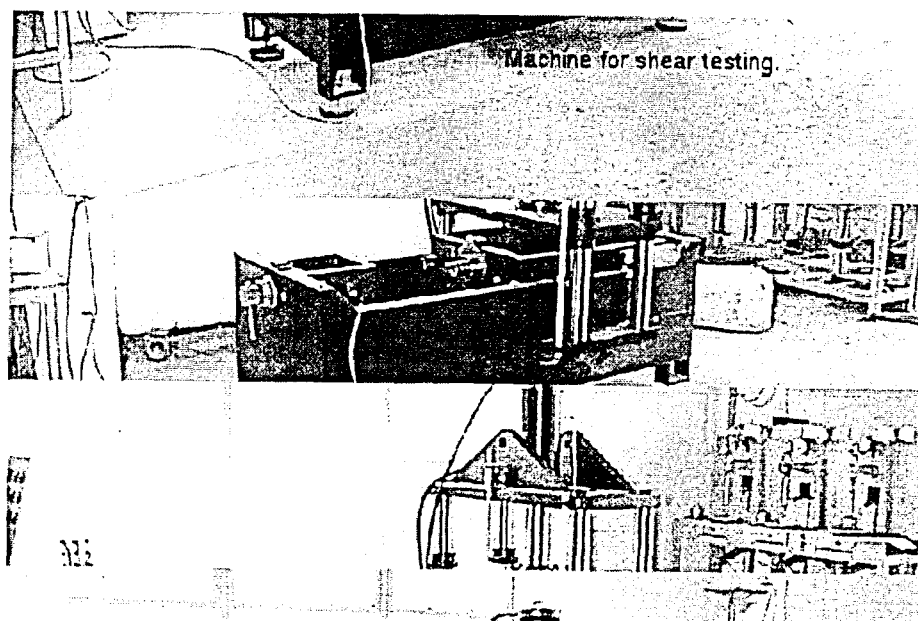


Figure 3.6 The large shear testing machine.

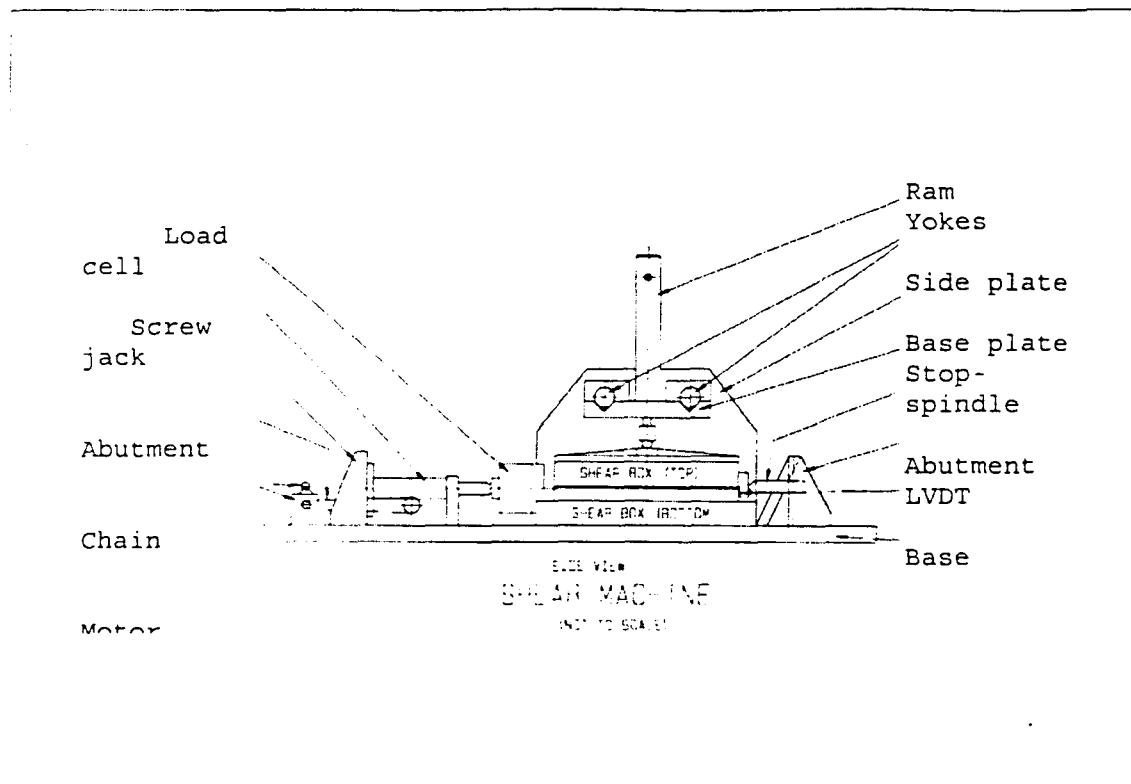


Figure 3.7 Schematic sketch of large shear testing machine (side view)

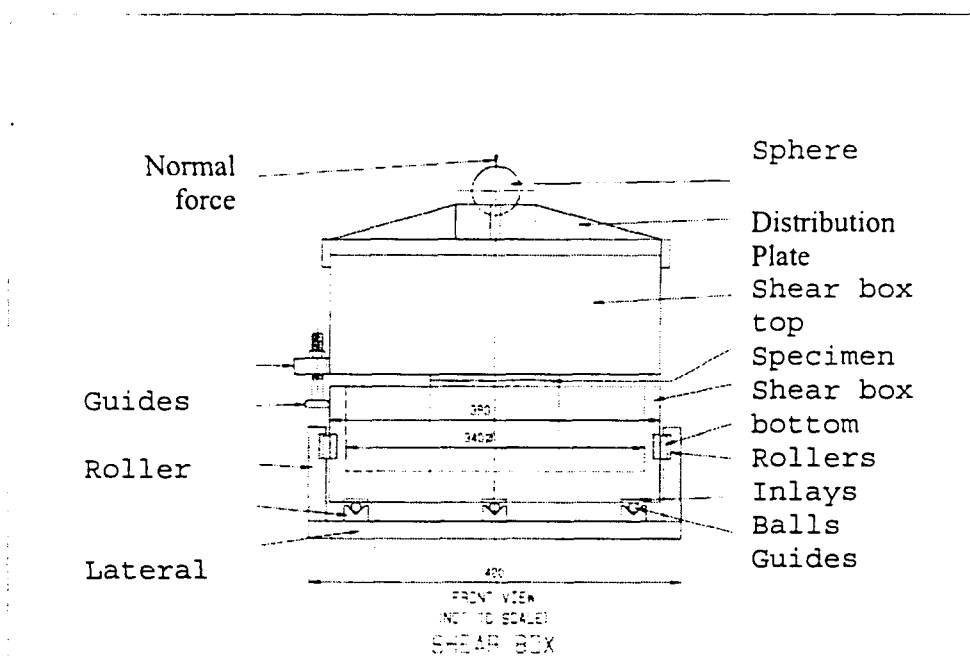


Figure 3.8 Schematic sketch of large shear testing machine (front view)

(i) Shear box assembly (specimen accommodation)

The shear box assembly consists of two different parts, a lower half and a top half. The lower half accommodates one half of the specimen and represents the mobile part of the shear box, i.e. shearing takes place underneath the top half, which is kept horizontally stationary. Via a yoke, the bottom part is in direct contact with the mechanism which provides the force necessary for shearing.

Suitable roller-bearings ensure low friction gliding of the lower half over a rigid, machined base plate. The base plate is fitted to a strong frame, to which all other stationary machine components are fitted. The lateral support of the bottom part is provided by needle bearings. The top half accommodates the other half of the specimen and is separated from the bottom part by a gap which is aimed to be 5 mm.

The direction of the shear force is in line with the shear plane. Provision is made for adjusting the gap between the bottom and top parts of the shear box and for adjusting the direction of the shear force to suit the specimen as described above.

To prevent side way-drifting of the top part during testing, side guides are provided, which are in firm touch with the corresponding outside flats of the bottom part.

Provision is made for testing the sample under wet conditions by a water bath. The water bath allows for immersion of the entire test sample in water. The water bath is constructed in such a way as not to interfere with either the transfer of loads onto the specimen or with the measuring of displacements.

Provision is made to protect the lower shear-box assembly from water and moisture when testing specimens under wet conditions.

Both shear box parts are equipped with clamps for temporary immobilization and hooks are provided at suitable positions on both parts to facilitate the handling of the equipment during assembly, testing and dismantling.

Three shear box assemblies were manufactured, having the following inside dimensions:

Box No. 1: 350 x 350 mm Square

Box No. 2: \varnothing 350 mm Round

Box No. 3: \varnothing 150 mm Round

All three boxes have sufficient wall thickness to minimise deformations caused by loads acting on them. Figure 3.9 illustrates the square box.

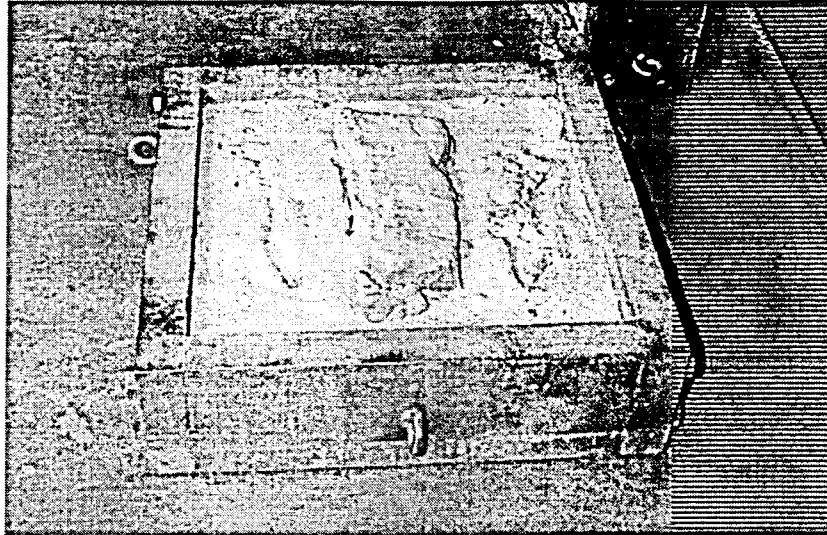


Figure 3.9 Bottom half of shearbox assembly with test specimen

(ii) Load distribution plate

On the top part of the shear box assembly a stiffened load distribution plate is placed. In the geometrical center of the stiffened plate a spherical seating is provided, through which the normal loads are applied evenly.

For each of the square or round boxes, two different load distribution plates were manufactured:

One plate which fits loosely over the outside of the top part and one which fits with enough clearance into the respective square or round cavity of the top part. The clearance of the plates on the sides of the shear box and the method of providing for vertical movement of the plates is sufficient to ensure free unhindered vertical travel of the load plates up to 10 mm.

(iii) Application of normal loads

The normal load is applied on the spherical seating of the load-distribution plate by means of a hydraulic cylinder. The maximum capacity is 200 kN. During the test the mechanism is able to maintain any specified load of up to 200 kN constant, to $\pm 2\%$, regardless of any volume change of the specimen. The apparatus was designed as to not allow tilting of the shear box with the specimen during testing. The reason for this is that no tilting takes place under a dam foundation as a result of confinement.

(iv) Application of shear forces

The shear force is applied in the horizontal direction. The mechanism which generates the force is a hydraulically operated and strain-controlled hydraulic jack. The shear force is applied continuously and does not exceed 500 kN.

The rate of shearing, i.e. the horizontal displacement, measured at the bottom part of the shear box assembly, within a certain period of time, can be pre selected in steps of 0.2 mm/min. from 0.2 mm/min. to 5.0mm/min. The maximum shear displacement is 50 mm.

(v) Data measurement and acquisition

All forces and displacements are measured electronically. The recording of the voltage outputs is recorded continuously. The measurement of the normal and the shear forces are done by means of suitable load-cells.

A total of five interchangeable load cells with capacities of 50, 100, 150, 200 and 500 kN can be used. Suitable mountings for the load cells are provided. The combined error for linearity and hysteresis of each load cell is less than 0,10 % of the RO (rated output mV/V \pm 0,1 %).

The measurement of the relative horizontal movement between the two halves of the shear box assembly (shear displacement) is measured by two LVDT's (linear variable differential transducers), with a stroke of 50 mm and a linearity of better than 0,25 % RO. The LVDT's are positioned at the upper left and right hand corners of the bottom part of the shear box assembly. The electrical wiring of the LVDT's is done in such a way, that their combined output represents the average displacement. The mountings (clamps) for the bodies of the LVDT's are rigid, and shock resistant. The contact points for the spring-return armatures are smoothened.

The vertical displacement (dilation) is measured by two LVDT's with a stroke of 20 mm and a linearity of better than 0,25 % RO. The two LVDT's are positioned in the middle and at opposite ends of the load distribution plate.

(b) Testing method for large shearbox

(i) Sampling procedure

Sampling of rock specimens with associated joint surfaces is a difficult procedure because a joint surface is a delicate surface that must be preserved in its original state for testing.

The size of the final sample is determined by the size of the shearbox assembly. Two boxes were used with the following dimensions: 350 x 350 mm square and 350 mm diameter.

Samples were carefully selected in a rock mass on site and the surrounding rock material removed. Samples were taken out by hand with the use of a hand spike “koevoet” and “Hilti” drill. Then the two rock material pieces with associated joint surface were carefully wedged out and placed on the floor and carefully packaged to be transported to the laboratory. Extra rock samples were taken as to have more samples than were actually needed for testing as sometimes samples get damaged during transportation and casting.

(ii) Sample preparation.

In the laboratory a suitable sample was selected and tied up with wire with the joint surfaces in their original relative position. Figure 3.10 illustrates this principle.

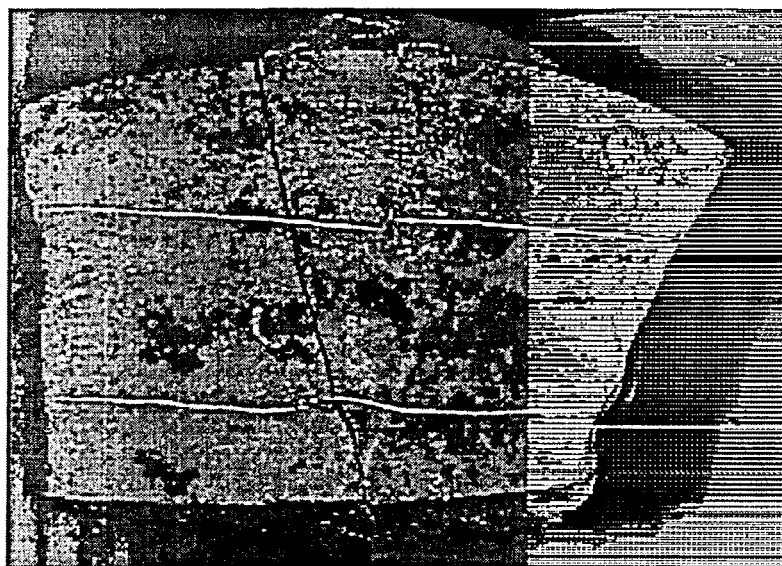


Figure 3.10 Rock sample with associated joint surface tied, up with wire ready to be cast.

The sample is then placed into the top box (upside down position) and the joint surface orientated parallel to the shear plane. It is positioned such that the shear surface is approximately 10 mm above the top of the shearbox rim. A casting agent (cement grout) is then prepared and cast into the top half of the box with the sample in position. The agent is poured into the box to about 20 mm below the rim of the box. The casting agent is made up of the following ingredients: 20 kg building sand, 5,25 kg cement, 2,25 kg slagment, 10 ml plastisizer, and $\pm 3,9$ liters water. The casting agent is then left for two days to set. Figure 3.7 illustrates a rock sample with joint cast in the shear box.

The bottom part of the box is then bolted onto a special jig to keep it in position and filled with casting agent to about 40 mm below of the rim of the box. The top part of the box with

the sample in place can now be turned around and gently lowered onto the bottom part until the joint surface is about 10 mm above the rim of the bottom part. Now it can be bolted to the jig and left for two days to set. When completely set, the wire holding the sample together can be cut and the moulds removed from the jig and moved to the testing machine.

(iii) Testing procedure

The prepared sample in the shear box assembly is placed into the shear box machine. The whole testing operation is computer controlled as described below. The software runs on an IBM AT or compatible machine, which has MS-DOS version 3.3 or later, installed. The PC has a VGA colour monitor. The software runs from a fixed disk drive no smaller than 80 Mega bytes.

The software supports a variety of shear testing procedures as well as keeping record of all the results. Mounted inside the PC is an ADC/DAC card, which interfaces the software to the testing machine. This interface enables the software to read the load signals and controls the speed of the drive motor. When the software is loaded, the first menu is activated on the screen. Selecting the options on the screen and entering the required information carries out the test by keyboard.

The normal load is now applied for at least 20 seconds before the shear load is activated. Normal stresses of 0.6, 0.9 and 1.2 MPa were decided upon and depending on the area of the sample to be tested, the corresponding loads were calculated and fed into the programme. The mass of the top half including the plate for transferring the load to the sample was determined and included in the calculation of the normal load. Shear load is applied at a rate of 2 mm per minute.

The data acquisition unit captures data every two seconds. These data consist of normal load by means of a pressure transducer, vertical movement by means of two vertical LVDT's, horizontal movement by means of two horizontal LVDT's and shear load by means of a load cell. The test was terminated when the horizontal movement reached a maximum of approximately 20-mm.

A test cycle was conducted for each normal load and the corresponding shear load obtained. Thereafter graphs of shear stress vs. normal stress were plotted and values for the angle of friction and cohesion were calculated.

Tests were carried out on basalt, dolerite, granite, sandstone and shale samples. Samples were tested a first time through three cycles dry, and then photographed (Appendix F). After thorough interpretation of the results it was decided to run another three cycles of testing dry

and then three cycles wet. (Submerged under atmospheric conditions). After the completion of a the “dry” tests the same samples were saturated and “wet” tests were done to compare the results and to get a “dry - wet” relationship.

(c) Evaluation of the large shear apparatus

The large shear apparatus is the only shear test apparatus of its kind in southern Africa. The **advantages** of the machine are that it can be used to determine the shear strength parameters of relative large rock specimens. The expertise has now also been developed to prepare samples, execute the test procedure and interpret the results. The machine could also be used to determine the shear strength parameters of other materials such as gravel's or even simulate rock fill materials.

The **disadvantages** of the machine is that it is difficult to take specimens from the site to test in the machine as a great effort is needed to ensure that a specimen is taken with both joint surfaces intact. Great care should be taken with the sampling and transportation process. The preparation and testing process is very time consuming. It is however felt that more representative results are obtained as larger surfaces can be tested.

Further testing on the machine should be carried out, as it is available for researchers in the Gauteng area.

3.2.4.3 Laser scanning device to measure joint surface roughness.

During the course of this investigation a laser-scanning device was developed in conjunction with the Department of Civil Engineering, University of Natal.

(a) The apparatus

The laser is built on a sturdy frame 750 mm long by 500 mm wide, allowing samples up to 600 mm by 350 mm. Figure 3.11 clearly shows the scanner head which moves in a longitudinal direction above the sample.

A laser displacement sensor is attached to this head, which is moved along the guide rails by a stepper motor driving a toothed belt by means of two toothed gear wheels.

The rotational movement of the stepper motor produces an incremental movement of the

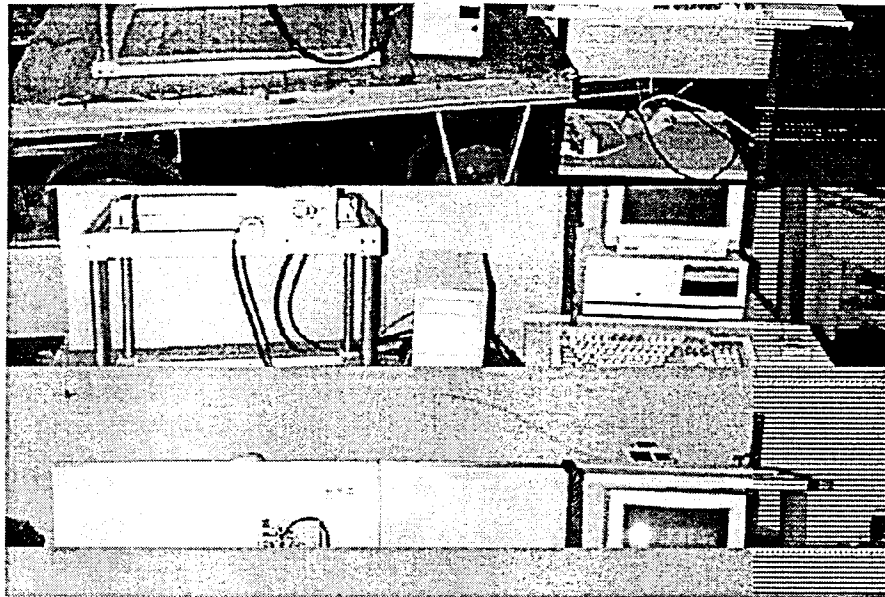


Figure 3.11 The laser scanning device

scanning head, which in turn allows the rock sample to be scanned in steps in the X-direction. This longitudinal scanning frame is attached, on one side, to the transverse moveable carriage, which allows movement in the Y-direction. The other end of the longitudinal frame is supported on a linear bearing, along which it moves. The transverse moveable carriage is driven along two guide rails by a second stepper motor arrangement. The size or number of steps and thus the speed of rotation of the stepper motors are determined by the number of electrical pulses and the frequency of the input signal, respectively. The laser displacement sensor uses a 3 mW helium-neon semiconductor laser diode, producing a light with a wavelength of 780 nm and a spot diameter less than 2 mm. It can measure distances between 50 and 130 mm, with a resolution of 50 μm at a 100 ms response time, or 150 μm with a 10 ms response time. The light is reflected off the surface to be measured and is received by a position sensing diode, which allows a stepped incremental signal to be output. This voltage output is directly related to the distance measured, so that the latter may be simply determined.

(b) Method of operation

The sample to be scanned is placed on the base plate against a reference bar in order to ensure accurate positioning, and is oriented such that the direction of shearing is parallel with the longitudinal scanning head. A wide range of sample thickness can be accommodated because

of the large measuring range of the laser sensor. Once the sample has been placed, the longitudinal and transverse scanning ranges of the apparatus can be set by positioning the micro switches appropriately. In this way only as small an area as required is scanned. The working sequence of the scanner is programmed and completely automated by the use of a IBM-compatible computer connected to a control box via an RS-232 serial port.

Once the scan program has been started, and the relevant information entered, scanning can commence. Both stepper motors are initially moved so that the laser displacement sensor is positioned at the starting point, as dictated by the positions of two micro switches. This point is to the left and below the actual sample to be scanned. The scanning head is then moved incrementally to the right in the X-direction by applying pulses to the stepper motor. When the scanning head reaches a limiting micro switch the head returns to the left limit of its travel and the entire longitudinal scanning frame is moved by one increment in the Y-direction. The scanner head then again begins to move to the right in the X-direction and the process is repeated until a fourth micro switch triggers the end of the scanning process.

The profile of the sample is only measured as the scanner head moves from left to the right in the X-direction. The X- and Y- coordinates are determined from the number of pulses fed to each of the stepper motors and the distance between the scanner head and the joint surface is measured at each increment directly by the laser sensor.

The increment in the X- and Y-directions can be set separately, such that the Y-direction increment can be any multiple of the X-direction increment. For a small joint surface approximately 80 mm by 55 mm in size, and using a scan increment of 0.5 mm, the entire surface can be scanned in 25 minutes, producing a data file containing approximately 18 000 data points.

The accuracy and relevance of the results that are obtained from the scanner are influenced by the increments between individual data points. A large increment will produce a coarse and largely non-representative profile whereas a very small increment may provide too much information for processing, and will greatly increase the time taken to build up a complete three dimensional picture of the surface roughness.

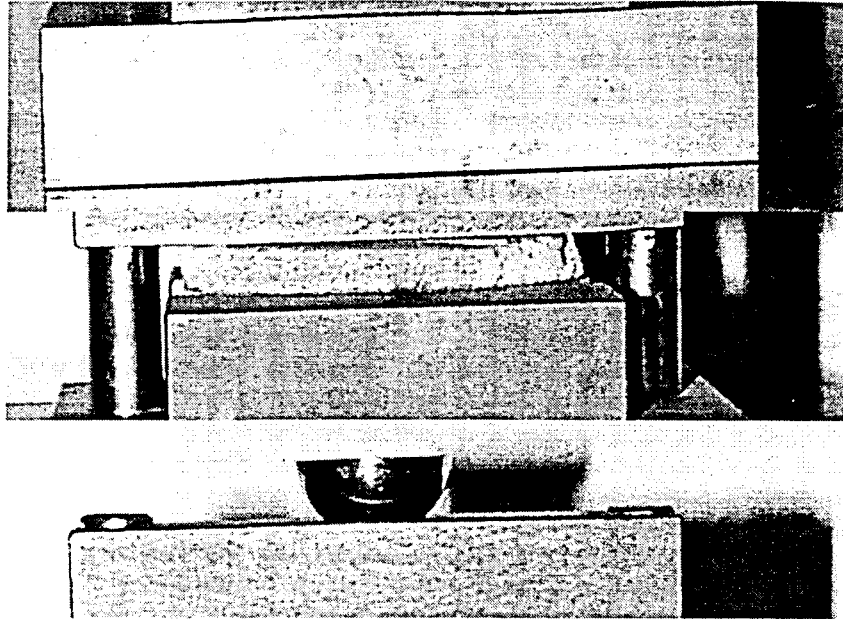


Figure 3.13 Punch shear apparatus

3.3 Deformation properties of rock material.

3.3.1 E-module (Young's modulus) and Poisson's ratio

Testing the deformation characteristics was carried out on a number of rock specimens taken from NX-size (54,5 mm diameter) borehole core. The specimens were prepared and tested in accordance with the relevant ISRM suggested methods (Brown, 1981). The determination of the UCS, Young's modulus and Poisson's Ratio was done concurrently. Testing was done in the Rock Mechanics Laboratory of the Technikon Pretoria.

3.4 Other engineering rock properties.

(a) Hardness (Schmidt hammer)

Hardness testing was carried out on a number of rock specimens taken from NX-size (54,5 mm diameter) borehole core. The specimens were prepared and tested in accordance with the relevant ISRM suggested methods (Brown, 1981) with a "L" type Schmidt hammer shown in Figure 3.14 Testing was done in the Rock Mechanics Laboratory of the Technikon Pretoria.

3.2.4.4 Alternative method of determining joint roughness.

An alternative method to measure joint roughness is with the use of a carpenter's comb. The carpenter's comb consists of a number of vertical steel or plastic pins that individually can move up or down to imitate the face of a two dimensional surface. This tool can be used to determine the unevenness of a joint surface in two dimensions by placing it directly onto the surface. Fig 3.12 illustrates this principle.

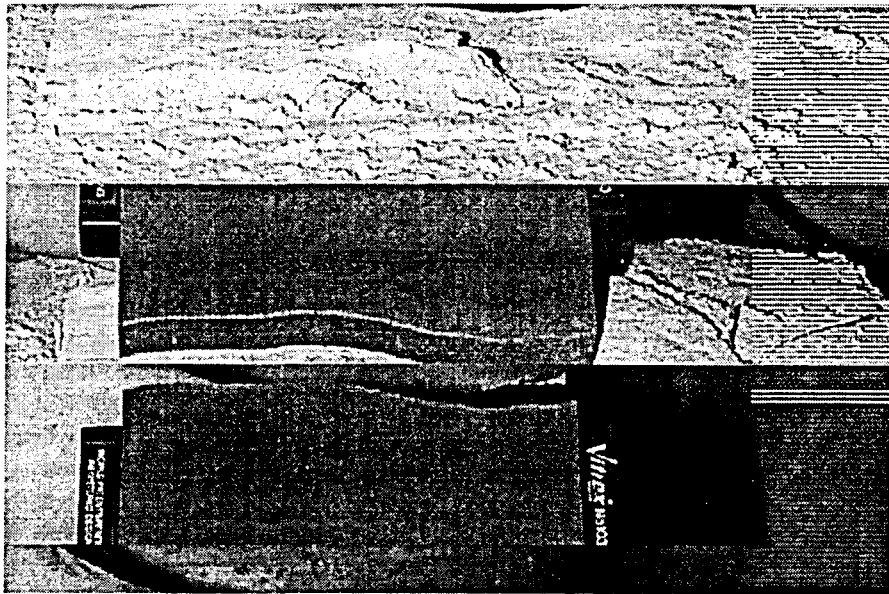


Figure 3.12 Carpenter's comb on rough joint surface

3.2.5 Punch shear strength (Intact shear strength).

The punch shear strength testing was carried out on a number of rock specimens prepared from NX-size (54,5 mm diameter) borehole core. The specimens were prepared and tested in accordance with the relevant ISRM suggested methods (Brown, 1981) in the punch shear apparatus illustrated in Figure 3.13. Testing was done in the Rock mechanics laboratory of the Technikon Pretoria.

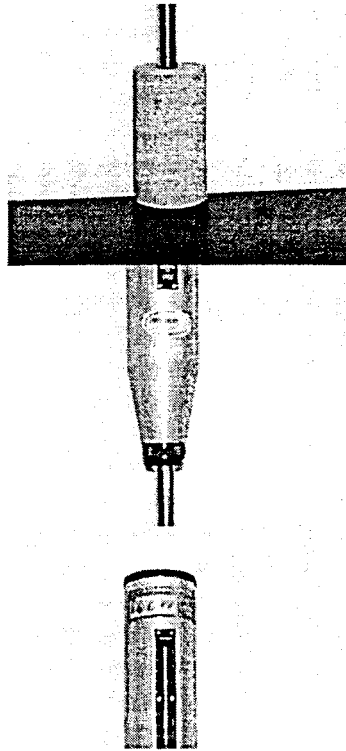


Figure 3.14 The Schmidt hammer

(b) Abrasiveness

Abrasiveness testing was carried out on a number of rock specimens taken from NX-size borehole core crushed to specification. The specimens were prepared and tested in accordance with the relevant ASTM suggested methods (ASTM C58) in the Los Angeles apparatus. Testing was done in the materials laboratory of the Department of Water Affairs and Forestry.

(c) Seismic wave velocity

Seismic wave velocity testing was carried out on a number of rock specimens taken from NX-size (54,5 mm diameter) borehole core. The specimens were prepared and tested in accordance with the relevant ISRM suggested methods (Brown, 1981) using a Pundit apparatus. Testing was done in the Rock Mechanics Laboratory of Technikon Pretoria with an apparatus on loan from the University of Pretoria.

(d) Water absorption index

Water absorption index testing was carried out on a number of rock specimens taken from borehole core. The specimens were prepared and tested in accordance with the relevant

ISRM suggested methods (Brown, 1981) Testing was done in the Rock Mechanics Laboratory of the Technikon Pretoria.

(e) Porosity

Porosity testing was carried out on a number of rock specimens taken from borehole core. The specimens were prepared and tested in accordance with the relevant ISRM suggested methods (Brown, 1981). Testing was done in the laboratory of the Council for Geoscience.

(f) Density

Density testing was carried out on a number of rock specimens taken from NX-size (54,5 mm diameter) borehole core. The specimens were prepared and tested in accordance with the relevant ISRM suggested methods (Brown, 1981). Testing was done in the Rock Mechanics Laboratory of the Technikon Pretoria.

(g) Swelling (Free swell)

Swelling (Free swell) testing was carried out on a number of rock specimens taken from borehole core. The specimens were prepared and tested in accordance with the relevant ISRM suggested methods (Brown, 1981). Testing was done in the Rock Mechanics Laboratory of EMATEK, CSIR.

(h) Slake durability

Slake durability testing was carried out on a number of rock specimens taken from crushed borehole core. The specimens were prepared and tested in accordance with ISRM suggested methods (Brown, 1981). Testing was done in the Rock Mechanics Laboratory of the Council for Geoscience.

CHAPTER FOUR

PRESENTATION AND DISCUSSION OF RESULTS

4.1 Rock types investigated.

During the planning stage of this study of rock material characteristics, it was envisaged to select as many of the rock types covering the surface and near surface in southern Africa as possible. Potential sites where rock material samples could be taken were identified. These sites were in most cases dam sites, although road cuttings and quarry sites were also included. Various rock types were sampled and subsequently tested. Figure 4.1 shows the origins of the samples discussed in this chapter.

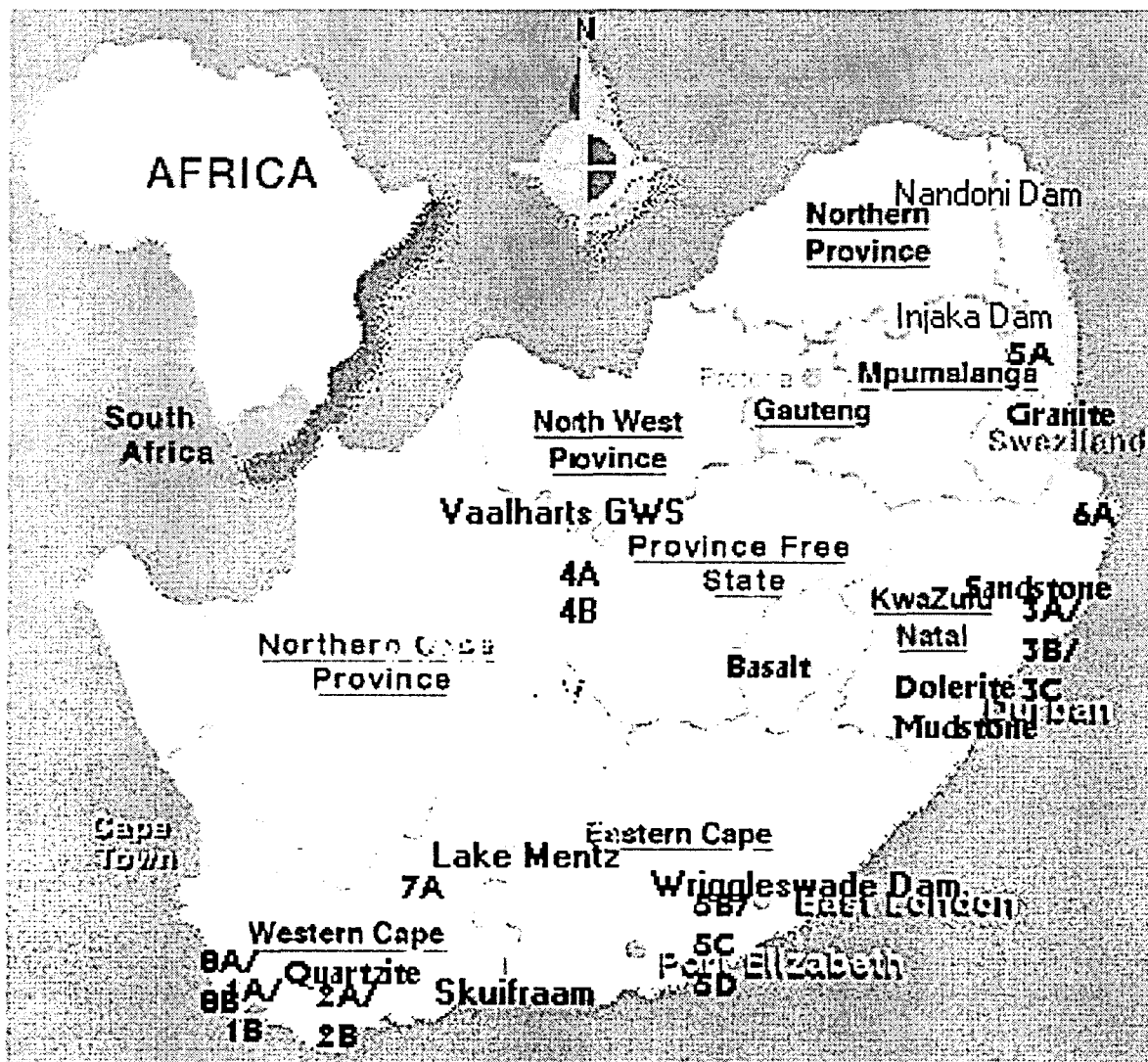


Figure 4.1 Location where samples of rock material were taken.

Table 4.1 lists the rock material types, sample numbers, the geological settings and the sites where the material specimens were sampled. The sample number refers to a specific set of rock type specimens, and can be used to locate the characteristics of the rock types listed in the tables in this chapter. These tables present the results of the research that was carried out on samples of selected southern African rock types. Borehole core samples and block samples were taken. Engineering characteristics were mainly determined on NX-size (54.4 mm diameter) borehole core samples. Borehole core samples were collected from dam sites where site investigations were in progress during 1992 and 1993.

ROCKTYPE	SAMPLE NUMBER	GEOLOGICAL SUCCESSION	SITE
Quartzite	1A	Cape Supergroup	Grootfontein Dam site, Citrusdal
Quartzite	1B	Cape Supergroup	Skuifraam Dam site, Franschhoek
Shale	2A	Cape Supergroup	Skuifraam Dam site, Franschhoek
Sandstone	2B	Cape Supergroup	Skuifraam Dam site, Franschhoek
Dolerite (Fine)	3A	Post Karoo	Qedusizi Dam, Ladysmith
Dolerite (Coarse)	3B	Post Karoo	Qedusizi Dam, Ladysmith
Mudstone	3C	Karoo Supergroup	Qedusizi Dam, Ladysmith
Shale	4A	Ventersdorp Supergroup	Vaalharts GWS
Sandstone	4B	Ventersdorp Supergroup	Vaalharts GWS
Granite	5A	Archaean	Injaka Dam, Marite River
Sandstone	5B	Karoo Supergroup	Wriggleswade Dam
Siltstone	5C	Karoo Supergroup	Wriggleswade Dam
Dolerite	5D	Post Karoo	Wriggleswade Dam
Rhyolite	6A	Karoo Supergroup	Pongolapoort Dam
Tillite	7A	Karoo Supergroup	Lake Mentz
Quartzite	8A	Cape Supergroup	Skuifraam Dam site, Franschhoek
Quartzite	8B	Cape Supergroup	Skuifraam Dam site, Franschhoek

Table 4.1 Selected southern African rock types (NX-cores) tested for engineering characteristics.

Block samples for shear testing in the large shear box were taken at the sites of dams under construction as well as at one road cutting. The purpose of the latter testing was to determine the peak and residual shear strength and the influence of the surface characteristics (mainly hardness and roughness) on the shear strength. Large shear tests were carried out on block

samples with surface areas ranging from approximately 100 x 100 mm to 300 x 300 mm. Table 4.2 presents the rock types and origins of the block samples that were tested. Only six rock types were tested in the large shear box apparatus due to the difficulties in obtaining samples as well as the duration of the testing process. Samples tested went through three phases of testing. The first phase was carried out dry and could, in hindsight, be seen as a learning curve for the new large shear apparatus. The second phase was carried out after problems with the machine were eliminated. Each sample was tested three times dry and then three times saturated. Eventually third phase tests were conducted on three additional granite specimens.

ROCK TYPE	ROCK SIMILAR TO	GEOLOGICAL SUCCESSION	SITE
Basalt	-	Karoo Supergroup	Lesotho Highlands Water Scheme
Dolerite	3A	Post Karoo	Qedusizi Dam, Ladysmith
Granite	5A	Archaean	Driekoppies Dam
Sandstone	-	Natal Group	N3 Cutting, Darnall
Mudstone(Shale)	3C	Karoo Supergroup	Qedusizi Dam, Ladysmith
Quartzite	8B	Cape Supergroup	Skuifraam Dam site, Franschhoek
Granite	1A-3A	Archaean	Nandoni Dam

Table 4.2 Selected rock types (large block samples) tested with the large shear box.

4.2 Presentation of results.

A comprehensive testing programme was carried out to determine the characteristics of the rock types investigated. Most of the testing was carried out in the laboratory of the Department of Civil Engineering at Technikon Pretoria and the Materials Laboratory of the Department of Water Affairs and Forestry in Pretoria West. Specialised testing that could not be conducted by these laboratories were carried out by other laboratories on contract. These included the rock mechanics laboratory of EMATEK, CSIR who conducted free swell testing, and the Engineering Geology Division of the Council for Geoscience who determined the

porosity and slake durability characteristics. The Materials Technology Division of the SABS carried out the Los Angeles tests on aggregate produced from the relevant rock types to determine abrasiveness. The Geology Department of the University of Pretoria carried out petrographic description of the rock types.

Results of all the are available in the appendixes recorded on the enclosed compact disc (CD). The different files can be read in Microsoft excel (.xls), Corel Quattro (.WB3), and Lotus Word Pro (.lwp). These files contain all the basic data as well as calculations and the graphics presented in the text.

Results of tests conducted on specimens are discussed for each rock type.

4.3 Discussion of rock material characteristics.

4.3.1 Quartzite of the Cape Supergroup.

Quartzite of the Cape Supergroup covers a substantial area from Vanrhynsdorp on the West Coast through Cape Town in the south to Port Alfred along the East Coast. Several samples of Quartzite of the Cape Supergroup were taken for testing. These included NX-size core samples as well as block samples for testing in the large shear box. Core samples were taken from Grootfontein Dam site (1A) and Skuifraam Dam site (1B, 8A and 8B) in the Western Cape. In addition, quartzite was also sampled at Skuifraam Dam site for large-scale shear tests. All the important engineering characteristics of the quartzite were determined during the testing programme. Testing methods are described in Chapter 2. Tables 4.3, 4.4, 4.5 and 4.6 describe the engineering characteristics of samples 1A, 1B, 8A and 8B respectively.

ROCK TYPE: Quartzite (1A)

ORIGIN: Cape Supergroup, Location: Grootfontein Dam site, Citrusdal

MACROSCOPIC DESCRIPTION:

Fine grained, unweathered, white to grey quartzite

PETROGRAPHIC DESCRIPTION: The rock consists of ± 55 % angular to sub-angular quartz and ± 5 % opaque minerals. Plagioclase feldspar, zircon and tourmaline are accessory minerals. The grain size of this clastic portion ranges from ± 0.06 to ± 0.25 mm. The matrix constitutes ± 40 % of the rock and consists mainly of mica (muscovite), kaolinite and some chlorite and/or smectite (determined by XRD). In places, the matrix is stained black, possibly by carbonaceous matter.

MATERIAL CHARACTERISTIC	PROPERTY VALUE			AVERAGE VALUE
	Min	Max	n	
STRENGTH CHARACTERISTICS				
Uniaxial compressive strength (UCS), MPa	294	357	3	329
Point load strength index (PLSI) MPa	8,08	14,14	13	11.8
Triaxial strength parameters , deg; MPa	-	-	1	$\phi = 59,2; c = 49,3$
Indirect tensile strength, MPa	21,7	28,6	5	23.5
Basic shear strength, deg	-	-	1	$\phi = 30,4$
Punch shear strength, MPa	43,9	64,7	5	53.1
DEFORMATION CHARACTERISTICS				
E-modulus, GPa	49,4	80,4	3	78.5
Poisson's ratio	0,1167	0.2085	3	0.163
GENERAL CHARACTERISTICS				
Hardness (Schmidt hammer)	51	58	20	53.75
Abrasiveness				n/a
Seismic wave velocity (P-wave), m/s	5283	5987	5	5641.6
Water absorption, %	0	0,81	3	0.53
Porosity, %	0,21	0,27	2	0,2450
Density, kg/m ³	2628	2734	8	2682
Swelling (Free swell), %	0,003	0,027	2	0,063
Slake durability (7 cycles), %	-	-	1	99,45

Table 4.3 Characteristics of selected specimens of Quartzite (1A) of the Cape Supergroup.

ROCK TYPE: Quartzite (1B)

ORIGIN: Cape Supergroup, Location: Skuifraam, Franschhoek

MACROSCOPIC DESCRIPTION:

Medium to coarse grained, massive pinkish white, unweathered quartzite

PETROGRAPHIC DESCRIPTION:

The rock consists of ± 95 % of sub-rounded quartz grains, which are recrystallized and show various degrees of undulatory extinction. The size of the quartz grains ranges from ± 0.5 to ± 2 mm. Approximately 5 % of the rock is matrix, consisting of mica, plagioclase and kaolinite.

MATERIAL CHARACTERISTIC	PROPERTY VALUE			AVERAGE VALUE
	Min	Max	N	
STRENGTH CHARACTERISTICS				
Uniaxial compressive strength (UCS), MPa	204	221	3	215
Point load strength index (PLSI)		-		n/a
Triaxial strength parameters, deg; MPa	-	-	15	$\phi = 53, c = 57$
Indirect tensile strength, deg; MPa	13,6	21,1	5	17,3
Basic shear strength, kPa	-	-	1	$\phi = 27.8, c = 9$
Punch shear strength, MPa	16,9	39,6	5	34,1
DEFORMATION CHARACTERISTICS				
E-modulus (50% UCS), GPa	51,0	84,4	3	65.25
Poisson's ratio	0.119	0,167	3	0,139
GENERAL CHARACTERISTICS				
Hardness (Schmidt hammer)	-	-		n/a
Abrasiveness	-	-		n/a
Seismic wave velocity (P-wave), m/s	4044	5785	3	4861.8
Water absorption, %	0	1,25	3	0,57
Porosity, %	0,328	0,362	2	0,345
Density. kg/m³	2580	2645	15	2625
Swelling (Free swell), %	0,006	0,025	2	0,016
Slake durability (7 cycles), %	-	-	1	99.09

Table 4.4 Characteristics of selected specimens of Quartzite (1B) of the Cape Supergroup.

ROCK TYPE: Quartzite (8A)

ORIGIN: Cape Supergroup Skuifraam Dam site, Franschhoek

MACROSCOPIC DESCRIPTION:

Fine to medium grained, massive, white to light grey, unweathered quartzite.

PETROGRAPHIC DESCRIPTION:

This quartzite consists of ± 65 % rounded to sub-rounded grains of quartz, exhibiting medium to strong undulatory extinction, ± 5 % interstitial opaque minerals, accessory zircon and ± 30 % matrix. The matrix consists of mica and kaolinite. The size of the quartz grains ranges from ± 0.045 to 5 mm.

MATERIAL CHARACTERISTIC	PROPERTY VALUE			AVERAGE VALUE
	Min	Max	n	
STRENGTH CHARACTERISTICS				
Uniaxial compressive strength (UCS), MPa	63	120	3	86
Point load strength index (PLSI), MPa	3,37	8,42	15	5.63
Triaxial strength parameters, deg; MPa	-	-	15	$\phi = 45,4, c = 29,1$
Indirect tensile strength, MPa	4,56	7,61	5	5,9
Basic shear strength, deg	-	-	1	$\phi = 28,5$
Punch shear strength, MPa	12,07	14,51	5	13.4
DEFORMATION CHARACTERISTICS				
E-modulus. GPa	26,9	41,8	3	36.4
Poisson's ratio	0,1779	0,5810	3	0.327
GENERAL CHARACTERISTICS				
Hardness (Schmidt hammer)	34	46	20	41,2
Abrasiveness	-	-	1	45.8
Seismic wave velocity (P-wave), m/s	4031	4440	4	4264.0
Water absorption, %	0,99	1,19	3	1.07
Porosity, %	0.267	0,325	2	0.297
Density, kg/m ³	2505	2595	15	2549
Swelling (Free swell), %	0,028	0,033	2	0.031
Slake durability (7 cycles), %	-	-	1	96.94

Table 4.5 Characteristics of selected specimens of Quartzite (8A) of the Cape Supergroup.

ROCK TYPE: Quartzite (8B)

ORIGIN: Cape Supergroup, Skuifraam Dam site, Franschhoek

MACROSCOPIC DESCRIPTION: Medium grained, massive, grey, unweathered quartzite.

PETROGRAPHIC DESCRIPTION: This quartzite contains ± 90 % angular to sub-angular quartz grains with varying undulatory extinction. The matrix comprises about 10 % of the rock and consists of mica and kaolinite. The quartz grains are ± 0.01 to ± 2 mm in diameter.

COMMENTS: The quartz grains have a “dirty” appearance.

MATERIAL CHARACTERISTIC	PROPERTY VALUE			AVERAGE VALUE
	Min	Max	n	
STRENGTH CHARACTERISTICS				
Uniaxial compressive strength (UCS), MPa	-	-	1	329
Point load strength index (PLSI), MPa	3,7	8,42	15	5,55
Triaxial strength parameters, deg; MPa	-	-	15	$\phi = 59,2, c = 49,3$
Indirect tensile strength, MPa	7,29	13,73	5	10.3
Basic shear strength, deg	-	-	3	$\phi = 30.4$
Punch shear strength, MPa	19,12	25,13	5	22,7
DEFORMATION CHARACTERISTICS				
E-modulus		-		-
Poisson's ratio		-		-
GENERAL CHARACTERISTICS				
Hardness (Schmidt hammer)	46	57	20	51.1
Abrasiveness	-	-	1	45,8
Seismic wave velocity (P-wave), m/s	4258	4963	4	4690
Water absorption, %	0,34	0,64	3	0,45
Porosity, %	0,25	0,31	2	0,282
Density, kg/m ³	2549	2617	15	2585
Swelling (Free swell), %	0,011	0,034	2	0,023
Slake durability (7 cycles), %	-	-	1	99,11

Table 4.6 Characteristics of selected specimens of Quartzite (8B) of the Cape Supergroup.

GENERAL COMMENTS ON RESULTS OF THE FOUR QUARTZITES TESTED DURING THIS INVESTIGATION:

The type of material, classified as quartzite or sometimes as sandstone of the Cape Supergroup, is very variable as is indicated by its engineering characteristics even when only unweathered rock is considered. For example, the uniaxial compressive strength varied between 86 and 329 MPa and triaxial strength parameter (internal angle of friction) between $45,4^{\circ}$ and $59,2^{\circ}$. The Brazilian tensile strength is between 5,9 and 28,1 MPa, the seismic wave velocity between 4264,0 and 5641,6 m/s, water absorption between 0,45 and 1,07 % and density between 2549,3 and 2681,9 kg/m³. It is recommended that the geological description of the material be studied when deciding on which values to choose from the tables above.

The basic friction angles for these materials were $30,4^{\circ}$, $27,8^{\circ}$ and $28,5^{\circ}$ and $30,4^{\circ}$. These values are very consistent and compares favourably with the value for quartzite of 26° - 35° in the literature. Due to the brittle nature of the rock material it was difficult to take samples for large scale shear testing. Nevertheless, sampling was attempted but eventually not one specimen suitable for testing was available.

4.3.2 Shale of the Cape Supergroup.

Shale of the Cape Supergroup covers a substantial area from Vanrhynsdorp on the West Coast through Cape Town in the south to Port Alfred along the East Coast. Several NX size core samples for testing were taken from Skuifraam Dam site (2A) in the Franschhoek area of the Western Cape. Shale was not sampled at Skuifraam Dam site for large-scale shear tests, as it was not present in the excavation on site during the sampling process. Results are presented in table 4.7 below.

A geological description of the shale is as follows:

ROCK TYPE: Shale (2A)

ORIGIN: Cape Supergroup, Location: Skuifraam, Franschhoek

MACROSCOPIC DESCRIPTION: Fine grained, layered, purple unweathered shale.

PETROGRAPHIC DESCRIPTION: Angular to subangular chips of quartz (± 0.02 to ± 0.08 mm in diameter), some flakes of mica (muscovite) and minor plagioclase feldspar constitutes approximately 40 % of the rock. The remaining ± 60 % is matrix consisting of carbonaceous material, mica and kaolinite.

COMMENTS: Layering of “matrix-rich” and “matrix-poor” zones can be observed on thin section scale.

MATERIAL CHARACTERISTIC	PROPERTY VALUE			AVERAGE VALUE
	Min	Max	N	
STRENGTH CHARACTERISTICS				
Uniaxial compressive strength (UCS), MPa	105	125	3	114
Point load strength index (PLSI), MPa	3,03	8,08	15	5,05
Triaxial strength parameters, deg; MPa	-	-	15	$\phi = 31,6, c = 42$
Indirect tensile strength, MPa	9,65	20,04	5	16,3
Basic shear strength, deg; kPa	-	-	1	$\phi = 31,7, c = 4$
Punch shear strength, MPa	21,8	40,4	5	33,8
DEFORMATION CHARACTERISTICS				
E-modulus (50% UCS), GPa	52,8	64,6	3	59,4
Poisson's ratio	0,213	0,307	3	0,2695
GENERAL CHARACTERISTICS				
Hardness (Schmidt hammer)	42	46	20	43,65
Abrasiveness		-		n/a
Seismic wave velocity (P-wave), m/s	5288	6034	5	5590
Water absorption, %	0,38	0,76	3	0,54
Porosity, %	0,196	0,23	2	0,213
Density, kg/m ³	2655	2786	15	2731
Swelling (Free swell), %	0,030	0,081	2	0,056
Slake durability (7 cycles), %	-	-	1	98,77

Table 4.7 Characteristics of selected specimens of Shale (2A) of the Cape Supergroup.

The results are similar to what would be expected of shale of this kind. The only result worth mentioning is the basic friction angle of $31,7^\circ$ that corresponds well to the 31° to 33° of shale in the literature.

4.3.3 Sandstone of the Cape Supergroup.

Sandstone of the Cape Supergroup covers a substantial area from Vanrhynsdorp on the West Coast through Cape Town in the south to Port Alfred along the East Coast. Core samples were taken from Skuifraam Dam site (2B) in the Franschhoek area of the Western Cape. Sandstone was not sampled at Skuifraam Dam site for large-scale shear tests, as it was not present in the excavation on site during the sampling process. Several NX-size core samples of sandstone of the Cape Supergroup were taken for testing. Results are presented in table 4.8 below. A geological description of the sandstone is as follows:

ROCK TYPE: Sandstone (2B)

ORIGIN: Cape Supergroup, Location: Skuifraam, Franschhoek.

MACROSCOPIC DESCRIPTION: Fine to medium grained, massive, white unweathered sandstone.

PETROGRAPHIC DESCRIPTION: This rock consists of ± 85 % of rounded to sub-rounded quartz grains. The majority of the quartz grains are between 0.04 and 0.2 mm in diameter, but some grains are up to ± 0.4 mm in size. Accessory minerals are tourmaline, zircon and opaque minerals. The matrix (± 15 %) consists mainly of thin elongated mica crystals (muscovite) and accessory amphibole.

COMMENTS: Layering of heavy mineral (tourmaline, zircon and opaque minerals) rich and heavy mineral poor zones can be observed on thin section scale.

MATERIAL CHARACTERISTIC	PROPERTY VALUE			AVERAGE VALUE
	Min	Max	n	
STRENGTH CHARACTERISTICS				
Uniaxial compressive strength (UCS), MPa	76	184	3	120
Point load strength index (PLSI), MPa	4,71	13,8	15	7,85
Triaxial strength parameters, deg: MPa	-	-	15	$\phi = 51, c = 51,7$
Indirect tensile strength, MPa	8,98	19,77	5	15,27
Basic shear strength, deg: kPa	-	-	1	$\phi = 27,9, c = 6,7$
Punch shear strength, MPa	6,36	39,42	5	32,8
DEFORMATION CHARACTERISTICS				
E-modulus (50% UCS), GPa	60,3	73,9	3	65,73
Poisson's ratio	0,1212	0,1869	3	0,1642
GENERAL CHARACTERISTICS				
Hardness (Schmidt hammer)	44	50	20	48,6
Abrasiveness	-	-	-	n/a
Seismic wave velocity (P-wave), m/s	4872	6012	5	5529
Water absorption, %	0,48	0,55	3	0,50
Porosity, %	0,30	0,38	2	0,34
Density, kg/m³	2563	2673	15	2620
Swelling (Free swell), %	0,011	0,014	2	0,013
Slake durability (7 cycles), %	-	-	1	97,96

Table 4.8 Characteristics of selected specimens of Sandstone (2B) of the Cape Supergroup.

The results are similar to what would be expected of sandstone of this kind. The only result worth mentioning is the base friction angle of $27,9^{\circ}$ that corresponds well to the 26° to 35° of sandstone in the literature.

4.3.4 Dolerite: post-Karoo.

Dolerite of post Karoo age is present in the central part of South Africa. It plays a vital role as foundation material for dams as well as a general construction material in the country. Several NX-size core samples of both fine and coarse-grained dolerite were taken from Qeduzisi Dam (3A and 3B) in the Ladysmith area of Kwa-Zulu Natal. Dolerite was also sampled at Qeduzisi Dam for large-scale shear tests.

Results are presented in tables 4.9 and 4.10 below.

The geological descriptions of the two dolerites are as follows:

ROCK TYPE: Dolerite (fine-grained) (3A)

ORIGIN: Karoo Supergroup, Location: Kliprivier, Ladysmith

MACROSCOPIC DESCRIPTION:

Fine crystalline, massive dark blue unweathered dolerite

PETROGRAPHIC DESCRIPTION:

This rock consists of $\pm 45\%$ lath shaped plagioclase feldspar crystals (± 0.02 to ± 0.5 mm in length), $\pm 45\%$ interstitial clinopyroxene (± 0.02 to ± 0.3 mm) and $\pm 10\%$ opaque minerals (magnetite). The plagioclase and the clinopyroxene are partly altered to kaolinite. Minor olivine phenocrysts (up to 1 mm in diameter) and some phenocrysts consisting of an aggregate of plagioclase (up to 1 mm in diameter) are observed.

COMMENTS: The presence of quartz (detected by X-ray diffraction - XRD) cannot be excluded.

MATERIAL CHARACTERISTIC	PROPERTY VALUE			AVERAGE VALUE
	Min	Max	n	
STRENGTH CHARACTERISTICS				
Uniaxial compressive strength (UCS), MPa	(97) *	263	2	263
Point load strength index (PLSI), MPa	10,44	12,46	6	11,6
Triaxial strength parameters, deg; MPa	-	-	15	$\phi = 33,9, c = 157$
Indirect tensile strength, MPa	31,3	34,7	4	32,6
Basic shear strength, deg; kPa	-	-	1	$\phi = 33,3, c = 6,7$
Punch shear strength, MPa	20,4	42,9	5	32,6
DEFORMATION CHARACTERISTICS				
E-modulus (50 % UCS), GPa	110,8	122,2	2	117
Poisson's ratio	0,287	0,291	2	0,289
GENERAL CHARACTERISTICS				
Hardness (Schmidt hammer)	57	62	20	59,65
Abrasiveness, %	-	-	1	9,5
Seismic wave velocity (P-wave), m/s	6496	7044	5	6776
Water absorption, %	0,39	0,56	3	0,47
Porosity, %	0,258	0,347	3	0,303
Density, kg/m ³	2940	2994	15	2969
Swelling (Free swell), %	0,006	0,007	2	0,007
Slake durability (7 cycles), %	-	-	1	99,66

* Note: Value excluded from average

Table 4.9 Characteristics of selected specimens of fine grained Dolerite (3A)

ROCK TYPE: Dolerite (coarse-grained) (3B)

ORIGIN: Post-Karoo, Location: Kliprivier, Ladysmith

MACROSCOPIC DESCRIPTION:

Fine crystalline, massive, dark blue, unweathered dolerite

PETROGRAPHIC DESCRIPTION:

The rock consists of ± 45 % lath shaped plagioclase feldspar crystals, which are 0.01 to 0.7 mm in length, ± 45 % interstitial clinopyroxene, which are $< \pm 0.5$ mm in size and ± 10 % opaque minerals (magnetite). Approximately 35 % of the clinopyroxene is altered. The alteration products, determined by XRD, are mica, kaolinite, smectite and/or chlorite and minor amphibole. Minor intergrowth between quartz and feldspar is observed.

MATERIAL CHARACTERISTIC	PROPERTY VALUE			AVERAGE VALUE
	Min	Max	n	
STRENGTH CHARACTERISTICS				
Uniaxial compressive strength (UCS)		-		n/a
Point load strength index (PLSI), MPa	10,77	11,45	2	11,1
Triaxial strength, deg; MPa	-	-	15	$\phi = 55,1, c = 25,2$
Indirect tensile strength, MPa	17,3	20,0	4	18,9
Basic shear strength, deg; kPa	20,42	-	3	$\phi = 36,3, c = 3$
Punch shear strength, MPa		22,98	4	21,7
DEFORMATION CHARACTERISTICS				
E-modulus		-		n/a
Poisson's ratio		-		n/a
GENERAL CHARACTERISTICS				
Hardness (Schmidt hammer)	57	60	20	58,4
Abrasiveness		-		n/a
Seismic wave velocity (P-wave), m/s	6673	7083	5	6927
Water absorption, %	0	0,52	3	0,24
Porosity, %	0,263	0,472	2	0,3674
Density, kg/m³	2934	2961	15	2947
Swelling (Free swell), %	0,022	0,025	2	0,024
Slake durability, %	-	-	1	98,38

Table 4.10 Characteristics of selected specimens of coarse grained Dolerite (3B)

COMMENTS: The uniaxial compressive strength for example is in the order of 260 MPa. The triaxial strength parameter (internal angle of friction) is very high between $33,9^\circ$ and $55,1^\circ$, Brazilian tensile strength is between 23,0 and 32,6 MPa, the seismic wave velocity between 6776 and 6927 m/s, water absorption is low, between 0,24 and 0,47 % and density between 2947,6 and 2969 kg/m³.

The basic friction angle for these materials that were tested were between $33,3$ and $36,3^\circ$. This value is very constant and compares favourably with the value of 36° in the literature.

Large-scale shear testing on joints was carried out. Tests were carried out on (i) a rough joint surface (JRC = 4-6) with no joint fill material and (ii) a joint surface with clay infilling. Tests were carried out under dry and saturated conditions. The joint surface was sheared repeatedly and the strength should be regarded as residual. The results are given in table 4.12.

ROCK TYPE: Dolerite (5D)

ORIGIN: Post-Karoo, Location: Wriggleswade

MACROSCOPIC DESCRIPTION:

Coarse crystalline, massive, dark blue, unweathered dolerite.

PETROGRAPHIC DESCRIPTION:

The rock consists of ± 55 % plagioclase feldspar, ± 30 % interstitial clinopyroxene, ± 5 % opaque minerals (magnetite) and ± 10 % alteration products (mica and kaolinite). Most of the grains are larger than 0.5 mm and can be up to 1 mm in diameter.

MATERIAL CHARACTERISTIC	PROPERTY VALUE			AVERAGE VALUE
	Min	Max	n	
STRENGTH CHARACTERISTICS				
Uniaxial compressive strength (UCS), MPa	225	297	4	257
Point load strength index (PLSI), MPa	10	14,8	14	12,7
Triaxial strength parameters, deg; MPa	226	-	15	$\phi = 48,4, c = 60.8$
Indirect tensile strength, MPa	16,39	18,26	5	17,2
Basic shear strength, deg; kPa	-	-	1	$\phi = 31, c = 0$
Punch shear strength, MPa	25,3	33,5	5	30,8
DEFORMATION CHARACTERISTICS				
E-modulus	118,4	194,7	4	156,4
Poisson's ratio	0,285	0,329	4	0,298
GENERAL CHARACTERISTICS				
Hardness (Schmidt hammer)	58	61	20	59,8
Abrasiveness	-	-	1	15,0
Seismic wave velocity (P-wave), m/s	6101	6609	5	6363
Water absorption, %	0	0	3	0
Porosity		-		-
Density, kg/m³	2936	2976	15	2961
Swelling (Free swell), %	0,017	0,098	2	0,058
Slake durability (7 cycles)	-	-	-	-

Table 4.11 Characteristics of selected specimens of coarse grained Dolerite (5D)

Large scale tests were successfully conducted on dolerite specimens. Table 4.12 indicates the influence that the condition of the joint surface has on the shear strength (This aspect is further discussed in chapter 5)

MATERIAL CHARACTERISTIC	VALUE
Friction angle of joint (Dry)	52,6°
Friction angle of joint (Wet)	43,6°
Friction angle of 1 mm clay filled joint (Dry)	17,0°
Friction angle of 1 mm clay filled joint (Wet)	14,9°

Table 4.12 Friction angles of selected specimens of post Karoo Dolerite (similar to Dolerite 3A).

4.3.5 Mudstone of the Karoo Supergroup.

Mudstone of Karoo Supergroup covers a large area in the central part of South Africa. It plays a role as foundation material for dams and is not a commonly used construction material in the country. Core samples of mudstone were taken from Qedusizi Dam (3C) in the Ladysmith area of Kwa-Zulu Natal. Several NX-size core samples of mudstone were taken for testing. Mudstone was also sampled at Qedusizi Dam site for large-scale shear tests. Results are presented in tables 4.13 and 4.14 below.

The geological description is as follows:

ROCK TYPE: Mudstone (3C)

ORIGIN: Karoo Supergroup, Location: Kliprivier, Ladysmith

MACROSCOPIC DESCRIPTION:

Fine grained, massive, dark brown, unweathered mudstone

PETROGRAPHIC DESCRIPTION: The mudstone consists of 20 % of angular quartz fragments, which are $< \pm 0.08$ mm in diameter in a matrix (80 %) of kaolinite, mica, chlorite and/or smectite plagioclase and possibly quartz.

COMMENTS:

The composition of the matrix has been determined by XRD.

Mudstone is usually a variable rock type in its different stages of weathering and its engineering characteristics are therefore not very constant.

MATERIAL CHARACTERISTIC	PROPERTY VALUE			AVERAGE VALUE
	Min	Max	n	
STRENGTH CHARACTERISTICS				
Uniaxial compressive strength (UCS), MPa	71	166	2	119
Point load strength index (PLSI), MPa	2,36	3,7	12	2.79
Triaxial strength parameters, deg; MPa	-	-	14	$\phi = 25, c = 47$
Indirect tensile strength, MPa	17,32	20,04	4	18.9
Basic shear strength, deg; kPa	-	-	1	$\phi = 32.7, c = 9.9$
Punch shear strength, MPa	32,91	36,89	5	36.3
DEFORMATION CHARACTERISTICS				
E-modulus, GPa	18,1	33,8	2	25.9
Poisson's ratio	0,137	0,2444	2	0.1912
GENERAL CHARACTERISTICS				
Hardness (Schmidt hammer)	34	41	20	38
Abrasiveness, %	-	-	1	11.4
Seismic wave velocity (P-wave),m/s	3423	3920	5	3675
Water absorption, %	2,56	3,92	3	3.19
Porosity, %	0,265	0,327	2	0.29
Density, kg/m³	2388	2505	14	2473
Swelling (Free swell), %	0,006	0.206	2	0,106
Slake durability (7 cycles), %	-	-	1	99,69

Table 4.13 Characteristics of selected specimens of Mudstone (3C) of the Karoo Supergroup.

COMMENTS: The mudstone tested was very homogeneous and layering was difficult to see in a hand sample. The uniaxial compressive strength for example is in the order of 119 MPa, the triaxial strength parameter (internal angle of friction) is 25°, the Brazilian tensile strength 18,9 MPa, the seismic wave velocity 3675 m/s, water absorption high, 3,19 % and density 2473 kg/m³. The basic friction angle obtained for this material is 32,7 °. It compares favourably with the value of between 31 and 33° in the literature.

Large-scale shear testing on joints was carried out. Tests were carried out on (i) a smooth joint surface (JRC = 8-10) with no joint fill material (only iron staining) and (ii) a joint surface with clay infilling. Tests were carried out under dry and saturated conditions. The joint surface was sheared repeatedly and the strength may be regarded as residual. Table 4.14 presents these results. They are further discussed in chapter 5.

MATERIAL CHARACTERISTIC	RANGE OF VALUES
Friction angle of joints (Dry)	32,8° - 37,0°
Friction angle of joints (Wet)	13,2° - 22,6°

Table 4.14 Friction angles of selected test specimens of Mudstone of the Karoo Supergroup (similar to Mudstone 3C).

4.3.6 Shale of the Ventersdorp Supergroup.

Shale of the Ventersdorp Supergroup occurs in the Northern Cape and Northwest Provinces. Samples (NX-core) were taken at the site of an investigation for a tunnel near Jan Kempdorp. No large samples could be taken for large scale shear testing.

The geological description of the shale is as follows:

ROCK TYPE: Shale (4A)

ORIGIN: Ventersdorp Supergroup, Location: Vaalharts

MACROSCOPIC DESCRIPTION:

Fine grained, layered, blue-grey, unweathered shale

PETROGRAPHIC DESCRIPTION:

The rock comprises of $\pm 40\%$ angular quartz grains, which are ± 0.02 to ± 0.05 mm in diameter, in a matrix ($\pm 60\%$) consisting of kaolinite, smectite and/or chlorite, mica, plagioclase feldspar and possibly clinopyroxene and quartz.

COMMENTS:

The composition of the matrix has been determined by XRD.

MATERIAL CHARACTERISTIC	PROPERTY VALUE			AVERAGE VALUE
	Min	Max	n	
STRENGTH CHARACTERISTICS				
Uniaxial compressive strength (UCS), MPa	211	309	2	260
Point load strength index (PLSI), MPa	3,37	9,43	12	6,4
Triaxial strength parameters, deg; MPa	-	-	15	$\phi = 43,8, c = 59,7$
Indirect tensile strength, MPa	23,3	30,3	5	29,1
Basic shear strength, deg; kPa	-	-	1	$\phi = 31,9, c = 10,5$
Punch shear strength, MPa	15,74	49,2	5	33,9
DEFORMATION CHARACTERISTICS				
E-modulus (50 % UCS), GPa	86,0	86,7	2	86,3
Poisson's ratio	0,2313	0.3015	2	0.2664
GENERAL CHARACTERISTICS				
Hardness (Schmidt hammer)	49	54	20	51,3
Abrasiveness, %	-	-	1	12,6
Seismic wave velocity (P-wave), m/s	5117	5567	5	5272,3
Water absorption, %	0,19	0,36	3	0,25
Porosity, %	0,344	0,418	2	0.3817
Density, kg/m ³	2725	2795	15	2762,3
Swelling (Free swell), %	0,020	0,050	2	0,035
Slake durability (7 cycles), %	-	-	1	99,41

Table 4.15 Characteristics of selected specimens of Shale (4A) of the Ventersdorp Supergroup.

Shale of the Ventersdorp Supergroup can be regarded as a metamorphic rock and is as such of higher quality than normal shale. It can almost be described as a slate. Its uniaxial compressive strength was determined as 260 MPa, the triaxial strength parameters (internal angle of friction and cohesion) are $43,8^{\circ}$ and 59,7 MPa, the Brazilian tensile strength 29,1 MPa, the seismic wave velocity 5272 m/s, water absorption low at 0,25 % and density 2762 kg/m³.

The basic friction angle for this material is $31,9^{\circ}$. This value is high in comparison with the value of between 25 and 30° in the literature. Large-scale shear testing on joints was not carried out.

4.3.7 Sandstone of the Ventersdorp Supergroup.

Sandstone of the Ventersdorp Supergroup occurs in the Northern Cape and Northwest Provinces. Samples (NX-core) were taken at the site of an investigation for a tunnel near Jan Kempdorp. No large samples could be taken for large scale shear testing.

The geological description is as follows:

ROCK TYPE: Sandstone (4B)

ORIGIN: Ventersdorp Supergroup, Location: Vaalharts

MACROSCOPIC DESCRIPTION: Fine to medium grained, massive, blue-grey, unweathered sandstone.

PETROGRAPHIC DESCRIPTION: The rock consists of ± 40 % angular to sub-angular quartz fragments (± 0.15 to ± 0.5 mm in diameter), ± 20 % feldspar grains (plagioclase and orthoclase), which are ± 0.2 to 0.4 mm in size and are mostly altered to sericite, and ± 5 % chert fragments, up to ± 0.4 mm in diameter. Accessory opaque minerals are observed. The matrix comprises ± 35 % of the rock and consists of mica, kaolinite, chlorite and/or smectite and some chips of quartz and mica. Large bands of chlorite, showing "flow structures" are observed within the matrix.

COMMENTS: Apart from the quartz fragments and the chips of mica all the minerals are altered. The rock was possibly subjected to dynamic metamorphism. Due to its mineralogy, this rock could be classified as a subgreywacke.

MATERIAL CHARACTERISTIC	PROPERTY VALUE			AVERAGE VALUE
STRENGTH CHARACTERISTICS	Min	Max	n	
Uniaxial compressive strength (UCS), MPa	142	162	2	152
Point load strength index (PLSI), MPa	5,05	10,77	15	7,53
Triaxial strength parameters, deg: MPa	-	-	15	$\phi = 37,5, c = 66,2$
Indirect tensile strength, MPa	15,5	17,3	5	16,3
Basic shear strength, deg: kPa	-	-	3	$\phi = 34,9, c = 3,3$
Punch shear strength, MPa	26.4	32.09	5	30.8
DEFORMATION CHARACTERISTICS				
E-modulus (50 % UCS), GPa	66,79	83,26	2	75.0
Poisson's ratio	0.208	0.259	2	0.233
GENERAL CHARACTERISTICS				
Hardness (Schmidt hammer)	49	58	20	53.6
Abrasiveness, %	-	-	1	25,3
Seismic wave velocity (P-wave), m/s	4618	5320	4	4556
Water absorption, %	0	0,4	3	0,13
Porosity, %	0,214	0,427	2	0,32
Density, kg/m ³	2632	2694	15	2672
Swelling (Free swell), %	0,023	0,130	2	0,077
Slake durability (7 cycles), %	-	-	1	98,92

Table 4.16 Characteristics of selected specimens of Sandstone (4B) of the Ventersdorp Supergroup.

Results are presented in table 4.16. Its uniaxial compressive strength was determined as 152 MPa, the triaxial strength parameter (internal angle of friction) is $37,5^\circ$, the Brazilian tensile strength 16,3 MPa, the seismic wave velocity 4556 m/s, water absorption low at 0,13 % and density 2672 kg/m³.

The basic friction angle for this material that was tested was $34,9^\circ$. This value is very high in comparison with the value of between 26 and 35° in the literature. Large-scale shear testing on joints was not carried out because rock material of this site could not be sampled as construction at the site had been completed.

4.3.8 Granite of the Basement Complex.

Granite of the Basement Complex covers a large area in the northern and eastern part of South Africa. It plays a role as foundation material for dams and other structures and is a often used construction material in the region. Core samples of granite were taken from Injaka Dam (5A) in the Bushbuck Ridge area of Northern Province. Granite was also sampled at Driekoppies Dam for large-scale shear tests. Results are available in tables 4.17 and 4.18 below. The geological description is as follows:

ROCK TYPE: Granite.

ORIGIN: Archaean granite, Location: Sabie River

MACROSCOPIC DESCRIPTION: Coarse crystalline, massive, pinkish-grey, unweathered granite.

PETROGRAPHIC DESCRIPTION: This granite consists of ± 50 % quartz with medium to strong undulatory extinction, ± 30 % plagioclase feldspar, ± 10 % orthoclase feldspar and ± 10 % mica (biotite). Accessory minerals are mica (muscovite), zircon, opaque minerals, tourmaline and apatite. The grains can be up to 1.5 mm in diameter, with most of the grains > 0.3 mm.

MATERIAL CHARACTERISTIC	PROPERTY VALUE			AVERAGE VALUE
	Min	Max	n	
STRENGTH CHARACTERISTICS				
Uniaxial compressive strength (UCS), MPa	199	216	2	208
Point load strength index (PLSI), MPa	5,72	13,47	15	8,82
Triaxial strength parameters, deg; MPa	-	-	15	$\phi = 49,8, c = 50,5$
Indirect tensile strength, MPa	9,82	11,69	5	10,5
Basic shear strength, deg; kPa	-	-	3	$\phi = 31, c = 6,3$
Punch shear strength, MPa	22,5	34,2	5	27,2
DEFORMATION CHARACTERISTICS				
E-modulus (50 % UCS), GPa	68,7	82,1	2	75,0
Poisson's ratio	0,258	0,268	2	0,263
GENERAL CHARACTERISTICS				
Hardness (Schmidt hammer)	52	58	20	54,85
Abrasiveness, %	-	-	1	29,5
Seismic wave velocity (P-wave), m/s	4259	5314	5	4889
Water absorption, %	0	0	3	0
Porosity, %	0,301	0,312	2	0,3069
Density, kg/m ³	2660	2696	15	2675
Swelling (Free swell),%	0,011	0,017	2	0,014
Slake durability (7 cycles), %	-	-	1	99,1

Table 4.17 Characteristics of selected specimens of Granite (5A) of the Basement Complex.

Granite is usually not a very variable rock type in its unweathered state and its engineering characteristics are usually very constant. The granite tested was very homogeneous in a hand

sample. The uniaxial compressive strength for example is in the order of 208 MPa, the triaxial strength is 49,8°, the Brazilian tensile strength 10,5 MPa, the seismic wave velocity 4889 m/s, water absorption very low at 0 % and density 2675 kg/m³.

The basic friction angle for this material was 31,0°. This value compares favourably with the value of between 31 and 35° in the literature. Large-scale shear testing on joints was carried out. Tests were carried out on three joint surfaces (JRC = 2-4, 4-6 and 8-10) with no joint fill material (only iron staining on joint surfaces). Tests were carried out under dry and saturated conditions. Three samples were tested in each case. The joint surface was sheared repeatedly and the strength can be regarded as residual. Table 4.18 presents these results. These results are further discussed in chapter 5.

MATERIAL CHARACTERISTIC	RANGE OF VALUES
Friction angle of joints (Dry)	27,1° - 40,0°
Friction angle of joints (Wet)	24,9° - 38,2°

Table 4.18 Friction angles of selected specimens of Granite of the Basement Complex (similar to Granite 5A).

4.3.9 Sandstone of the Karoo Supergroup.

Sandstone of the Karoo Supergroup covers a large area in the central part of South Africa. It plays a role as foundation material for dams and is generally not used as construction material in the country. Core samples of sandstone were taken from Wriggleswade Dam (5B). Several NX-size core samples of sandstone were taken for testing. Results are available in tables 4.19 below.

The geological description is as follows:

ROCK TYPE: Sandstone (5B)

ORIGIN: Karoo Supergroup, Location: Wriggleswade

PETROGRAPHIC DESCRIPTION:

The rock consists of ± 30 % angular to subangular quartz fragments showing various degrees of undulatory extinction, ± 20 % fragments of chert, ± 30 % altered fragments of feldspar, ± 10 % other highly altered fragments and ± 10 % matrix. Accessory minerals are zircon and opaque minerals. The matrix and the highly altered fragments consists of mica, kaolinite and chlorite and/or smectite (determined by XRD).

The grain size of the fragments ranges from 0.15 to 0.35 mm.

MATERIAL CHARACTERISTIC	PROPERTY VALUE			AVERAGE VALUE
	Min	Max	n	
STRENGTH CHARACTERISTICS				
Uniaxial compressive strength (UCS), MPa	188	234	3	207
Point load strength index (PLSI), MPa	6,06	10,77	15	8,84
Triaxial strength parameters, deg; MPa	-	-	12	$\phi = 57,8, c = 32,5$
Indirect tensile strength, MPa	10,57	12,92	5	11,9
Basic shear strength, deg; kPa	-	-	1	$\phi = 35,9, c = 0$
Punch shear strength, MPa	17,77	22,85	5	20,1
DEFORMATION CHARACTERISTICS				
E-modulus, GPa	42,0	47,5	3	41,2
Poisson`s ratio	0,135	0,240	3	0,193
GENERAL CHARACTERISTICS				
Hardness (Schmidt hammer)	54	58	20	53,55
Abrasiveness, %	-	-	1	25,3
Seismic wave velocity (P-wave), m/s	3509	4125	5	4056
Water absorption, %	0,99	2,18	3	1,67
Porosity, %	0,267	0,422	2	0,345
Density, kg/m ³	2520	2553	12	2529
Swelling (Free swell), %	0.023	0.162	2	0.093
Slake durability (7 cycles), %	-	-	1	99,6

Table 4.19 Characteristics of selected specimens of Sandstone (5B) of the Karoo Supergroup.

The uniaxial compressive strength for example is 207 MPa. There is dolerite in the vicinity which may be the reason for the high strength values of the sediments from Wriggleswade.

The triaxial strength (internal angle of friction) is 57,8°, the Brazilian tensile strength 11,9 MPa, the seismic wave velocity 4056 m/s, water absorption 1,67 % and density 2529 kg/m³. The basic friction angle for this material is 35,6 °.

4.3.10 Siltstone of the Karoo Supergroup.

Siltstone of the Karoo Supergroup covers a large area in the central part of South Africa. It plays a role as foundation material for dams and is generally not used as a construction material in the country. Core samples of siltstone were taken from Wiggleswade Dam. Siltstone was also sampled at Qeduzisi Dam for large-scale shear tests. Results are available in tables 4.20 below.

The geological description is as follows:

ROCK TYPE: Siltstone (5C)

ORIGIN: Karoo Supergroup, Location: Wiggleswade

PETROGRAPHIC DESCRIPTION: The rock is extremely fine grained and optical identification of the minerals is not possible. XRD analysis showed the presence of mainly quartz and plagioclase feldspar with minor mica, kaolinite, smectite and/or chlorite. The grain size is approximately 0.01 mm.

MATERIAL CHARACTERISTIC	PROPERTY VALUE			AVERAGE VALUE
	Min	Max	n	
STRENGTH CHARACTERISTICS				
Uniaxial compressive strength (UCS), MPa	255	257	2	256
Point load strength index (PLSI), Mpa	3,70	6,73	15	5,15
Triaxial strength parameters, deg; MPa	-	-	15	$\phi = 34,9, c = 83,1$
Indirect tensile strength, Mpa	19,45	24,24	5	22
Basic shear strength, deg; kPa	-	-	1	$\phi = 38,2, c = 9$
Punch shear strength, Mpa	32,13	57,99	5	49,1
DEFORMATION CHARACTERISTICS				
E-modulus, Gpa	63,33	71,53	2	67,4
Poisson's ratio	0,212	0,262	2	0,237
GENERAL CHARACTERISTICS				
Hardness (Schmidt hammer)	52	60	20	56,1
Abrasiveness, %	-	-	1	12,4
Seismic wave velocity (P-wave), m/s	5169	5802	5	5426
Water absorption, %	0	0,43	3	0,28
Porosity, %	0,297	0,299	2	0,298
Density, kg/m ³	2671	2769	15	2711
Swelling (Free swell), %	0,114	0,476	2	0,296
Slake durability (7 cycles), %	-	-	1	99,59

Table 4.20 Characteristics of selected specimens of Siltstone (5C) of the Karoo Supergroup.

Siltstone is a variable rock type in its different stages of weathering and its engineering characteristics are not very constant. The siltstone tested was very homogeneous and layering was difficult to see in a hand sample. The uniaxial compressive strength for example is 256 MPa perpendicular to the bedding planes which is very high for a siltstone, the triaxial strength is 34,9°, the Brazilian tensile strength 22 MPa, the seismic wave velocity 5426 m/s, water absorption low at 0,28 % and density 2711 kg/m³. The basic friction angle for this

material that was tested was 38,2°. This value is very high compared with the value of between 31 and 33° in the literature. No testing on large samples was undertaken.

4.3.11 Rhyolite of the Karoo Supergroup.

Rhyolite of the Karoo Supergroup covers a small area in the eastern part of South Africa. It plays a role as foundation material for dams (Pongolapoort Dam) and is generally used as construction material in that area. Core samples of Rhyolite were taken from Pongolapoort Dam (6A) in the Pongola area of KwaZulu/Natal. Rhyolite was not sampled for large-scale shear tests. Results are available in table 4.21 below. The geological description of the rhyolite was not carried out. The reason for this is that no specimen was available at the time for the geological description.

MATERIAL CHARACTERISTIC	PROPERTY VALUES			AVERAGE VALUE
	Min	Max	n	
STRENGTH CHARACTERISTICS				
Uniaxial compressive strength (UCS), MPa	122	176	3	152
Point load strength index (PLSI), Mpa	7,41	9,43	15	8.6
Triaxial strength parameters, deg; Mpa	-	-	12	$\phi = 37.6, c = 55.6$
Indirect tensile strength, Mpa	12,81	16.73	5	14.7
Basic shear strength, deg; kPa	-	-	1	$\phi = 35, c = 12$
Punch shear strength, Mpa	19.8	31.5	5	25.8
DEFORMATION CHARACTERISTICS				
E-modulus (50 % UCS). Gpa	44.6	65.23	3	56.8
Poisson's ratio	0.236	0.256	3	0.245
GENERAL CHARACTERISTICS				
Hardness (Schmidt hammer)	48	50	20	49.6
Abrasiveness, %	-	-	1	19.6
Seismic wave velocity (P-wave), m/s	4354	4683	5	4544
Water absorption, %	1,60	2,64	3	2.29
Porosity, %	0,294	0,343	2	0.318
Density, kg/m ³	2499	2537	12	2518
Swelling (Free swell), %	0,012	0,013	2	0.013
Slake durability (7 cycles), %	-	-	1	98.99

Table 4.21 Characteristics of selected specimens of Rhyolite (6A) of the Karoo Supergroup.

Rhyolite is a variable rock type in its different stages of weathering and its engineering characteristics are not very constant. The rhyolite tested was not homogeneous and pseudo

layering was difficult to see in a hand sample. The uniaxial compressive strength for example is in the order of 152 MPa, the triaxial strength parameter (internal angle of friction) is 37,6°, the Brazilian tensile strength 14,7 MPa, the seismic wave velocity 4544 m/s, water absorption high at 2,29 % and density 2518 kg/m³. The basic friction angle for this material that was tested was 35°. This value compares favourably with the value of 31° for porphyry (a similar type of rock) in the literature. No testing on large samples was undertaken.

4.3.12 Tillite of the Karoo Supergroup.

Tillite of Karoo Supergroup occurs along the periphery of the Karoo basin. It plays a role as foundation material for dams e.g. Goedertrouw Dam and is generally used as construction material in the country. Several NX-size core samples of tillite were taken from Lake Mentz (7A) in the Jansenville area of the Eastern Cape. Tillite was not sampled for large-scale shear tests. Results are available in table 4.22 below.

MATERIAL CHARACTERISTIC	PROPERTY VALUE			AVERAGE VALUE
	Min	Max	n	
STRENGTH CHARACTERISTICS				
Uniaxial compressive strength (UCS), MPa	293	340	3	317
Point load strength index (PLSI), MPa	5,05	9,15	15	6,5
Triaxial strength parameters, deg; MPa	-	-	15	$\phi = 51,3, c = 57,6$
Indirect tensile strength, MPa	15,62	19,41	5	18,1
Basic shear strength, deg. kPa	-	-	1	$\phi = 32,6, c = 2,7$
Punch shear strength, MPa	29,14	39,93	5	35,3
DEFORMATION CHARACTERISTICS				
E-modulus (50% UCS), GPa	81,13	82,5	3	81,7
Poisson's ratio	0,251	0,288	3	0,267
GENERAL CHARACTERISTICS				
Hardness (Schmidt hammer)	50	58	20	54,75
Abrasiveness, %	-	-	1	12,5
Seismic wave velocity (P-wave), m/s	5373	5987	5	5781
Water absorption, %	0	0	3	0
Porosity, %	0,276	0,344	2	0,31
Density, kg/m ³	2665	2708	15	2692
Swelling (Free swell), %	0,066	0,075	2	0,071
Slake durability (7 cycles), %	-	-	1	99,31

Table 4.22 Characteristics of selected specimens of Tillite (7A) of the Karoo Supergroup.

ROCK TYPE: Tillite (7A)

ORIGIN: Karoo-Supergroup, Lake Mentz.

PETROGRAPHIC DESCRIPTION:

The rock consists of $\pm 40\%$ angular fragments and chips of quartz and minor feldspar, $\pm 10\%$ fragments of altered rocks (consisting of clinoziosite, kaolinite, chlorite and/or smectite). The matrix comprises $\pm 50\%$ of the rock. About 90% of the quartz fragments and chips are ± 0.018 to ± 0.36 mm in diameter and $\pm 10\%$ are up to 2 mm in size. The rock fragments are up to 0.5 mm large.

COMMENTS: No identification of the matrix was possible.

Tillite is a variable rock type in its different stages of weathering and its engineering characteristics are not very constant. The Tillite tested during this investigation was very homogeneous and unweathered. The uniaxial compressive strength for example 317 MPa, the triaxial strength (internal angle of friction) is $51,3^\circ$, the Brazilian tensile strength 18,1 MPa, the seismic wave velocity 5781 m/s, water absorption very low at 0% and density 2692 kg/m³. The base friction angle for this material is $32,6^\circ$. This value is average. No base friction angle could be found for tillite in the literature. No large specimens could be sampled.

4.4 Correlation of some rock properties

It is to be expected that there should be some relation between the various rock properties. This relation was studied for some properties and is presented below. In every case the trend line is shown on the correlation graph.

4.4.1 The relation between uniaxial compressive strength and point load strength.

The relation between uniaxial compressive strength (σ_c) and Point load strength (I_s) of the different rock types investigated were studied by correlating the two properties. Figure 4.2 illustrates this relationship. A reasonable correlation exists between the UCS and the point load strength. The correlation coefficient was determined as 0,6953. The relationship between the UCS and point load strength was found to be:

$$\sigma_c = 25,8 I_s$$

Bieniawski (1975) found the relationship to be: $\sigma_c = 24 I_s$

Since Bieniawski's research in 1975 a number of researchers investigated this relationship. It was found that the relationship between UCS and PLSI is dependent on the fabric of the rock

type. For example, testing the PLSI of a sedimentary rock parallel to its bedding planes would give a lower PLSI value than testing it perpendicular to the bedding planes. It is only in rock types with a massive fabric that some correlation could be expected.

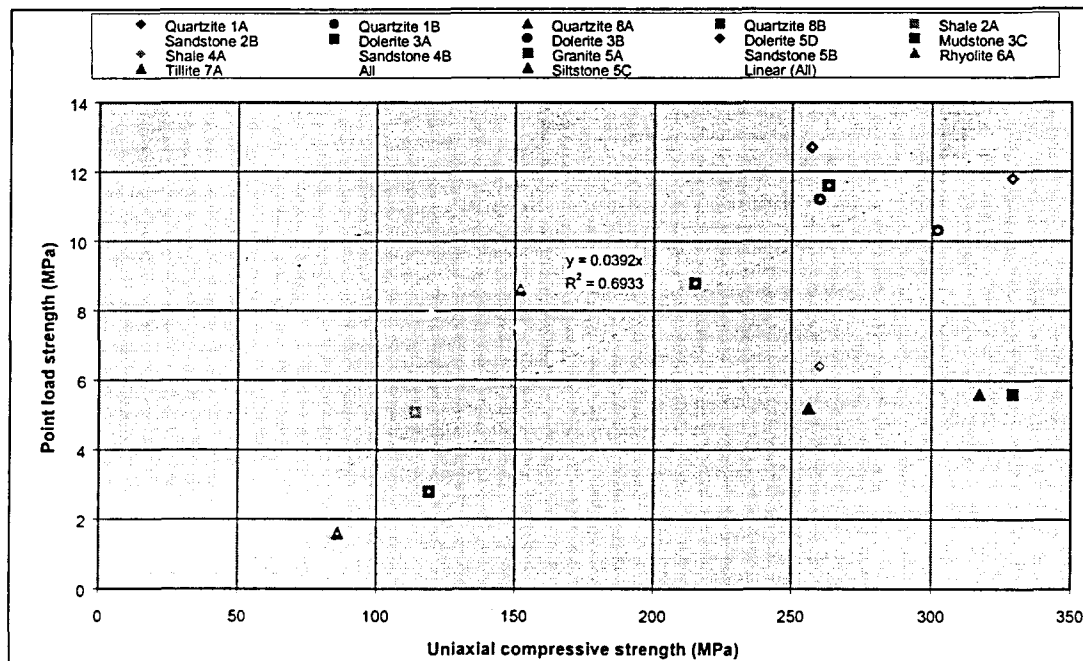


Figure 4.2 Correlation of point load strength vs uniaxial compressive strength.

An attempt was made to correlate UCS with PLSI. Rock types with anisotropy were not included in the calculation of the correlation coefficient. Rock types excluded from the calculation were Shale 4A, Siltstone 5C, Rhyolite 6A, Quartzite 8B and Sandstone 2B. Rock types with a more massive fabric gave a correlation coefficient of 0,6933. This indicates that there is some correlation between UCS and PLSI in rocks with a more massive structure.

4.4.2 The relation between Schmidt hammer hardness and uniaxial compressive strength.

Figure 4.3 illustrates the relation between Schmidt hammer hardness and uniaxial compressive strength. The curve was forced through the origin. The reason for this was to obtain a figure showing the origin and the scatter of observations. The relationship between UCS and Schmidt rebound number was found to be exponential. There is a very good correlation between these two properties as can be expected.

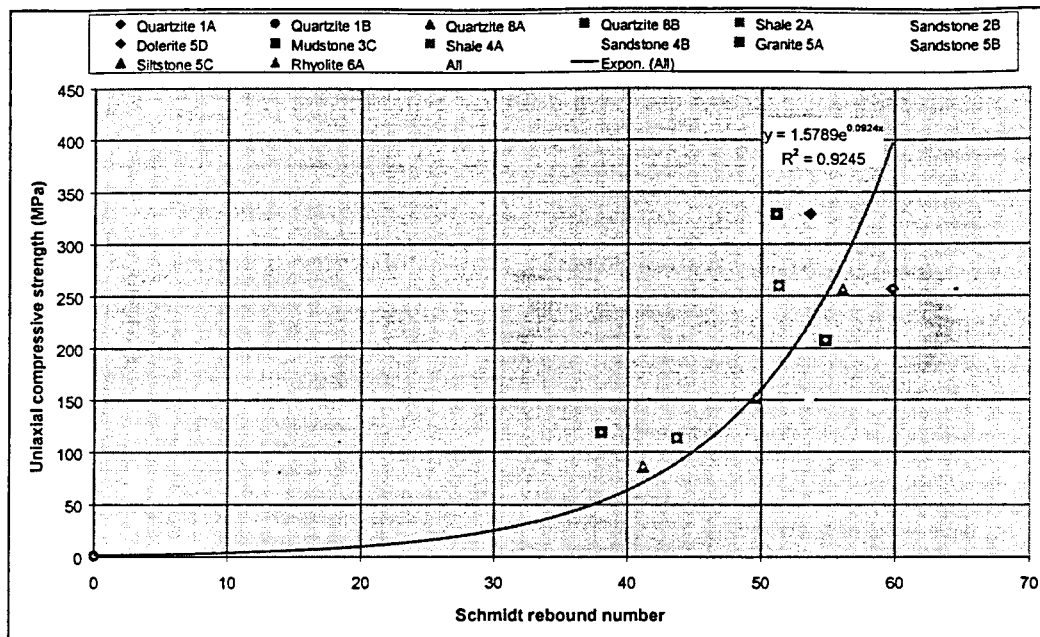


Figure 4.3 Correlation of Schmidt rebound number vs uniaxial compressive strength.

The correlation coefficient is 0,9245.

4.4.3 The relation between punch shear strength and uniaxial compressive strength.

Figure 4.4 illustrates the relation between punch shear strength and uniaxial compressive strength. The coefficient of correlation (R^2) is 0,6035. The relationship between the punch and uniaxial shear strength was found to be $UCS = 7,4$ punch shear strength.

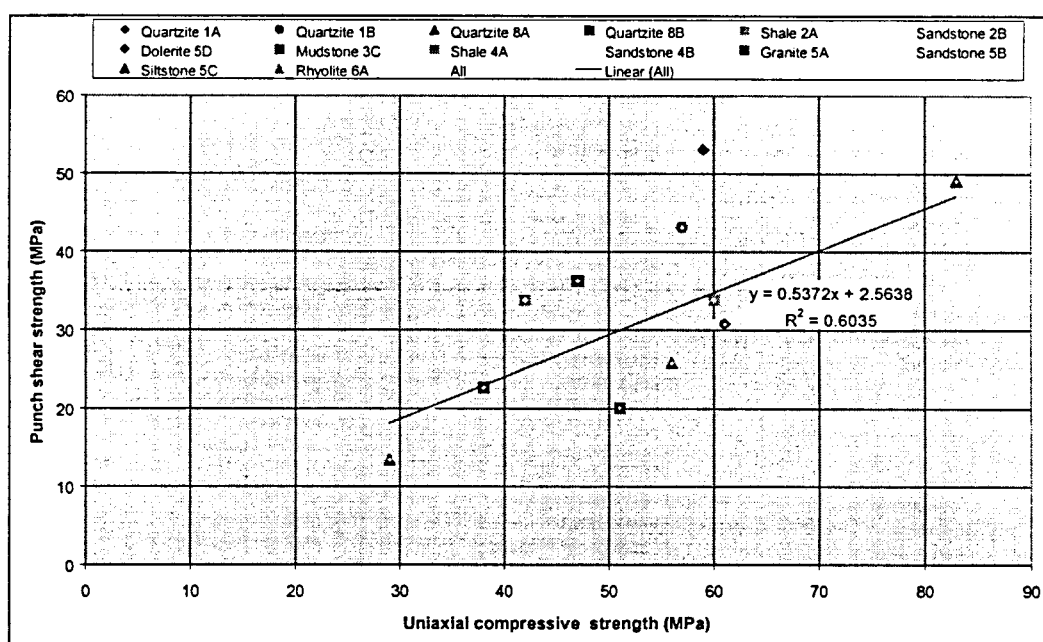


Figure 4.4 Correlation of punch shear strength vs uniaxial compressive strength.

4.4.4 The relation between Modulus of elasticity and Uniaxial compressive strength.

A correlation of tangent modulus vs uniaxial compressive strength was carried out for the rock types investigated. This correlation is a modified rock classification developed by Deere and Miller (1966). Modulus ratios of 500:1 and 200:1 are indicated on Figure 4.5

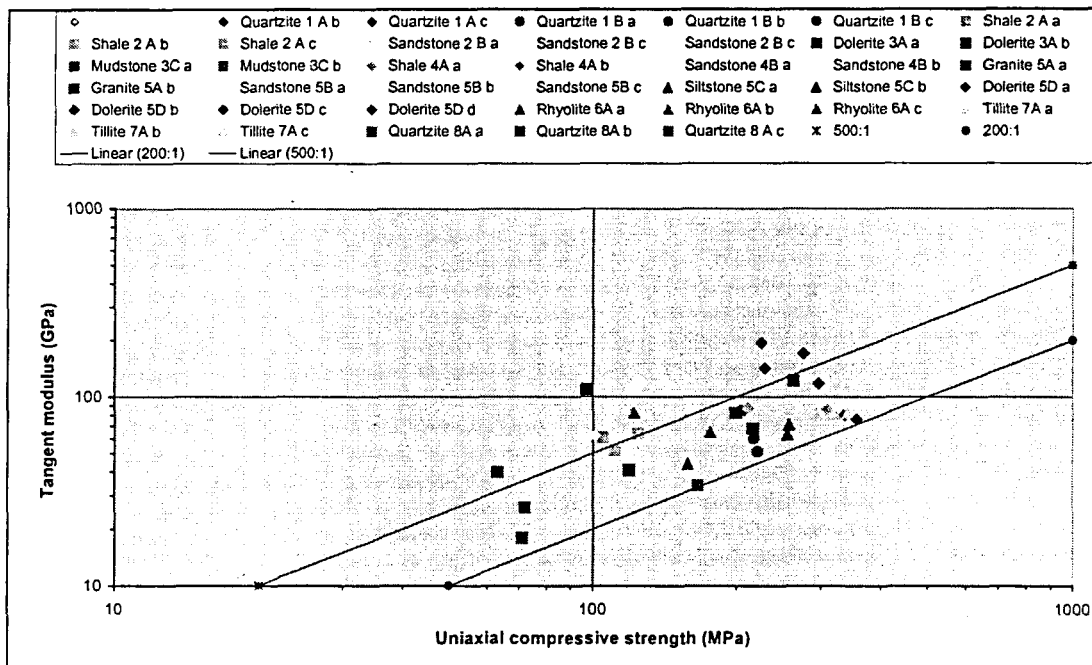


Figure 4.5 Correlation of tangent modulus vs uniaxial compressive strength

The various rock types seem to group together on the graph. Because UCS and E moduli were determined during the same test, the results of individual specimens could be plotted.

4.4.5 The relation between punch shear strength and Brazilian tensile strength.

The relation between punch shear strength vs tensile strength is illustrated in Figure 4.6. There is a very good correlation ($R^2 = 0,9205$) to be seen, after the points for Dolerite 3A, 3B and Shale 4A were omitted. The relationship between the tensile strength and punch shear strength was found to be: Brazilian tensile strength = 0,5 punch shear strength.

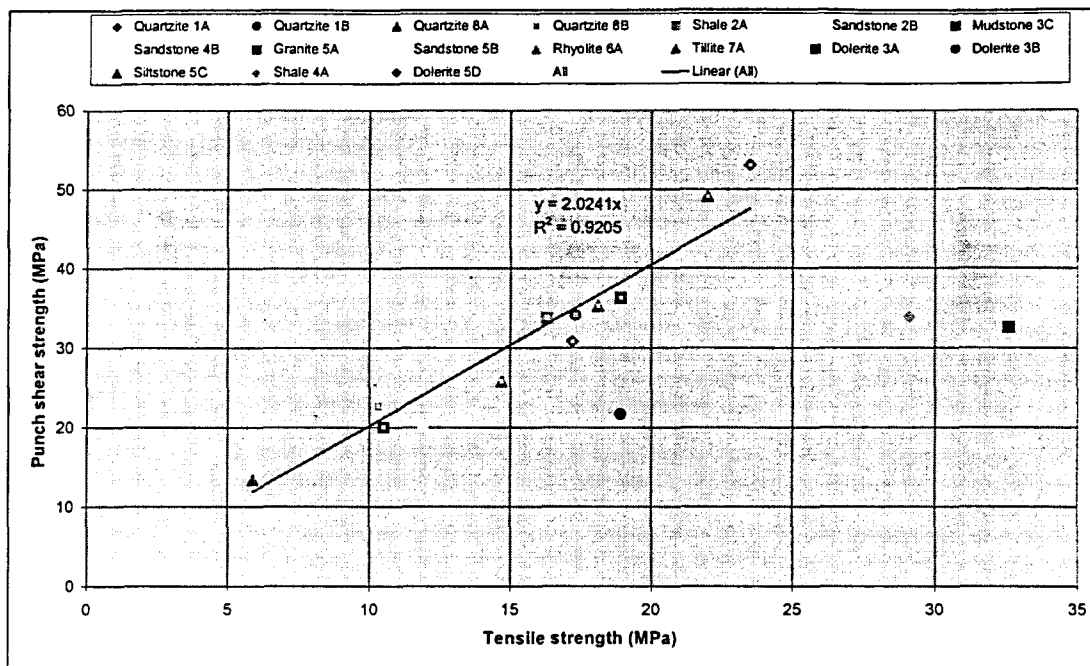


Figure 4.6 Correlation of punch shear strength vs tensile strength.

4.4.6 The relation between density and seismic wave velocity.

The relation between density and seismic wave velocity is illustrated in Figure 4.7

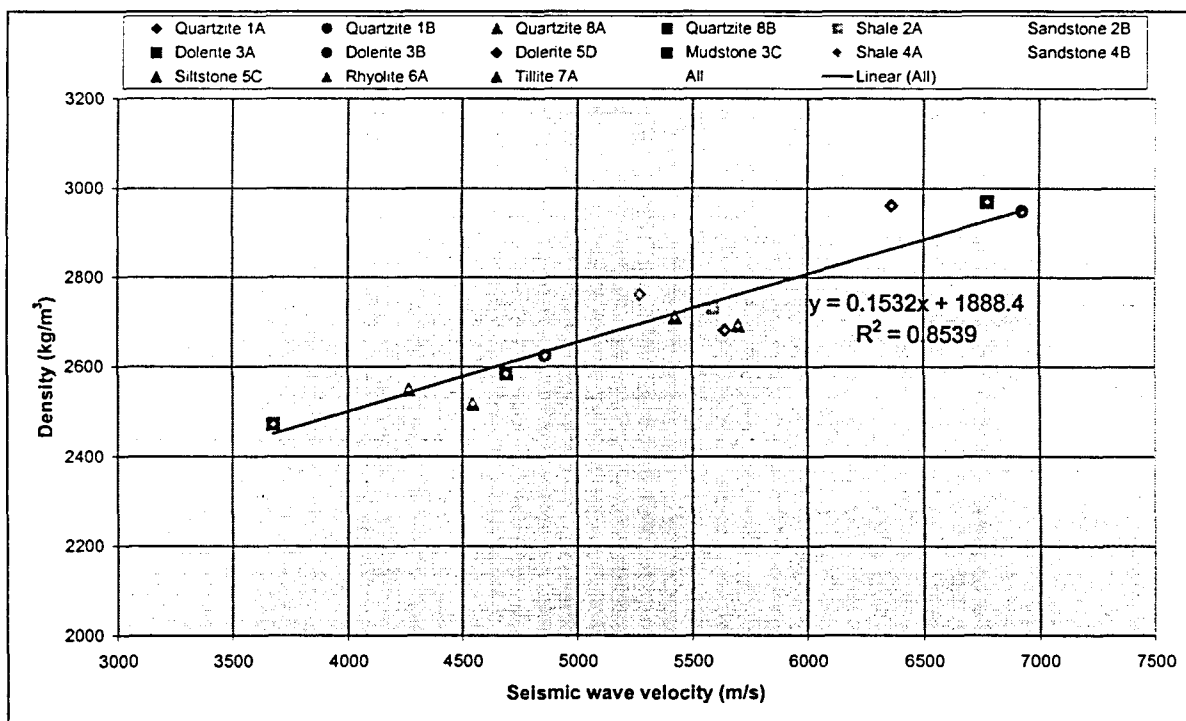


Figure 4.7 Correlation of density vs seismic wave velocity.

There is a very close relation between density and seismic wave velocity as can be expected. The coefficient of correlation (R^2) is 0,8539. The relationship between the seismic wave velocity and density was found to be seismic wave velocity = 5,57 density - 9763.

4.4.7 The relation between punch shear strength and cohesion from triaxial testing.

The relationship between punch shear strength and the cohesion of the triaxial test for the different rock types was analysed as it was expected that there should be a good relation between the two. This relation was indeed found. The coefficient of correlation (R^2) is 0,6075

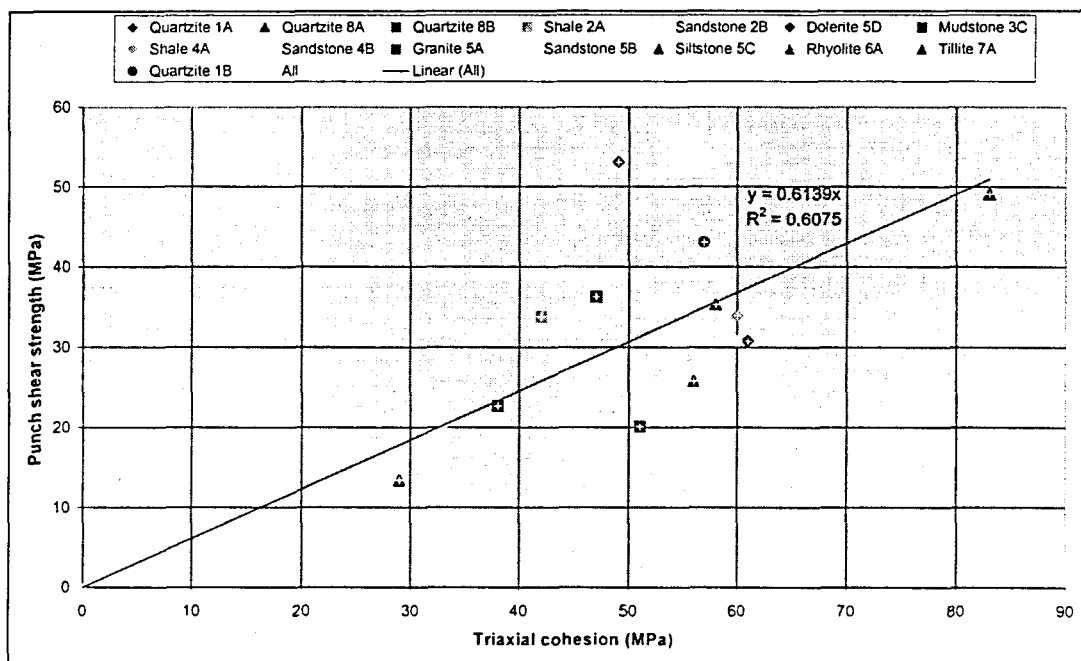


Figure 4.8 Correlation of punch shear strength vs triaxial cohesion.

4.4.8 Conclusion

Engineering properties were correlated to investigate the relationships between the different properties for the rock types investigated. In most cases a statistically acceptable correlation could be established. It must be kept in mind that rock material is usually not very uniform and can not be compared to other engineering materials such as aluminium, steel and even concrete as far as its properties are concerned. These engineering materials are much more uniform and research of their characteristics give much better correlation coefficients. A correlation coefficient of 0,7 and above for rock material can be considered as statistically acceptable.

4.5 Shear testing on large shear apparatus.

4.5.1 Phases of testing and testing procedure.

The shear-testing programme of natural joint surfaces of various types of rock eventually consisted of three phases of testing. The three phases of testing were:

(a) The first phase consisted of three tests at different vertical stresses, i.e. at approximately 600, 900 and 1200 kPa on dry rock samples. It was expected that this test phase would result in the determination of the peak shear strengths.

However, after analysis of the data it was decided to check the large shear apparatus for any faults as the tests appeared to have been wrongly executed and the results thus difficult to interpret. After adjustments to the apparatus and amendments to the software controlling the machine the second and third phases were carried out. Adjustments to the apparatus included fastening of loose screws and LVDT attachments. The software was partially rewritten to change the commands regulating the horizontal and vertical forces. During the first phase of testing the horizontal and vertical forces were wrongly initiated simultaneously, which meant these forces both increased concurrently to the set level. This was changed to allow the vertical force to reach its predetermined level before the horizontal force was initiated. Results of this testing phase are presented in Appendix E on the compact disc (CD) included in this report.

The results obtained during the first phase of testing must be regarded as unreliable as they were not conducted in accordance with international testing methods. They are however included and compared with residual shear strength results as obtained from the second and third phases, as much time and effort was spent in the sample preparation and execution of the testing.

(b) The second phase consisted of two sub phases, in this report referred to as phases 2A and 2B. Phase 2A was conducted on the same rock specimens as tested in Phase 1. This was done after adjustments to the large shear machine and software controlling the shear process had been made. The same normal stresses as used during the Phase 1 described in, were applied. At the beginning of this stage each specimen had already been sheared three times during Phase 1 and it was accepted that the results obtained were for residual shear strength. (Peak shear strength can only be determined once on every specimen during the first test on the joint surface). Supportive documentation is available in Appendix G.

Phase 2B was carried out immediately after Phase 2A without removing the specimen from the apparatus. All tests were conducted in the same manner as during phase 2A, but the

shearbox was filled with water to simulate submerged conditions. Supportive documentation is available in Appendix G.

(c) The third phase of the investigation involved the taking of the three new samples. They were numbered Granite 1C, 2C and 3C and prepared as described in chapter two of this report. Testing during this Phase (3A) was carried out at effective normal stresses of approximately 600, 900, 1200 and 1500 kPa. It was decided to use four normal loads, as this would give greater accuracy with four points on the shear stress vs. normal stress graph. Testing was also carried out in a forward direction and then the sample was cleaned (all debris of the previous test removed by blowing it off the surface), turned 180° around, placed in the testing machine and tested in the opposite direction (reverse). The reverse tests were also carried out at the same normal stresses. Thereafter the samples were tested in the forward direction under submerged conditions, using the same four normal loads. This was Phase 3B of the investigation. Supportive documentation is available in Appendix J.

4.5.2 Data analysis.

A detailed analysis of the results of the shear tests on large samples was carried out to determine the shear strength of the different rock types as well as the influence of geotechnical characteristics of the joint surfaces on the shear strength.

Barton and Choubey (1977) have shown that the relationship between shear stress and normal stress for lower stresses (both under 3 MPa) and smooth joints ($JRC = 5$) are linear. For higher stresses (shear stress up to 6 MPa and normal stress up to 4 MPa) on rough joints ($JRC = 20$) the relationship is curved. The relationship in all cases originates at 0.

Tests were conducted at normal stresses between 0,5 and 1,5 MPa. Normal stresses under a concrete dam are in this order of magnitude.

Analysis of the results of each test on each sample consisted of selecting three points on the graph of horizontal load vs horizontal displacement and evaluating the horizontal load (kN) and vertical load (kN) at each of these points. From the graph of vertical displacement vs horizontal displacement the deviation from horizontal (positive or negative) in degrees was determined to calculate the “corrected” shear load and normal load. The shear and normal stresses were then calculated. The normal stresses for all the samples were then plotted vs the shear strength (dry and saturated, see appendix I). Regression plots were then drawn and the coefficient of correlation and slope and X-intercept (c) calculated. (See appendix T for tables).

The **calculated peak friction angle** is the value of the friction angle as calculated with Barton’s formula. The **measured maximum residual friction angle** is the friction angle

determined by the highest shear load observation points on the shear load vs. displacement graph. The **measures minimum residual friction angle** is the friction angle determined by the lowest shear load observation points on the shear load vs. displacement graph. The **measures average residual friction angle** is the friction angle determined by the average shear load observation points (horizontal part of the graph) on the shear load vs. displacement graph.

4.6 Rock types tested

Specimens tested with the large shear apparatus during Phases 1 and 2 are listed in table 4.23. Five rock types were tested. These included three (3) basalt samples, three (3) dolerite samples, seven (7) granite samples, three (3) sandstone samples and three (3) mudstone samples. Some specimens were damaged during the first phase of testing and were not available for the subsequent testing programme.

Specimen	Origin	Surface characteristics	Schmidt Rebound	JRC	First cycle	Second cycle	Third cycle
Basalt 1	Lesotho	Rough, hard	54	8-10		Yes	Yes
Basalt 2	Lesotho	Rough, hard	56	8-10	Yes	Yes	Yes
Basalt 3	Lesotho	Rough, hard	52	6-8	Yes	Yes	Yes
Dolerite 1	Qedusizi	Rough, hard	46	4-6	Yes	Yes	Yes
Dolerite 2	Qedusizi	Rough, hard	40	2-4	Yes		
Dolerite 3	Qedusizi	Soft clay 1 mm	51	4-6	Yes	Yes	Yes
Granite 1	Driekoppies	Rough, hard	67	2-4		Yes	Yes
Granite 2	Driekoppies	Rough, hard	58	10-12	Yes		
Granite 3	Driekoppies	Rough, hard	60	8-10		Yes	Yes
Granite 4	Driekoppies	Rough, hard	65	8-10	Yes		
Granite 5	Driekoppies	Rough, hard	61	8-10	Yes	Yes	Yes
Granite 6	Driekoppies	Rough, hard	61	8-10	Yes	Yes	Yes
Granite 7	Driekoppies	Rough, hard	56	6-8	Yes	Yes	Yes
Sandstone 1	Natal	Rough, hard	22	6-8	Yes	Yes	Yes
Sandstone 2	Natal	Rough, hard	28	12-14	Yes		
Sandstone 3	Natal	Rough, hard	26	6-8	Yes		
Mudstone 1	Qedusizi	Rough, hard	28	2-4	Yes	Yes	Yes
Mudstone 2	Qedusizi	Rough, hard	40	2-4	Yes	Yes	Yes
Mudstone 3	Qedusizi	Rough, hard	40	2-4	Yes	Yes	Yes

Table 4.23 Specimens tested during the first and second phases of testing.

A suitable site for sampling specimens for the third phase of testing was located at the Nandoni Dam presently under construction in the Northern Province near Thohoyandou. A number of large samples were taken for shear testing in the laboratory. These samples were all taken from the quarry at the dam site as no suitable samples could be found in the dam foundation. They were all excavated from the rock mass with hand held tools. Care was taken that the joint surfaces were not damaged during the sampling process. Table 4.24 gives a description of the three granite specimens tested.

Specimen	Surface characteristic	Schmidt rebound number	JRC
Granite 1C	Rough clean	62	8 – 10
Granite 2C	Rough - FeO ₂ stained	61	8 – 10
Granite 3C	Rough - hard joint fill	58	8 – 10

Table 4.24 Granite specimens tested during the third phase of the investigation.

Although the three samples were taken from the same granite site it was not possible to get samples from the same continuous in situ joint surfaces. On closer inspection it was found that there were some variations in the characteristics of the joint surface sampled. Granite 1C had the smallest surface area of 15950 mm². The surface was not stained or covered by any joint fill. Granite material formed the contact surface. Granite 2C had a surface area of 30600 mm². The surface was lightly stained with iron oxide. No joint fill was present. Slightly weathered granite material formed the contact surface. Granite 3C had a surface area of 31500 mm². The surface was covered with joint fill in the form of a greenish secondary mineral. The joint fill material formed the contact surface. The joint roughness (JRC) of the three samples was approximately the same.

4.6.1 Basalt

Three basalt specimens were tested, two of which through phases 1, 2A and 2B. Table 4.25 presents a summary of the results obtained for phases 2A and 2B. The plots of shear stress vs normal stress for phases 2A and 2B are shown in Figure 4.9. The shear strength parameters are listed in table 4.25

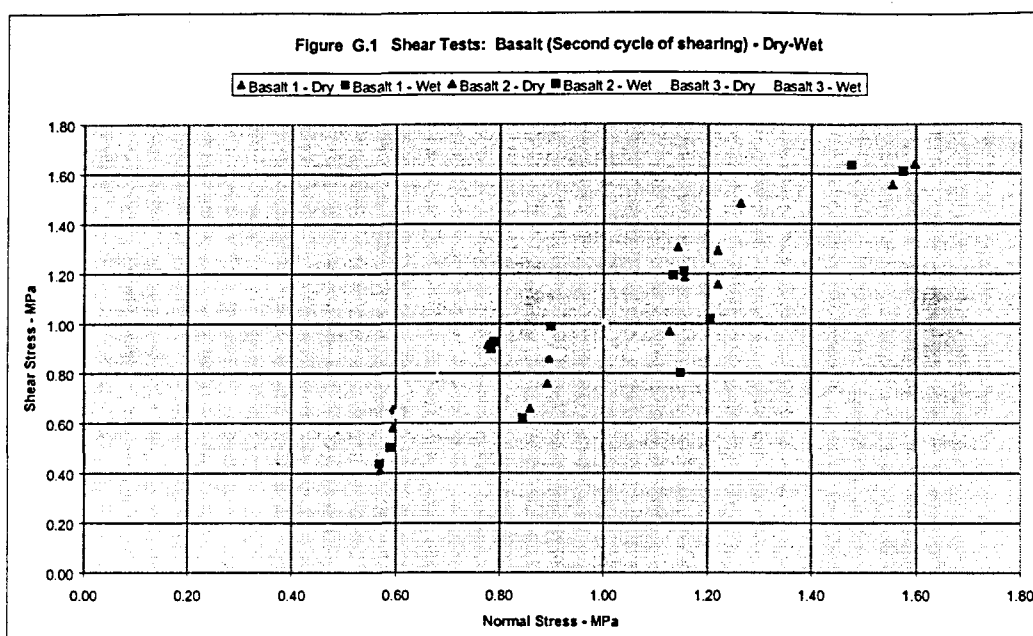


Figure 4.9 Shear stress vs normal stress observations of Basalt - Phases 2A and 2B of shearing of Basalt 1, 2 and 3.

Specimen	Angle of friction (degrees)		Apparent Cohesion (kPa)	Correlation coefficient of observation points on normal - vs. shear stress graph
	Value	Average		
Basalt 1 - Phase 2A (dry)	44		0	0,9256
Basalt 2 - Phase 2A (dry)	49	44	166	0,8839
Basalt 3 - Phase 2A (dry)	38		240	0,9934
Basalt 1 - Phase 2B (wet)	40		82	0,7952
Basalt 2 - Phase 2B (wet)	48	42	137	0,8248
Basalt 3 - Phase 2B (wet)	37		190	0,9962

Table 4.25 Shear strength parameters of basalt as determined during test Phases 2A and 2B.

DISCUSSION: The angle of friction seems to be reasonable as the basic friction angle for basalt has been reported as being between 35° and 38° (Coulson, 1972). The average submerged residual friction angle was determined as 42°. This is expected as Basalt is a hard rock (UCS or JCS = 200 MPa and Schmidt hardness = 53 - 57) with rough joint surface. The JRC was determined as 9.

4.6.2 Dolerite

Two of three Dolerite specimens were tested through the second phase of shearing. Figure 4.10 illustrates the normal stress vs. shear stress of Dolerite in the second phase of shearing (dry and submerged). The test results are listed in table 4.26.

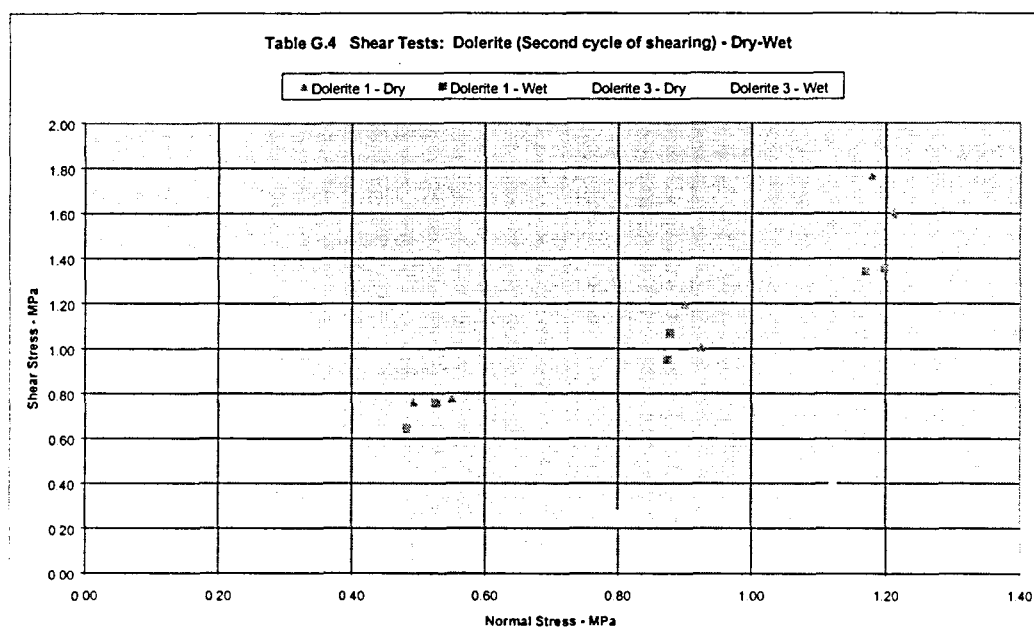


Figure 4.10 Shear stress vs normal stress observations of Dolerite - phases 2A and 2B of shearing (dry and submerged) of Dolerite 1 & 3

Specimen	Angle of friction (degrees)	Apparent cohesion (kPa)	Correlation Coefficient of observation points on normal - vs. shear stress graph
Dolerite 1 - Second phase (dry)	52,6	39	0,8872
Dolerite 3* - Second phase (dry)	17,0	95	0,8167
Dolerite 1 - Second phase (wet)	43,6	205	0,9731
Dolerite 3* - Second phase (wet)	14,9	8,5	0,8577

Dolerite 3* with 1mm clay layer on joint

Table 4.26 Friction angles and apparent cohesion for Dolerite as determined by this study.

DISCUSSION: Two of the three dolerite specimens were tested. There was a distinctive difference between the shear surfaces of the two specimens. Dolerite 1 was a hard, rough surface whilst Dolerite 3 had approximately one millimetre of clay on its surface. Shear strength of the two surfaces can thus not be compared nor correlated.

The angle of friction for Dolerite 1 was determined as 52,6° during phase 2A. This value seems to be high, as the basic friction angle for dolerite is 36°. The residual friction angle of Dolerite 1 was determined as 43,6° submerged (test phase 2B). This value seems to be on the high side, however it must be kept in mind that dolerite is a hard rock (UCS = 250 MPa, and Schmidt rebound number: 46). Another factor explaining the medium high friction angle is the roughness of the joint surface. The JRC is between 10 and 12. The roughness index was found to be 3,7. This "roughness index", a measure of roughness, was developed during this investigation and is fully described on page 4-60 of this report.

The residual friction angle of Dolerite 3 (on the clay filled joint) was determined as 17° dry and 14,9° submerged. These values seem to be on the low side, however it must be kept in mind that the joint fill is soft clay about 1mm thick. Another factor explaining the low friction angle is the smoothness of the joint surface. The JRC is 4 - 6. The roughness index is 7,7.

4.6.3 Granite

(a) Results of testing during phases 1, 2A and 2B

Seven specimens of Granite were tested, four through phases 1, 2A and 2B of testing. Table 4.27 shows the shear strength parameters obtained. Three specimens were tested in detail during phase 3 of this project.

The shear stress vs normal stress observations for phase 2A and 2B (dry and saturated) are plotted in Figure 4.11.

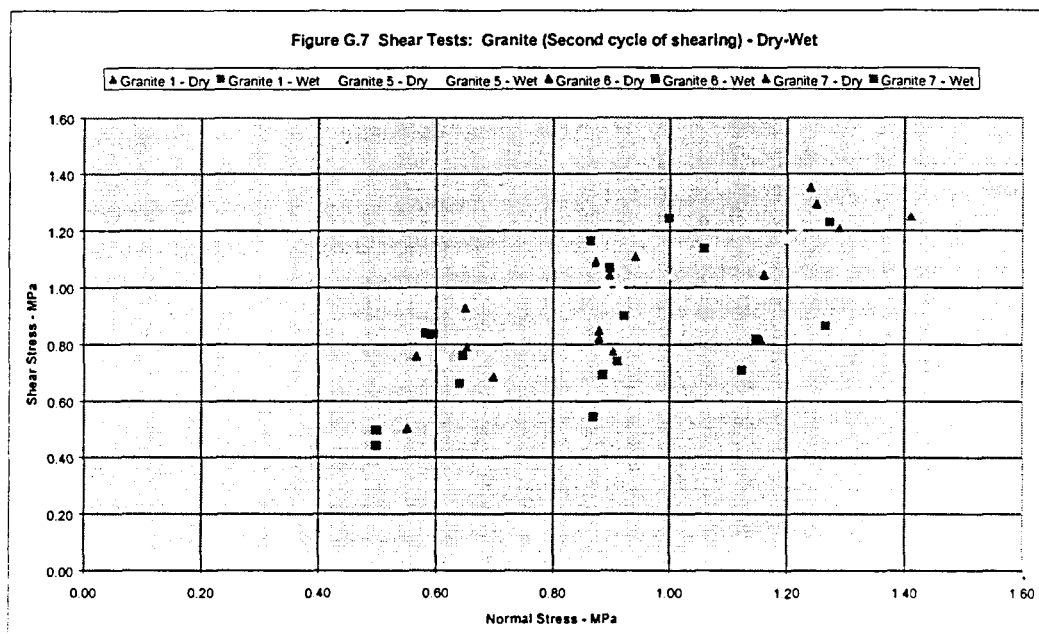


Figure 4.11 Shear stress vs normal stress observations of Granite – Phase 2A and 2B of shearing (dry and submerged)

Rock type and test phase	Angle of friction (degrees)		Apparent cohesion (kPa)	Correlation coefficient of observation points on normal - vs. shear stress graph
	Value	Average		
Granite 1 – Phase 2A (dry)	35,8	34,6	261	0,8092
Granite 5 – Phase 2A (dry)	40,0		231	0,9771
Granite 6 – Phase 2A (dry)	27,1		56	0,6152
Granite 7 – Phase 2A (dry)	35,3		440	0,9746
Granite 1 – Phase 2B (wet)	28,8	29,9	343	0,5883
Granite 5 – Phase 2B (wet)	37,5		279	0,9882
Granite 6 – Phase 2B (wet)	24,9		230	0,8364
Granite 7 – Phase 2B (wet)	28,2		394	0,8491

Table 4.27 Shear strength parameters of Granite as determined during phases 2A and 2B.

DISCUSSION: Four of the seven granite specimens were tested during the Phases 2A and 2B of testing. The granite specimens were moderately hard with rough surfaces. The basic friction angle for granite, 31° to 35° as reported by Coulson, (in Barton and Choubey, 1977) is in the same order of magnitude as the results obtained during this project. The residual friction angle of granite was determined as $34,6^{\circ}$ dry and $29,9^{\circ}$ submerged. These values seem to be as what could be expected as it must be kept in mind that granite is a moderately hard rock (UCS or JCS = 150 MPa and Schmidt rebound number 56 to 65). Another factor explaining the moderately high friction angle is the roughness of the joint surface. The JRC is 8 - 10. The roughness index is between 3,7 to 12,3.

(b) Results of testing during phase 3A and 3B

During the interpretation of the test results of Phase 2 it became clear that there were large variations between the calculated (peak) friction angles and the tested maximum residual friction angles. The reasons for this were unclear. It could be that, although the cumulative shear distance was in the order 80 mm after the first test and as much as 180 mm after the sixth test, the residual shear strength had not been reached for some samples with hard joint surfaces.

A further set of rock samples were selected and tested with great care and put through a cycle of four tests to try to determine the shear strength more accurately.

The results of the Phase 3 tests were evaluated and corrected for the shear angle with the horizontal and from the shear load vs. horizontal displacement graph (appendix J). A maximum, minimum and a general average called “other value” were determined and plotted on a shear stress vs. normal stress graphs. The angle of friction, cohesion and correlation coefficient for the trend line was determined for the forward, reverse and wet tests.

The test results of the third phase are summarised for each sample as follows:

(i) Granite 1C

Figure 4.12 is a graph of the shear stress vs. normal stress. The diamonds present the forward test result, the triangles the reverse and the circles the saturated test results. In each case a maximum (blue), minimum (red) and other (yellow) value is presented.

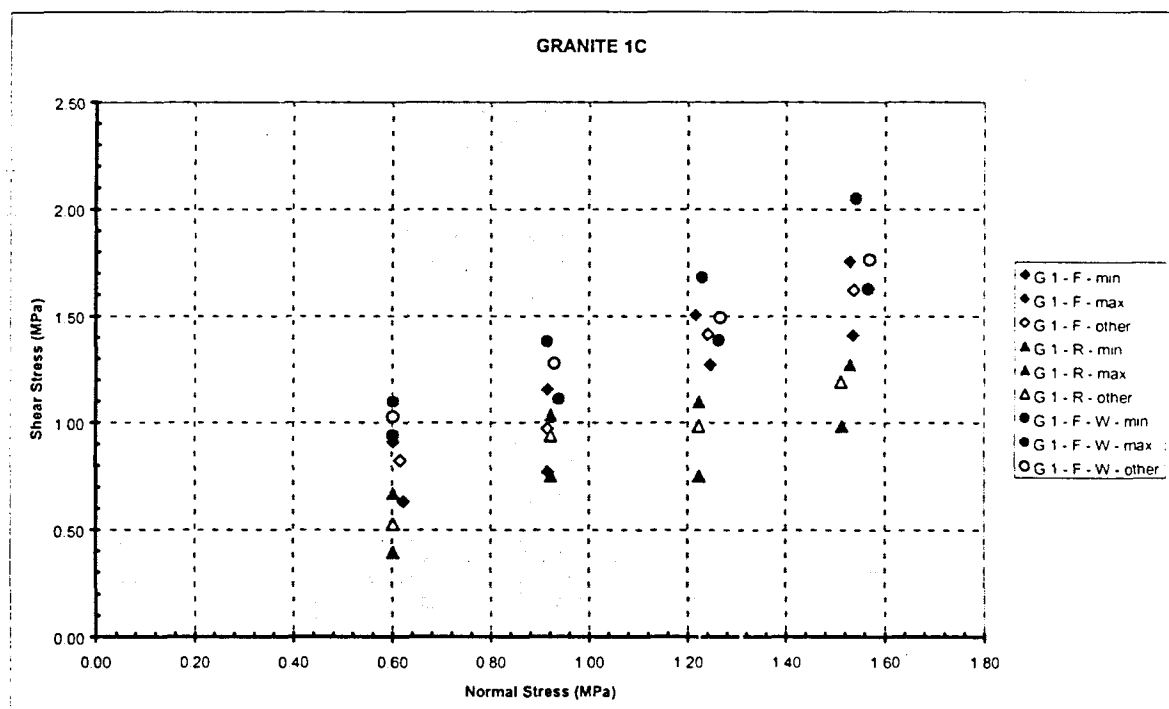


Figure 4.12 Shear stress vs. normal stress observations for Granite 1C.

The results for Granite 1C are summarised in Table 4.28

Shear direction and size	Apparent cohesion kPa	Friction angle Degrees	Correlation Coefficient of observation points on normal - vs. shear stress graph
Forward – minimum	228	42,7	0,9502
Forward – maximum	333	43,1	0,9937
Forward – other	215	42,7	0,9705
Reverse – minimum	99	30,3	0,8870
Reverse – maximum	369	31,3	0,9162
Reverse – other	192	34,0	0,9024
Forward (Wet) – minimum	476	35,8	0,9887
Forward (Wet) – maximum	471	45,2	0,9969
Forward (Wet) – other	575	36,7	0,9960

Table 4.28 Results of shear testing on Granite 1C.

DISCUSSION: The test in a forward direction yielded an angle of friction of between 42,7 and 43,1 degrees. The value for reverse is approximately 10 degrees lower, between 30,3 and 34 degrees. The value for the saturated sample's minimum and other is between 35,8 and 36,7 degrees. This is a good average. The maximum value of 45,2° is unexpected and no reasonable explanation could be found.

(ii) Granite 2C

Figure 4.13 is a graph of the shear stress vs. normal stress. The diamonds present the forward test result, the triangles the reverse and the circles the saturated test results. In each case a maximum (blue), minimum (red) and other (yellow) value is presented.

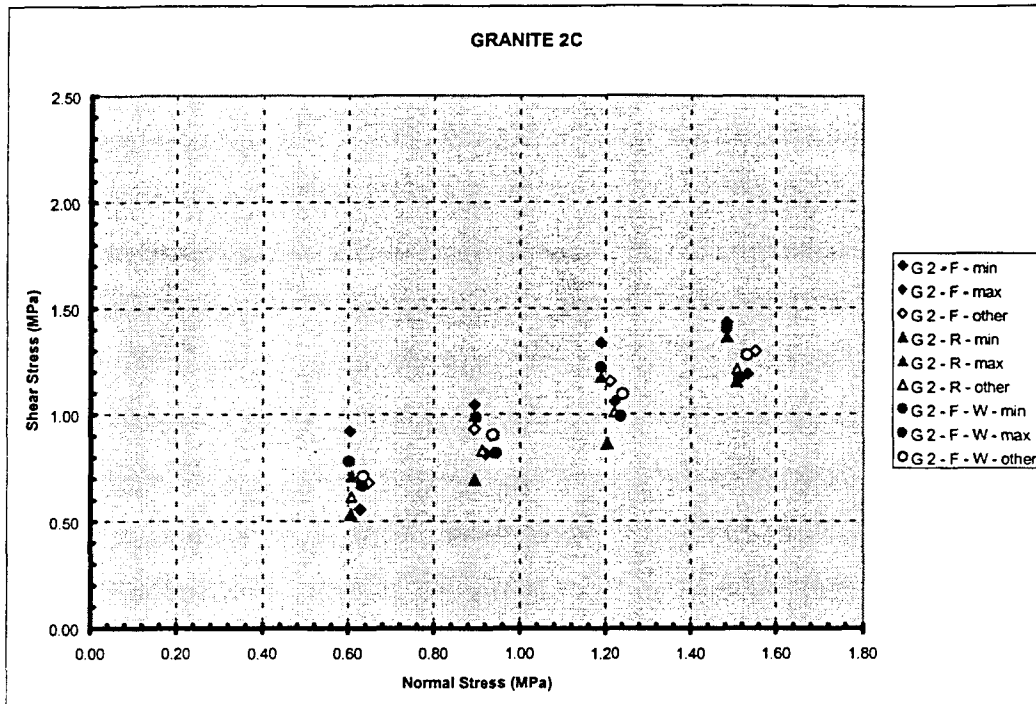


Figure 4.13 Shear stress vs. normal stress observations for Granite 2C.

The results for Granite 2C are summarised in Table 4.29.

Shear direction and size	Apparent cohesion kPa	Friction angle Degrees	Correlation Coefficient of observation points on normal - vs. shear stress graph
Forward – minimum	145	35,2	0,9764
Forward – maximum	536	31,8	0,9608
Forward – other	290	34,0	0,9662
Reverse – minimum	101	34,0	0,9802
Reverse – maximum	297	36,3	0,9874
Reverse – other	222	33,2	0,9984
Forward (Wet) – minimum	294	29,8	0,9955
Forward (Wet) – maximum	350	35,7	0,9978
Forward (Wet) – other	309	32,4	1,000

Table 4.29 Results of shear testing on Granite 2C.

DISCUSSION: The test in a forward direction yielded an angle of friction of between 31,8 and 34,0 degrees. The value for reverse is approximately the same, between 33,3 and 36,3 degrees. The value for the saturated sample's minimum and other is between 29,8 and 35,7 degrees.

(iii) Granite 3C

Figure 4.14 is a graph of the shear stress vs. normal stress. The diamonds present the forward test result, the triangles the reverse and the circles the saturated test results. In each case a maximum (blue), minimum (red) and other (yellow) value is presented.

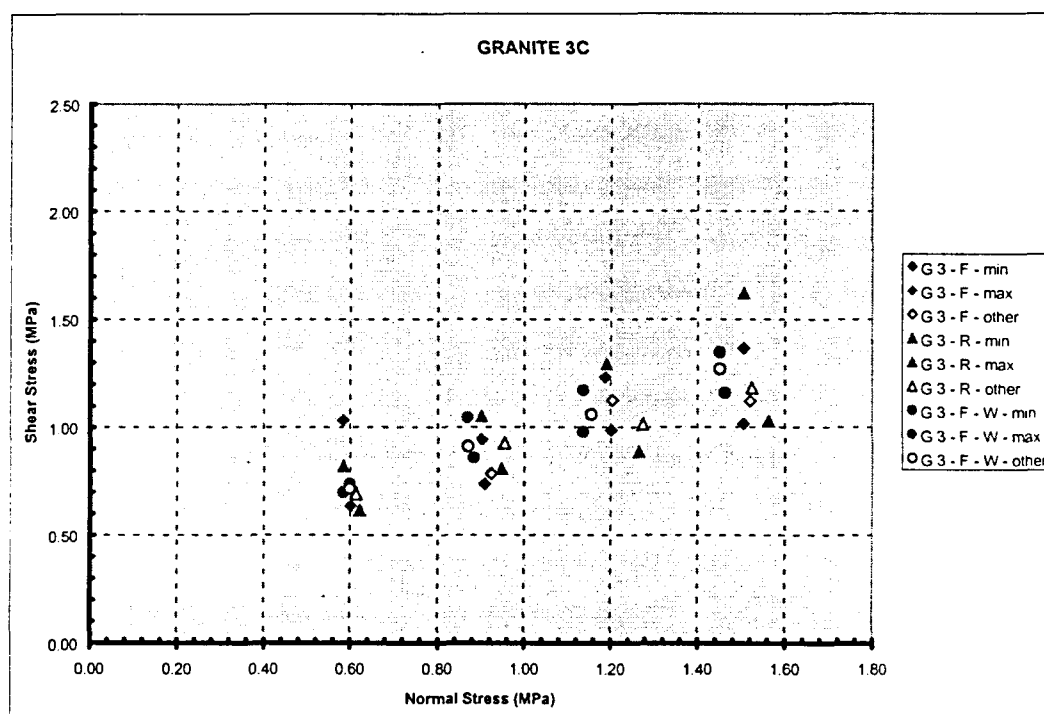


Figure 4.14 Shear stress vs. normal stress observations for Granite 3C.

The results for Granite 3C are summarised in Table 4.30

Shear direction and size	Apparent cohesion kPa	Friction angle Degrees	Correlation coefficient of observation points on normal - vs. shear stress graph
Forward – minimum	355	24,8	0,9216
Forward – maximum	705	22,7	0,7443
Forward – other	392	27,1	0,8426
Reverse – minimum	382	22,8	0,9778
Reverse – maximum	290	40,9	0,9930
Reverse – other	393	27,1	0,9716
Forward (Wet) – minimum	394	27,5	0,9989
Forward (Wet) – maximum	376	34,6	0,9573
Forward (Wet) – other	339	32,5	0,9962

Table 4.30 Shear stress vs. normal stress for Granite 3C.

DISCUSSION: The joint surface of Granite 3C was covered by approximately 1 mm of joint fill material. The joint fill comprised of a secondary green mineral, probably chlorite in an unweathered form. The joint surface had prominent striations in the direction of shearing. The test in a forward direction yielded an angle of friction of between 22,8 and 27,1 degrees. The values obtained for the reverse tests were 22,8°, 27,1° and 40,9°. The friction angle of 40,9° is very high and can not be explained. This test result is regarded as credible as the observations on the Normal stress vs. Shear stress graph gave a coefficient of correlation of 0,9930. The values obtained for the saturated sample's minimum is between 27,5 and for the other value 34,6 degrees.

4.6.4 Sandstone

Three specimens of Sandstone were tested, of which only one was tested through phases 1, 2A and 2B. The shear stress vs normal stress observations for phase 2A and 2B (dry and submerged) are plotted in Figure 4.15.

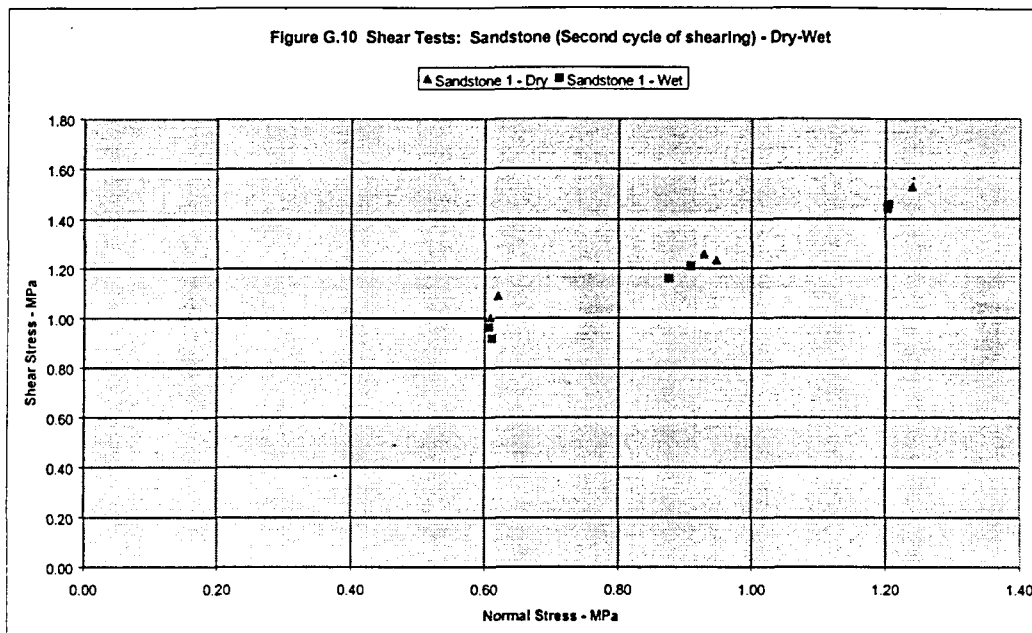


Figure 4.15 Shear stress vs normal stress observations of Sandstone – Phase 2A and 2B of shearing (dry and submerged)

Rock type and test phase	Angle of friction (degrees)		Apparent cohesion (kPa)	Correlation coefficient
	Value	Average		
Sandstone 1 – Phase 2A (dry)	37,6	-	558	0,9706
Sandstone 1 – Phase 2B (wet)	40,5	-	422	0,9944

Table 4.31 Shear strength parameters of Sandstone as determined during this study.

DISCUSSION: One sandstone specimen was tested through Phases 1, 2A and 2B. Sandstone 1 had a hard rough surface. The basic friction angle for sandstone is 26° - 35° as reported by Coulson, (in Barton and Choubey, 1977). The residual friction angle of sandstone 1 was determined as $37,6^{\circ}$ dry and $40,5^{\circ}$ saturated. These values seem to be moderately high, however it must be kept in mind that sandstone is a hard rock (UCS or JCS = 180 MPa and Schmidt rebound number is 22 - 26). Another factor explaining the high friction angle is the roughness of the joint surface. The JRC is between 10 and 12. The roughness index is 12,5.

4.6.5 Mudstone

Three specimens of Mudstone (Please note: Mudstone is referred to as Shale on the plates in the appendices) were tested, all three specimens through phases 1, 2A and 2B. Table 4.32 presents the shear strength parameters as determined during this study.

The shear stress vs. normal stress observations for the second phases (dry and submerged) are plotted in Figure 4.16.

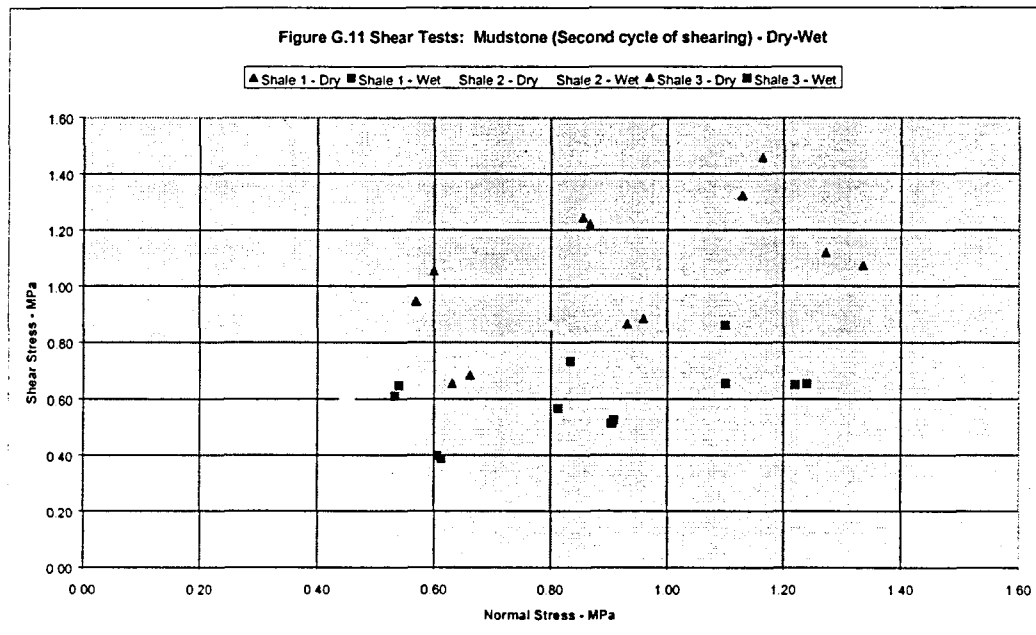


Figure 4.16 Shear stress vs. normal stress observations of Mudstone – Phase 2A and 2B of shearing (dry and submerged)

Rock type and test phase	Angle of friction (degrees)		Apparent cohesion (kPa)	Correlation Coefficient of observation points on normal - vs. shear stress graph
	Value	Average		
Mudstone 1 – Phase 2A (dry)	32,8	34,9	257	0,9785
Mudstone 2 – Phase 2A (dry)	37,0		252	0,9936
Mudstone 3 – Phase 2A (dry)	35,2		598	0,9260
Mudstone 1 – Phase 2B (wet)	22,6	16,8	141	0,9974
Mudstone 2 – Phase 2B (wet)	14,6		446	0,8450
Mudstone 3 – Phase 2B (wet)	13,2		487	0,3161

Table 4.32 Shear strength parameters of Mudstone as determined by this study.

DISCUSSION: Three mudstone specimens were tested. The basic friction angle for Mudstone is between 31° and 33° as reported by Coulson, (1972). The residual friction angle of mudstone was determined as 34,9° dry and 16,8° submerged. These values seem to be slightly on the high side during dry testing and very low during saturated conditions, however it must be kept in mind that Mudstone is a soft rock (UCS or JCS = 120 MPa and Schmidt rebound number between 28 and 40). Another factor explaining the average friction angle during dry testing is the smoothness of the joint surface. The JRC is between 2 and 4. The roughness index is 6,2 to 10.

4.7 Determination of hardness and roughness of joint surfaces tested in the large shear apparatus.

4.7.1 Hardness of joint surfaces

The strength of rock material is usually expressed in terms of uniaxial compressive strength (UCS). There is a very good correlation between UCS and Schmidt hammer (L) hardness of rock material but this is density sensitive. Figure 2.1 (Deere and Miller, 1966) gives this correlation (p 2-14 of this report). The Schmidt hammer hardness and densities for rock types used for the investigation, namely Basalt, Dolerite, Granite, Shale and Sandstone were determined and the corresponding uniaxial compressive strength were predicted using the same figure 2.1. The results of this exercise for the rock types tested are presented in table 4.33. There is a substantial difference between the predicted and the measured uniaxial compressive strength in some cases for the different rock types.

ROCK SAMPLE	DENSITY (measured) kg/m ³	SCHMIDT REBOUND NUMBER	UCS PREDICTED (MPa)	UCS MEASURED (MPa)
Basalt 1	2710	57	230 ± 100	162**
Basalt 3	2710	53	185 ± 80	
Dolerite 1	2969	46	170 ± 80	263
Dolerite 3	2969	51	180 ± 80	
Granite 1	2675	67*	300 ± 100	208
Granite 5	2675	61*	250 ± 100	
Granite 6	2675	61*	250 ± 100	
Granite 7	2675	56	190 ± 100	
Mudstone 1	2473	28	45 ± 22	119
Mudstone 2	2473	40	75 ± 30	
Mudstone 3	2473	32	50 ± 30	
Sandstone 1	2528	22	35 ± 20	86

(* Extrapolated) (** From literature, van Rooy, 1990)

Table 4.33 Hardness of joint surfaces determined as by Schmidt hammer and expressed in terms of uniaxial compressive strength .

4.7.2 Determination of roughness of joint surfaces

Roughness is certainly the most important joint surface characteristic determining the shear strength thereof. It is thus very important to have an instrument that can measure the roughness very accurately. A laser scanning apparatus that can measure the roughness of joint surfaces was developed in conjunction with the Department of Civil Engineering of the University of Natal. This apparatus is described in chapter three.

The surface roughness of all the rock samples tested in the large shear machine was determined with the laser apparatus before shear testing started. The raw data were processed with the software package "Micro station" and the results are presented in appendix M. Two sets of visual data are provided, namely (i) a contour diagram of the surface area as well as (ii) three roughness profiles through each sample. The three sections were taken along the centre-line of the sample; along the direction of shearing and on each side of the centre-line approximately 50 mm away respectively.

The roughness profile of each sample was also determined with a carpenter's comb. This was done along the centre-line of each sample. Placing the measured profile on top of Barton's profile as an overlay, a visual comparison of a roughness profile could be made. A reasonable correlation between the two methods was found. Figure 4.18 illustrates this finding. The complete set of profiles is presented in appendix N.

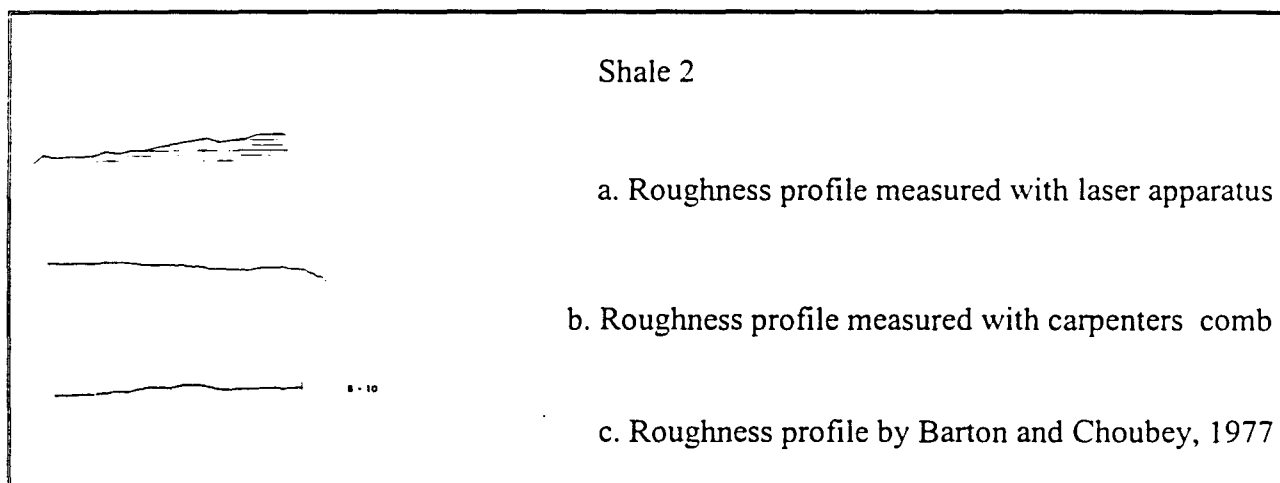


Figure 4.18 A comparison between roughness profiles along the centreline of a specimen determined by (a) the laser apparatus (b) the carpenters comb and (c) roughness profile by Barton and Choubey (1977).

A comparison of the roughness profiles taken from each sample with the typical roughness profiles developed by Barton and Choubey (1977) (figure 2.4 in this report) produced a JRC value for each of the samples tested. Table 4.34 gives the JRC for samples tested.

ROCK SAMPLE	JRC RANGE	GEOTECHNICAL DESCRIPTION OF SURFACE
Basalt 1	8 - 10	Rough, undulating, cooling joints, unweathered Basalt
Basalt 2	8 - 10	Rough, undulating, cooling joints, unweathered Basalt
Basalt 3	6 - 8	Rough, undulating, cooling joints, unweathered Basalt
Dolerite 1	4 - 6	Rough, undulating, cooling joints, unweathered Dolerite
Dolerite 3	1 - 2	Smooth planar joint filled with 1 mm clay, unweathered Dolerite
Granite 1	2 - 4	Smooth planar, cooling joint, unweathered Granite
Granite 5	8 - 10	Rough, planar, techtonic joints, unweathered Granite
Granite 6	8 - 10	Rough, planar, techtonic joints, unweathered Granite
Granite 7	6 - 8	Rough, planar, techtonic joints, unweathered Granite
Granite 1C	8 - 10	Rough, planar, techtonic joints, unweathered Granite
Granite 2C	8 - 10	Rough, planar, techtonic joints, unweathered Granite
Granite 3C	8 - 10	Rough, planar, techtonic joints, unweathered Granite
Mudstone 1	2 - 4	Smooth planar, bedding joints, unweathered Mudstone
Mudstone 2	2 - 4	Smooth planar, bedding joints, unweathered Mudstone
Mudstone 3	2 - 4	Smooth planar, bedding joints, unweathered Mudstone
Sandstone 1	6 - 8	Rough, undulating, bedding joints, slightly weathered Sandstone

Table 4.34 Measured joint roughness coefficient (JRC) for large rock samples tested

Another way to express roughness is to determine the volume of material above the lowest point on the shear surface of a rock specimen. Further analysis of the data obtained with the laser apparatus indicated that it was indeed possible to calculate the volume of material above the lowest point on the shear surface. The shear surface area was also calculated. This was done for all specimens tested in the large shear apparatus and for which roughness determinations with the laser apparatus were done. To normalise this value the calculated volume is divided by the surface area of the specimen tested. The volume-area ratio is a

measure of joint roughness, hereafter called the **roughness index**. Table 4.35 is a summary of the volumes and surface areas calculated as well as the roughness index (effective roughness).

ROCK SAMPLE	SURFAC EAREA (mm ²)	VOLUME (mm ³)	ROUGHNESS INDEX (effective roughness) (mm)	RESIDUAL ANGLE OF FRICTION (degrees) (Dry)
Basalt*				
Dolerite 1	32409	113504	3,50	52,6°
Dolerite 2	31943	286164	8,96	-
Dolerite 3	14972	116010	7,75	-
Granite 1	17148	63725	3,72	35,8°
Granite 2	46151	565190	12,25	-
Granite 3	41431	400467	9,65	-
Granite 4	38978	551303	14,14	-
Granite 5	21566	265649	12,32	40,0°
Granite 6	15058	126932	8,43	27,1°
Granite 7	15805	102023	6,46	35,3°
Mudstone 1	31256	314552	10,05	32,8°
Mudstone 2	10304	64401	6,21	27,0°
Mudstone 3	12365	99869	8,07	35,2°
Sandstone 1	18373	236771	12,89	47,1°
Sandstone 3	21554	271383	12,59	-

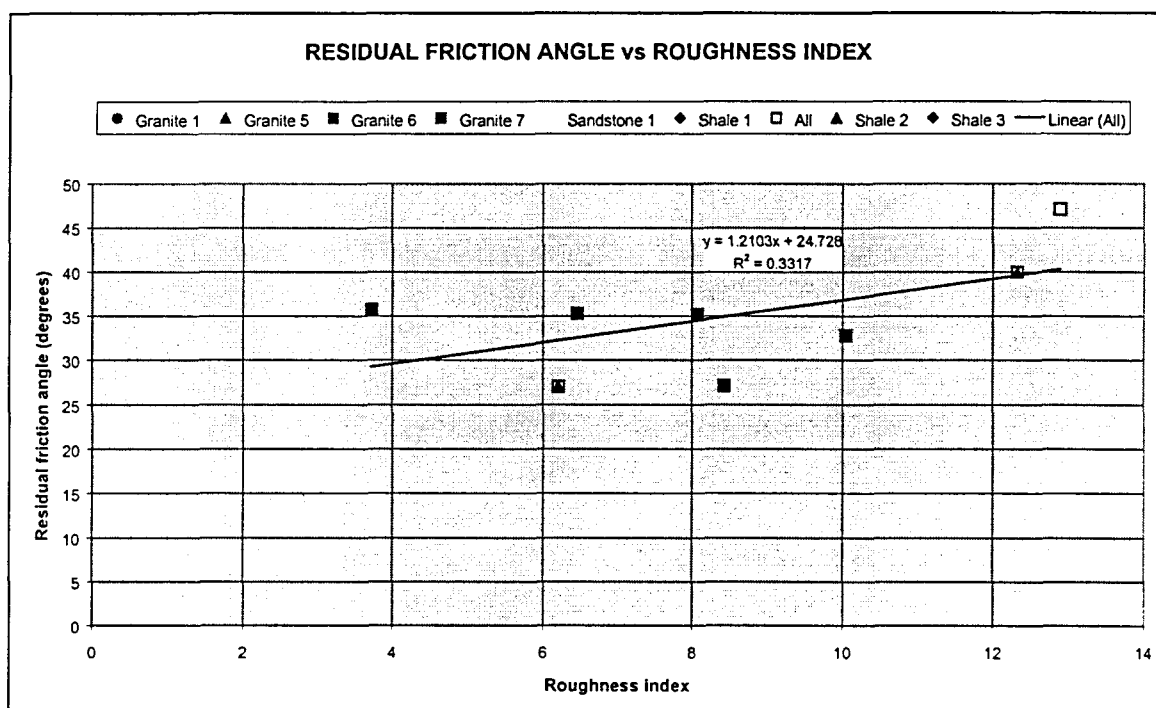
* Basalt specimens were not scanned for roughness

*Warning: A number of the joint surfaces were at an angle when scanned. The calculated volume values obtained for many of the rock samples were therefore influenced.

Table 4.35 Calculated roughness index for large samples tested during phase 2.

A correlation between the roughness index and the shear strength was then attempted. Figure 4.19 is a plot of residual friction angle against roughness index. Inspection of the volumes obtained through the surface scan and subsequent analysis revealed very large volumes for

joint surfaces that were relatively smooth (see Mudstone 1,2 and 3). It was subsequently realised that some of the joint surfaces were at an angle when scanned and that the volume values obtained for many rock samples were thus not reflecting the true representation. This is also substantiated by the very weak correlation obtained for data in Figure 4.19. Although the results from this attempt are disappointing, it is still believed that this method can be used to quantify roughness, but it will require some refinement. This method should receive attention during further studies in this field. It is also recommended that the relation between the peak friction angle and the effective roughness be further investigated.



*Warning : the joint surfaces were at an angle when scanned and that the volume values obtained for many rock samples were not correct.

Figure 4.19 Correlation between friction angle and effective roughness.

4.7.3 Correlation of joint roughness, hardness and shear strength

A detailed analysis of the results of the shear tests on large samples was carried out to determine the shear strength of the different rock types, as well as the effect of geotechnical characteristics of joint surfaces on the shear strength.

The analysis of each sample consisted of selecting three points on the graph of horizontal load vs horizontal displacement and reading off the horizontal load (kN) and vertical load (kN) of

each of these points. From the graph of Vertical displacement vs Horizontal displacement the deviation from horizontal (positive or negative) in degrees was determined.

Rock type	Residual angle of friction	Apparent cohesion (kPa)	Number of Tests	Number of points
Basalt (dry)	38,5° - 49,2°	0 - 240	6	22
Basalt (submerged)	37,0° - 48,2°	83 - 190	3	18
Dolerite (dry)	52,6°	40	1	6
Dolerite (submerged)	43,6	205	1	6
Dolerite (dry - clay infill)	17°	95	1	6
Dolerite (submerged - clay infill)	14,9°	9	1	6
Granite (dry)	27,1° - 40,0°	57 - 440	5	30
Granite (submerged)	24,9° - 38,2°	280 - 394	5	30
Mudstone (dry)	32,8° - 37,0°	252 - 598	3	18
Mudstone (submerged)	13,2° - 22,6°	141 - 487	3	18
Sandstone (dry)	37,6°	558	1	6
Sandstone (submerged)	40,5	422	1	6

*All the testing was done at approximately 0,6; 0,9 and 1,2 MPa normal stress

Table 4.35 Shear strength parameters for samples tested in the large shear apparatus during Phase 2.

The shear and normal stresses are then calculated. The normal stresses for all the samples are then plotted vs the shear stresses (dry and submerged) - (see Appendix G). Regression plots were then drawn and the coefficient of correlation and slope and intercept (C) calculated (see appendix T for tables). A second set of calculations of these characteristics was done with the X-intercept equal to zero. This way the angle of friction was determined by taking the value with the highest correlation coefficient. Table 4.35 illustrates the range of values for angle of friction and cohesion for the different types of rock

4.8 Discussion of testing and results of Phase 2.

It can be assumed that the effective normal stress (σ_n) under a concrete dam foundation of moderate size is in the order of 1 MPa or 1000 kPa. This was the reasoning for choosing effective normal stresses of 600, 900, 1200 kPa for testing during the phase 2 and effective normal stresses of 600, 900, 1200 and 1500 kPa during the phase 3.

Roughness was determined with a carpenter's comb and compared with Barton and Choubey's (1977) roughness profiles and the joint roughness coefficient (JRC) was so obtained. The hardness of joint surfaces was determined with a Schmidt hammer and the joint wall compressive strength (JCS) calculated using Barton and Choubey's (1977) formula.

The contribution to the angle of friction by roughness and hardness was determined by using formula [5.1]. By adding the basic friction angle to this value, the total friction angle can be determined. Table 4.37 presents these results of this calculation for rock types tested for Phase 2 of the investigation.

Rock type	JRC	JCS (MPa)	Basic friction ϕ_b (degrees)	Contribution of JRC & JCS to friction angle (degrees)	Calculated peak friction angle Barton (degrees)
Basalt 1	9	234	35	21	56
Basalt 3	7	188	35	16	51
Dolerite 1	5	163	36	11	47
Granite 1	5	347	31	13	44
Granite 5	9	280	31	22	53
Granite 6	9	280	31	22	53
Granite 7	7	213	31	16	47
Mudstone 1	3	42	31	5	36
Mudstone 2	3	76	31	6	37
Mudstone 3	3	51	31	5	36
Sandstone 1	7	32	31	10	41

Table 4.37 Friction angles for rock types as calculated with the Barton and Choubey (1977) empirical equation for shear strength at normal stress (σ_n) = 1000 kPa.

The contribution of hardness and roughness of the joint surfaces to the total friction angle of the joint plane varied between a minimum of 5° and a maximum of 22°. The minimum values of 5° and 6° are for the Mudstone with smooth and moderately hard joint plane surfaces. The basic friction angle for Mudstone is 31°. The total friction angle is thus 36° to 37°. The maximum values of 13° to 22° were found to be that for granite where the joint surfaces was rough and hard. The basic friction angle for Granite is also 31°. The total friction angle is thus 44° to 53°.

The calculated **peak** friction angle was then compared with the maximum **residual** friction angle as determined by testing of joint planes during this study. Table 4.38 presents the results of this comparison. Normally, calculated **peak** friction angle should not be compared with **residual** friction angles, in this case they were, as the maximum value determined is the only value that was obtained with the available specimens.

Rock type	Calculated peak friction angle (Barton) (degrees)	Determined residual friction angle (dry) (by testing) (degrees)	Difference in friction angle	
			<i>Degrees</i>	<i>Percentage</i>
Basalt 1	56	44	-12	-21,4
Basalt 2	56	49	-7	-12,5
Basalt 3	51	38	-13	-25,5
Dolerite 1	47	52,6	+6	+12,8
Dolerite 3 (Clay)	48	17	-	-
Granite 1	44	36	-8	-18,2
Granite 5	53	40	-13	-24,5
Granite 6	53	27	-26	-49
Granite 7	47	35	-12	-25,5
Mudstone 1	36	33	-3	-8,3
Mudstone 2	37	37	0	0
Mudstone 3	36	35	-1	-3
Sandstone 1	41	38	-3	-7,3

Table 4.38 Difference between the calculated peak and tested residual friction angles for rock types tested during phase 2. (Calculated peak friction angle = 100%).

Ideally, calculated peak friction angles (with Barton's empirical formula) should be compared with tested peak friction angles. When testing rock specimens for shear strength in a large shear apparatus where high normal stresses are applied, only the result of the first shear is a true peak test result. The following cycles of testing take place on a surface damaged by previous testing. To obtain the angle of friction (ϕ) and the cohesion of a joint surface at least three (3), but preferably four (4), tests must be carried out at different normal loads. The angle of friction of a test carried out in this manner can thus not be called a "peak". In this chapter "residual" refers to the results obtained as described above. There is thus merit in the argument of comparing the peak and "maximum residual" friction angles.

It is obvious from table 5.2 that the differences between calculated and tested friction angles are small, between 0° and 3° for rock with smooth moderately hard joint surfaces (in this case Mudstone 1, 2 and 3). Greater differences, 7° to 13° were found for rock with very hard and rough joint surfaces (Basalt 1,2 and 3) as well as for Granite (phase 2 testing) where the difference varies between 8° and 26° .

An even greater difference was found for Dolerite 3 (see table 5.3). A peak friction angle of 48° was calculated but the a cycle of three tests gave a residual friction angle of 17° . This is because Dolerite 3 had a clay layer as joint fill material for which Barton's equation does not make provision.

The conclusion from this research is that Barton's equation is applicable for smooth and moderately hard joint surfaces. Higher friction angles were calculated by Barton's equation than were determined in the laboratory for hard rough joint surfaces. It is generally accepted that Barton's formula is not applicable for filled joints.

The effect of water on the shear strength is demonstrated in table 4.39 where the tested friction angle (dry) and tested friction angle (submerged) are listed.

Rock type	Determined residual friction angle $\phi_{(Dry)}$ (degrees)	Determined residual friction angle $\phi_{(Saturated)}$ (degrees)	Difference between dry and saturated friction angles ϕ (degrees)
Basalt 1	44	40	-4
Basalt 2	49	48	-1
Basalt 3	38	37	-1
Dolerite 1	52,6	43,6	-9
Dolerite 3 (Clay)	17	14,9	-2,1
Granite 1	35,8	28,8	-7
Granite 5	40,0	37,5	-2,5
Granite 6	27,1	24,9	-2,2
Granite 7	35,3	28,2	-7,1
Mudstone 1	32,8	22,6	-10,2
Mudstone 2	37	14,6	-22,4
Mudstone 3	35,2	13,2	-22
Sandstone 1	37,6	40,5	+2,9

Table 4.39 Difference between dry and saturated friction angles.

The effect of water on the friction angles of different rock types is illustrated in table 4.39. From this table it is evident that, as can be expected, rock types with hard, rough joint surfaces are only slightly influenced by the presence of water as far as friction angles are concerned. This is especially true for Basalt (with JRC = 7 - 9 and JCS = 188 - 234 MPa) where the difference between dry and submerged is between 1 and 4 degrees.

The influence of water is the greatest on friction angles of smooth moderately hard joint surfaces JRC = 3 and JCS = 43 - 76 MPa where the differences between dry and saturated is 10,2 degrees for Mudstone 1 and 22 to 22,4 degrees for Mudstone 2 and 3.

The friction angles for clay filled joints is affected by water. The friction angle of a clay filled joint tested for Dolerite 3 is as low as 17°. Submerged in water it falls to 14,9°.

4.9 Discussion of testing and results of Phase 3

During the interpretation of the test results of phase 2 it became clear that there were large variations between the calculated (peak) friction angles and the tested residual friction angles. The reasons for this were unclear. It could be that, although the cumulative shear distance was in the order 80 mm after the first cycle (three dry tests) and as much as 180 mm after the sixth test (another three saturated cycles), the real residual shear strength had not been reached for some of the samples with hard joint surfaces.

It was decided to investigate a further set of rock samples with great care and through four cycles of testing to try to determine the shear strength more accurately.

Rock type	JRC	JCS (MPa)	Basic friction ϕ_b (degrees)	Contribution of JRC & JCS to friction angle (degrees)	Calculated peak friction angle Barton (degrees)
Granite 1C	9	185	31	20,4	51,4
Granite 2C	9	190	31	20,7	51,7
Granite 3C	9	205	31	20,8	51,8

Table 4.40 Friction angles for granite as calculated with the Barton and Choubey (1977) empirical equation for shear strength at normal stress (σ_n) = 1000 kPa.

From table 5.4 it is evident that all three granite samples had the same roughness coefficient (profile). The JRC was equal to 9 in all three cases. The joint compressive strengths were also very much the same, in the order of 200 kPa. The contribution of these two characteristics to the friction angle in all three examples is expected to be the same, as calculated in table 4.40. The calculated contribution was between 20,4° and 20,8°. However, the tested other residual friction angle was between 36° (for Granite 1C) and 7,4° (for Granite 2C) higher than the calculated peak angle of friction. The tested angle of friction is lower than the calculated peak for Granite 3C with joint fill material present. See table 4.41 for this information.

Rock type	Calculated peak friction angle (Barton) (degrees)	Tested maximum residual friction angle (dry) (by testing – other) (degrees)	Difference in friction angle	
			Degrees	Percentage
Granite 1C	51,4	42,3	-9,1	-18
Granite 2C	51,7	34,0	-17,7	-34
Granite 3C	51,8	27,1	-27,7	-48

Table 4.41 Difference between the calculated peak and tested residual friction angles for granite tested during Phase 3. (Percentages calculated in relation to calculated peak).

The influence of water on the residual friction angle is shown in Table 4.42. From this figure it is evident that water saturated joints have a negative effect on the friction angle. This influence is between 1,6 and 6 degrees. However, during testing of granite 3C (with a secondary mineral as joint fill material) it was found that the presence of water had a positive effect on the angle of friction. The residual angle of friction in a saturated state was 5,4° higher than the dry residual friction angle.

Rock type	Tested residual friction angle $\phi_{(Dry)}$ (degrees)	Tested residual friction angle $\phi_{(Saturated)}$ (degrees)	Difference between dry and saturated friction angles ϕ (degrees)
Granite 1C	42,7	36,7	-6
Granite 2C	34,0	32,4	-1,6
Granite 3C	27,1	32,5	+5,4

Table 4.42 Difference between dry and saturated friction angles of granite specimens tested.

CHAPTER FIVE

ESTIMATION OF SHEAR STRENGTH USING A GEOTECHNICAL CHARACTERISATION OF THE JOINT SURFACE

5.1 Introduction

Geotechnical characteristics of joint surfaces in a rock mass can usually be described with relative ease on site. Sampling and testing of these joints is much more difficult and do take a long time to carry out. Design engineers usually want to have an estimate of the shear strength of joint sets in a rock fairly early during the design stage of a structure in a rock mass. If the shear strength could be linked to a geotechnical description of the joints in a rock mass then a first estimate of the shear strength could be made. This would satisfy the immediate need of the design engineer. A preliminary design could then be done at an early stage while sampling and testing for actual design purposes is carried out. This research concentrated on doing just that. The findings are discussed in this chapter.

The shear strength of joint surfaces in a rock mass has been a difficult parameter to determine. Several researchers, including Amadei and Seab (1990), Barton and Choubey (1977), Goodman (1976), Nicholson (1983) and other authors have investigated this problem. This chapter contributes to the existing knowledge of shear strength by describing the results of shear tests on a number of southern African rock types tested on the large shear machine described in chapter three. The rock types used for the investigation were Basalt, Dolerite, Granite, Shale and Sandstone.

5.2 Joint surface parameters

The shear strength parameters of joints in a rock mass are affected by a number of factors as described in Chapter 2. To simulate these factors in a laboratory is virtually impossible and here only the most important factors are discussed once more. These are:

- (i) Hardness of the joint surface
- (ii) Roughness of the joint surface
- (iii) The influence of water
- (iv) The effects of joint fill material

An attempt was made to estimate the shear strength parameters by describing geotechnical properties of the joint surface, including hardness, roughness, joint fill material present and the presence of water. These factors were correlated with the shear strengths measured during large scale shear testing.

5.3 The theory of shear strength in jointed rock.

Barton and Choubey (1977) described the empirical relation of shear strength of joints in rock as follows:

$$\tau = \sigma_n \tan [JRC \log_{10} (JCS/\sigma_n) + \phi_b]$$

where τ = peak shear strength (kPa)
 σ_n = effective normal stress (kPa)
 JRC = joint roughness coefficient
 JCS = joint wall compressive strength (kPa)
 ϕ_b = basic friction angle (obtained from residual shear tests on flat unweathered rock surfaces) (degrees)

From this relation it is apparent that there are three important factors determining the shear strength of joints in rock. They are:

- (i) the basic friction angle of the rock material,
- (ii) the joint roughness (JRC), and
- (iii) the joint wall compressive strengths (JCS).

The following portion of the formula above can express the contribution of roughness and hardness of the joint surface to the total friction angle:

$$[JRC \log_{10} (JCS/\sigma_n)] \dots\dots\dots [5.1]$$

5.4 Classification of joint surfaces for the prediction of shear strength

5.4.1 Joint surfaces in hard rock

(a) Joints with no joint fill material present

In a rock mass where joint surfaces are characterised by moderate to high joint roughness coefficient values (JRC above 6 according to Barton and Choubey, 1977) and moderate to high joint compressive strength values (UCS above 80 MPa), the shear strength is determined by these characteristics. The peak shear strength can be calculated using Barton and Choubey's empirical formula (1977). In essence the peak angle of friction consists of the basic friction angle plus the contribution of the hardness plus that of the roughness.

Granite 1C serves as an example:

Characteristic	Empirical value By Barton	Tested value
Basic friction angle		31°
$JRC \log_{10} (JCS/\sigma_n)$	13°	
Peak angle of friction	44°	43,1°
Residual angle of friction		37,0°
Residual angle of friction (saturated)		27,5°

Table 5.1 Friction angle characteristics of Granite 1C.

The tested peak angle of friction is actually not a peak, due to practical constraints, but is a maximum of the first three tests (at different normal loads) on the shear surface. This maximum and calculated peak for the specimen corresponds quite well.

(b) Joints with staining on hard and rough joints

These joints have the same characteristics as the joints described in (a) above

Example from this research programme is Granite 2C:

Characteristic	Empirical value	Tested value
Basic friction angle		31°
$JRC \log_{10} (JCS/\sigma_n)$	12°	
Peak angle of friction	43°	35,2°
Residual angle of friction		31,8°
Residual angle of friction (saturated)		29,8°

Table 5.2 Friction angle characteristics of Granite 2C.

The tested peak angle of friction is actually not a peak, due to practical constraints, but is a maximum of the first three tests on the shear surface.

The shear strength of Granite with joints that are not filled in any way and those that are stained can be determined by the empirical formula of Barton and Choubey (1977).

The following conclusions could be made for unfilled joints and joints that are lightly stained in hard rock:

- (i) the basic friction angle is the minimum friction angle of a particular joint
- (ii) the contribution of the roughness and hardness of the joint could be added to the basic friction angle to obtain a design parameter.
- (iii) the angle of friction is not significantly affected negatively by the presence of water.

5.4.2 Joints in rock with fill material present

In the case where joints are filled with a secondary mineral or soft fill material, the peak shear strength can not be determined by the empirical formula of Barton and Choubey (1977). During the testing programme three samples were tested that indicated that rock with filled joint material has angles of friction considerably lower than was expected. The results are illustrated in Table 5.3 below.

Characteristic	Granite 3C (Phase 3)	Mudstone (Phase 2)	Dolerite (Phase 2)
Basic friction angle	31,0°	31,0°	36,0°
Calculated peak friction angle	40,9°	46,2°	49,9°
Measured max. residual friction angle	22,1°	35,2°	17,0°
Measured saturated max. residual friction angle	27,5°	14,6°	14,9°

Table 5.3 Comparison of basic, calculated peak, measured max. residual and measured saturated max. residual friction angles of some rock types tested.

(i) An example from this research programme is Granite 3C:

In this case the joint fill material (chlorite) results in a maximum residual friction angle much lower than the basic friction angle of the rock.

(ii) Another example is the Mudstone tested during Phase 2.

In this case the joint fill material (a very thin layer of clay) results in a maximum residual friction angle much lower than the basic friction angle of the rock.

(iii) Another example is the Dolerite tested during Phase 2.

In this case the joint fill material (a 1 mm thick layer of clay) results in a maximum residual friction angle much lower than the basic friction angle of the rock.

For filled joints in moderate to hard rock or joints in soft rock, the following conclusions can be made :

(i) the basic friction angle of the rock material is **not** the minimum friction angle of a particular joint. The minimum can be substantially lower than the basic angle of friction.

(ii) the angle of friction is affected negatively by the presence of water if the infill consists of clay.

5.5 Application of shear strength in the design of concrete dam foundations.

In the design of the stability of a concrete dam foundation the worst possible situations must be designed for. This includes joint sets with unfavourable dip, full water uplift pressure acting on joint surfaces and the maximum force on the concrete structure as a result of water in the reservoir at maximum overflow conditions.

Important parameters used in the design of concrete dam foundations include the following:

- * the orientation of important joint sets in the rock foundation
- * the shear strength of joints in the rock mass
- * the direction and size of the forces acting on the rock foundation as a result of
 - (i) the concrete structure and
 - (ii) the water in the reservoir
 - (iii) the uplift pressure of the water

Instability can occur as a result of sliding of the concrete structure along an unfavourable joint set with insufficient shear strength, or rotation of the concrete structure around the toe of the structure. The design of every structure, including the foundation as part of the structure, should be treated separately and investigated in detail.

5.6 Guidelines for the use of information contained in this report

It is important to note that the results of the research conducted during this study is very specific to the rock specimens tested during the conducted testing programme.

CHAPTER SIX

CONCLUSIONS

6.1 The **objectives** of this research project were:

(a) to determine and to analyse, the shear strength of joints in a number of rock types, sampled at different locations and to link these strengths to the conditions of the foundations and in particular the condition of the surfaces of the rock joints. The information so obtained can then serve as a data bank for the design of new dams and for the evaluation of the safety of existing dams, and

(b) to determine the characteristics of a number of southern African rock types to serve as preliminary design parameters to allow safer and more economical designs for the foundations of concrete dam walls.

The results for (a) were obtained for a small number of rock types, including dolerite, granite, mudstone and quartzite and to some extent for basalt and sandstone, whilst the results for (b) were reached for most common southern African rock types.

6.2 A comprehensive literature study was conducted that found that although engineering characteristics of rock material are investigated on a continuous basis for civil and other engineering applications, this information is not readily available to the engineering community as clients and contractors regard it as confidential information. This report is probably the most comprehensive source of engineering characteristics of southern African rock types available today.

6.3 This report describes the strength, deformation and general characteristics of quartzite, shale, sandstone, dolerite, mudstone, granite, rhyolite and tillite in detail.

6.4 The emphasis was placed on the shear strength of discontinuities in rock. The basic shear strength parameters of the different rock materials were determined as part of the determination of rock material characteristics. The angle of friction obtained for the different materials correspond very well with those in the literature.

6.5 It was also envisaged to determine the peak and residual shear strength parameters of important southern African rocks. To achieve this objective the Department of Water Affairs and Forestry, in association with the technical subcommittee for this project, had a large shear box apparatus built that was used for testing of large specimens as well as rock fill material. This report describes the design and construction of the apparatus, the test method as well as results of shear testing large specimens.

6.6 Testing with the large shear box apparatus was conducted in three phases. During the first phase the peak shear strength parameters were determined under dry conditions. The second phases (2A and 2B) involved determination of the residual shear strength parameters under dry and submerged conditions and the third phases (3A and 3B) a record of the polishing effect after repeated testing of three granite samples under dry and submerged conditions. The same specimens were used through phases 1, 2A and 2B.

6.7 The first phase was carried out between 28 September 1995 and 10 June 1996. It was intended to determine the peak shear strength parameters during this phase. This phase of testing consisted of three cycles of shear testing under increasing normal stress. Normal stresses for the testing were in the order of 600; 900 and 1200 kPa.

6.8 Evaluation of the test results of the first phase revealed certain problems. The shear load vs. shear displacement graphs was difficult to interpret. Further detailed investigation discovered a problem with the software controlling the shear- and normal load actuators. With the start of the shear test the normal- and shear loads increased simultaneously. The normal load should have been at a set maximum before the shear load was applied. When this was realised a specialist consultant in the person of Mr UW Vogler was appointed to help with the interpretation of results as well as supervision over the second and third phases.

6.9 Before the second and third phases the shear apparatus was inspected and all bolts and LVDT's fastened properly. The software used to drive the apparatus was scrutinised to ensure correct instruction during testing.

6.10 The second and third phases were carried out between 25 March 1998 and October 2000. The aim was to determine the residual shear strength parameters during this phase. These tests were conducted under dry and submerged conditions. Each phase of testing consisted of three cycles of shear testing under increasing normal stress. Normal stresses for the testing were in the order of 600; 900 and 1200 kPa for Phase 2 and 600; 900; 1200 and 1500 kPa for Phase 3.

6.11 The shear strength parameters of joints in rock are mainly influenced by (i) the hardness and (ii) the roughness of the joint surfaces. Both these parameters were during the study. The hardness of each joint surfaces was determined with a Schmidt hammer and related to the uniaxial compressive strength as reported by Barton and Choubey, 1977.

6.12 A two dimensional laser scanning device was developed by the the Department of Civil Engineering of the University of Natal during the investigation of the hydraulic roughness of unlined boarded tunnels. This was a project funded by the Water Research Commission. As part of this research project a three dimensional laser scanning device was developed and built in association with the Department of Civil Engineering of the University of Natal. This device measures x, y and z co-ordinates on a rock joint surface on a grid pattern. This information can be manipulated with software on a computer to produce a contour diagram of the joint surface area. From this joint roughness profiles can be obtained.

6.13 The roughness of each shear surface was also determined with a carpenter's comb and related to typical roughness profiles after Barton and Choubey, 1977. A method was also developed to present a three dimensional image of the topography of a joint surface that could be used to quantify joint roughness. Another way to express roughness is to determine the volume of material above the lowest point on the shear surface of a rock specimen. Further analysis of the data obtained with the laser apparatus indicated that it was indeed possible to calculate the volume of material above the lowest point on the shear surface. The shear surface area could also be calculated. This was done for all specimens tested in the large shear apparatus and for which roughness determination with the laser apparatus was done. To normalise this value the calculated volume is divided by the surface area of the specimen tested. The roughness index is a measure of joint roughness.

6.14 A third phase of investigation was undertaken to determine the validity of the test results during the second phase of testing. This phase concluded the project during October 2000. Three Granite samples were tested in detail. Every sample was tested in a forward as well as reverse direction. Tests were also carried out with the sample saturated. Four normal loads were applied to have four observation points on the graph to correlate. It is concluded that although problems were encountered during the second phase of testing, the results can be used with confidence.

6.15 Emphasis was placed on the shear strength parameters of joints, especially the angle of friction. Two types of joints are recognised in nature: (a) joints with no or little fill material where the shear strength is strongly influenced by the characteristics of the rock material and (b) joints with fill material where the shear strength is determined by the characteristics of the fill material. The major part of this research concentrated on (a) joints with no or little fill material. The three major characteristics determining the shear strength parameters of this type of joint are (i) the base shear strength of the rock material, (ii) the roughness profile along the joint surface and (iii) the hardness of the material on the joint surface.

6.16 This study contributes to the knowledge of shear strength on southern African rocks types, in particular on the sampling of specimens, preparation of specimens for testing in the large shear apparatus, the measurement of the roughness and hardness of the joint surface, the testing procedure. To a lesser extent the study provides typical values of the shear strength characteristics of the rock joints. Further work still needs to be done in this regard.

CHAPTER SEVEN

RECOMMENDATIONS

7.1 This report contains a comprehensive database of engineering characteristics of rock types that can be used as a guide for initial safety and design purposes. It must be kept in mind that sampling and testing of large rock specimens is a time consuming process and engineering design parameters are usually needed in the early phases of a civil engineering project. The results of this study can be used for preliminary design purposes. It is recommended that for the design of any major structure a comprehensive study of the engineering characteristics of the foundation material should still be undertaken.

7.2 It is recommended that a new project be initiated to investigate the shear strength of representative southern African rock types in further detail in a systematic manner. Such an investigation can build on the knowledge obtained in this investigation. It is important to keep the variables such as rock type, weathering, and hardness as few as possible and to investigate the influence of joint roughness.

7.3 The roughness index, developed during this project, should be further investigated.

CHAPTER EIGHT

REFERENCES

Amadei, B. and Seab, S (1990) Constitutive models of rock joints. Rock Joints, Balkema, Rotterdam, 1990.

Barton, N. and Choubey, V (1977) The Shear Strength of Rock Joints in Theory and Practice. Rock Mechanics 10, 1 - 54, 1977

Barton, N. (1971) A relation between joint roughness and joint shear strength. Proc. Int. Symp. on Rock Mech. Rock Fracture. Nancy. Paper I-8

Barton, N. (1982) Modelling Rock Joint Behaviour from In Situ Block Tests: Implications for Nuclear Waste Repository Design. Technical Report ONWI-308, Terra Tek, Inc, September 1982.

Barton, N. and Bandis, S. (1991) Review of Predictive Capabilities of JRC-JCS Model in Engineering. Norwegian Geotechnical Institute, Publication Nr 182, Oslo, 1991.

Barton, N. (1991) Scale effects of Sampling Bias? Norwegian Geotechnical Institute, Publication Nr 182, Oslo, 1991.

Barton, N.R. (1974) A review of the shear strength of filled discontinuities. Publication 105. Norwegian Geotechnical Institute, Oslo.

Bieniawski, Z. T. (1975) The point load test in geotechnical practice. Engineering Geology, Vol 9, pp 1 - 11.

Bridges, M.C. (1975) Presentation of fracture data for Rock Mechanics. Proceedings of the 2nd Australian - New Zealand Conference on Geomechanics. Brisbane.

Brink, A. B. A. (1983) Engineering Geology of Southern Africa. The Karoo Sequence - Volume 3. Building Publications, Pretoria.

Brink, A. B. A. (1983) Engineering Geology of Southern Africa. The first 2 000 million years of geological time - Volume 1. Building Publications, Pretoria.

Broch, E and Franklin, J. A. (1972) The point load strength test. Int. Jl. Rock Mechanics and Mining Science, Vol 9, pp 669 - 697.

Brown, E. T. (Ed) (1981) Rock characterisation, Testing and Monitoring. International Society for Rock Mechanics (ISRM) suggested methods, Pergamon Press.

Cook N. G. W. (1988) Natural joints in rock: Mechanical, Hydraulic and Seismic Behaviour and Properties under Normal Stress. Int. J. Rock Mech. Min. Sci. & Geomech. Abstr. Vol 29, No 3, pp 198-223, 1992.

Coulson, J.H. (1972) Shear strength of flat surfaces in rock. Proc. 13th Symposium on Rock Mechanics. Urbana, Ill., 1971 (E.J.Cording, Ed.). pp 77 – 105 (1972)

De Toledo, P.E.C. and De Freitas, M.H. (1993) Laboratory testing and parameters controlling the shear strength of filled rock joints. Geotechnique 43, No 1, pp 1 - 19.

Deere, D.U. and Miller, R.P. (1966) Engineering classification and index properties of rock. Technical report No. AFNL-TR-65-116 Air Force Weapons Laboratory, New Mexico.

Fookes, P.G. and Denness, B. (1969) Observational studies on fissure patterns in Cretaceous sediments of South East England. Geotechnique, 19, No 4, pp 453 - 477.

Fourmaintraux, D. (1975) Quantification of discontinuities in rock from mafic origin. Rock Mechanics, 7, pp83 - 100

Gabrielsen, R.H. (1990) Characteristics of joints and faults. Proceedings of the International Son Rock Joints, Loen. Balkema, Rotterdam.

Geertsema, A. J. (1986) Die Ingenieursgeologie van sandsteen in die Natal Groep. M. Sc. Thesis, University of Pretoria, 1986.

Gillette, D. R., Sture, S., Ko, H., Gould, M. C. and Scott, G. S. (1983) Dynamic Behaviour of Rock Joints. 24th U S Symposium on Rock Joints, June 1983.

Goodman, R.E. (1970) The deformability of joints. In: Determination of the in-situ modulus of deformation of rocks. Special technical publication, No 477, pp 174 - 196. American Society for Testing and Materials, Philadelphia.

Goodman, R.E. (1976) Methods of Geological Engineering in Discontinuous Rocks, West, St Paul.

Hakami, E and Barton, N. (1991) Aperture Measurement and Flow experiments Using Transparent Replicas of Rock Joints. Norwegian Geotechnical Institute, Publication Nr 182, Oslo, 1991

Haverland, M. L. and Slebir, E. J. (1971) Methods of performing and interpreting in situ shear tests. Engineering and Research Centre, Bureau of Reclamation, U S Department of the Interior. Proceedings of the 13th Symposium on Rock Mechanics. University of Illinois at Urbana-Champaign, August 30 - September 1, 1971.

Hoek, E and Bray, J. (1977) Rock slope engineering. The Institution of Mining and Metallurgy, London.

Hudson, John A. (1993) Comprehensive Rock Engineering. Volume 1 - 5. Pergamon Press
ISRM (1978) Suggested method for determining the Uniaxial Compressive Strength of Rock Materials. ISRM Committee on Laboratory Tests, September 1978.

ISRM (a) (1974) Suggested method for Determining Shear Strength. Committee on standardisation of Laboratory and Field tests, February 1974.

ISRM (b) (1977) Suggested method for Determining Tensile Strength. Committee on standardisation of Laboratory and Field tests, March 1977.

ISRM (c) (1977) Suggested Method for Determining Hardness and Abrasiveness of Rocks. Committee on standardisation of Laboratory and Field tests. Document 5, March 1977.

ISRM (d) (1977) Suggested Method for Determining Sound Velocity. Committee on standardisation of Laboratory and Field tests. Document 4, March 1977.

ISRM (e) (1977) Suggested Methods for Determining Water Content, Porosity, Absorption, and related properties and Swelling and Slake-Durability Index Properties. Committee on standardisation of Laboratory and Field tests. Document 2, December 1977.

ISRM (f) (1977) Suggested Method for Petrographic Description of Rocks. Committee on standardisation of Laboratory and Field tests. Document 6, March 1977.

ISRM (g) (1977) Suggested method for Determining the Strength of Rock Material in Triaxial Compression. Committee on standardisation of Laboratory and Field tests, March 1977.

Jaeger, J. C. (1959) Frictional properties of joints in rock. Geofis. Pura Appl. Milano. pp 148 - 158.

Kutter, H.K. (1974) Rotary shear testing of rock joints. In: Advances in rock mechanics, pp 254 - 262. Proc. 3rd Congr. Int. Soc. Rock Mech, Denver.

Ladanyi, H.K. and Archambault, G. (1977) Shear strength and deformability of filled indented joints. Proc. 1st Int. Symp. Geotech, pp 317 - 326. Structural Complex Formations, Capri.

Lupini, J.F, Skinner, A.E. and Vaughan, P.R. (1981) The drained residual strength of cohesive soils. Geotechnique, No 2, pp 181 - 213.

Makurat, A., Barton, N., Rad, N. S. and Bandis, S. (1991) Joint Conductivity variation due to normal and shear deformation. Norwegian Geotechnical Institute, Publication Nr 182, Oslo, 1991.

Makurat, A., Barton, N., Tunbridge, T. and Vic, G.. (1991) The Measurement of the Mechanical and Hydraulic Properties of Rock Joints at Different Scales in the Stripa project. Norwegian Geotechnical Institute, Publication Nr 182, Oslo, 1991.

Makurat, A., Barton, N., Vic, G., Chrysanthakis, P. and Monsen, K. (1991) Jointed Rock Mass Modelling. Norwegian Geotechnical Institute, Publication Nr 182, Oslo, 1991.

Maschek, R. K. A. (1989) Sabie River Development Scheme. Injaka Dam Site. Uniaxial compressive strength tests on core specimens. Unpublished report of the Geological Survey of South Africa, Pretoria.

Nicholson, Glenn A. (1983) In situ and laboratory shear device for rock: A comparison. Technical Report GL-83-14. Geotechnical Laboratory. U S Army Engineer Waterways Experimental Station, Vicksburg, Mississippi.

Pegram, G.G.S. and Pennington, M.S. (1996) A Method for Estimating the Hydraulic Roughness of Unlined Bored Tunnels. Report to the Water Research Commission by the Department of Civil Engineering, University of Natal. WRC Report No 579/1/96.

Pereira, J.P. (1990) Mechanics of filled discontinuities. Proceedings of an International Conference on mechanics of jointed and faulted rock, pp 375 - 380. Vienna.

Price, N.J. (1966) Fault and Joint development in Brittle and semi-Brittle rock. Pergamon, Oxford.

Priest, Stephen D. (1993) Discontinuity analysis for rock engineering. Chapman & Hall, London.

Richards, L.R. (1975) The shear strength of joints in weathered rock. Ph.D Thesis. University of London, Imperial College, pp 1 – 427.

Spencer, E.W. (1969) Introduction to the structure of the Earth. McGraw-Hill. New York.

Stacey, T.R. (1980) A simple device for direct shear testing of intact rock. Jnl. of the SA Institution of Mining and metallurgy. March, 1980

Sun, W.H, Zheng, T.M. and Li, M.Y. (1981) The mechanical effect of the thickness of weak intercalary layers. Proceedings of an International symposium on weak rock, pp 49 - 54, Tokyo.

U S Bureau of Reclamation. Procedure for performing Direct and Sliding Friction Testing of Rock Core. Draft Internal report USBR 6250-92.

Van der Walt, A. (1992) Specifications for Large Shear Machine. Internal report of the Department of Water Affairs, Pretoria, 1992

Van Rooy, J.L. (1991) Some Rock Durability Aspects of Drakensberg Basalts for Civil Engineering Construction. PhD thesis, University of Pretoria.

Vogler, U. W. (1985) Code of practice for determining the punch shear strength on plates of intact rock material. Geomechanics Division, CSIR, Pretoria 1985. pp 1 - 5.

Ward, J. R., Jermy, C. A. (1985) Geotechnical Properties of South African Coal-bearing Strata. Proceedings of a ISRM Symposium on Rock Mass Characterisation, Randburg, November 1985.

Whitten, D.G.A. and Brooks, J.R.V. (1972) A Dictionary of Geology. Penguin, Harmondsworth.

Wilbowo, J. T., Amadei, B., Sture, S., Robertson, A. B. and Price, R. (1992) Shear Response of A Rock Joint Under Different Boundary Conditions: An Experimental Study. The Proceedings of an International Conference on Fractured and Jointed Rock Masses, Lake

Ziegler, T.W. (1972) In Situ Testing for the Determination of Rock Mass Shear Strength. Technical Report S-72-12 U.S. Army Engineer Waterways Experimental Station, Vicksburg, Miss.